

Universidade Federal de Juiz de Fora
Engenharia Elétrica
Programa de Pós-Graduação em Engenharia Elétrica

Thiago Fernandes do Amaral Nogueira

**Statistical Modeling of the Brazilian In-Home Channels: PLC and Cascade
of PLC and Wireless**

Juiz de Fora

2018

Ficha catalográfica elaborada através do Modelo Latex do CDC da
UFJF com os dados fornecidos pelo(a) autor(a)

Nogueira, Thiago.

Statistical Modeling of the Brazilian In-Home Channels: PLC and Cascade of PLC and Wireless / Thiago Fernandes do Amaral Nogueira. – 2018.
78 f. : il.

Orientador: Moisés Vidal Ribeiro

Coorientador: Guilherme Ribeiro Colen

Dissertação de Mestrado – Universidade Federal de Juiz de Fora, Engenharia Elétrica. Programa de Pós-Graduação em Engenharia Elétrica, 2018.

1. Caracterização estatística. 2. Comunicação híbrida. 3. Comunicação via rede de energia elétrica. 4. Comunicação sem fio. 5. Metodologia de modelagem. I. Vidal Ribeiro, Moisés, orient. II. Ribeiro Colen, Guilherme, coorient. III. Título.

Thiago Fernandes do Amaral Nogueira

**Statistical Modeling of the Brazilian In-Home Channels: PLC and Cascade
of PLC and Wireless**

Dissertação de mestrado apresentada ao Programa de Pós-Graduação em Engenharia Elétrica da Universidade Federal de Juiz de Fora, na área de concentração em sistemas eletrônicos, como requisito parcial para obtenção do título de Mestre em Engenharia Elétrica.

Orientador: Moisés Vidal Ribeiro

Coorientador: Guilherme Ribeiro Colen

Juiz de Fora

2018

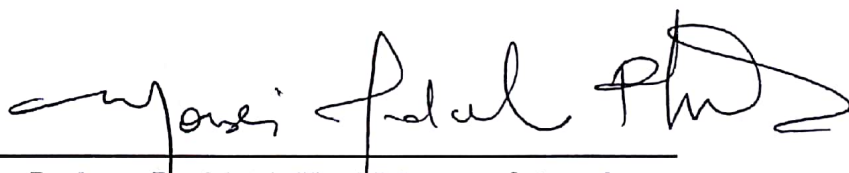
Thiago Fernandes do Amaral Nogueira

Statistical Modeling of the Brazilian In-Home Channels: PLC and Cascade
of PLC and Wireless

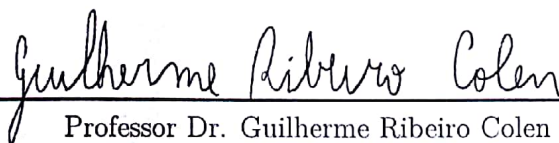
Dissertação de mestrado apresentada ao Programa de Pós-Graduação em Engenharia Elétrica da Universidade Federal de Juiz de Fora, na área de concentração em sistemas eletrônicos, como requisito parcial para obtenção do título de Mestre em Engenharia Elétrica.

Aprovada em: 06/09/2018

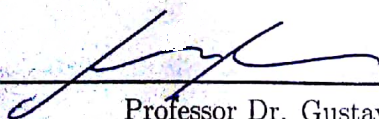
BANCA EXAMINADORA



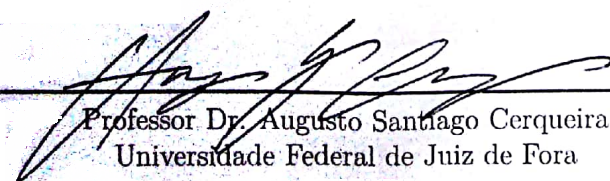
Professor Dr. Moisés Vidal Ribeiro - Orientador
Universidade Federal de Juiz de Fora



Professor Dr. Guilherme Ribeiro Colen
Centro de Instrução Almirante Wandenkolk



Professor Dr. Gustavo Fraidenraich
Universidade Estadual de Campinas



Professor Dr. Augusto Santiago Cerqueira
Universidade Federal de Juiz de Fora

Dedico este trabalho aos meus pais José Joaquim e Margarida, minha namorada Laís e ao meu filho Heitor.

ACKNOWLEDGEMENTS

Agradeço a Deus por me guiar e me rodear de pessoas maravilhosas desde o primeiro momento de minha vida.

Aos meus pais José Joaquim Nogueira e Margarida Luiza Fernandes Nogueira, sem seu apoio e ensinamentos eu jamais teria chegado tão longe.

A minha namorada Laís Machado Bernardinelli, pelo amor, carinho, amizade e cumplicidade.

Ao Professor Moisés Vidal Ribeiro, por toda orientação, paciência e incentivo.

Ao Professor Guilherme Ribeiro Colen, pela orientação e apoio.

A todos amigos que contribuíram de alguma forma para este trabalho. Em especial aos colegas do laboratório pelo aprendizado compartilhado e todas conversas.

“If I have seen further it is by standing on the shoulders of Giants.”
(Isaac Newton)

RESUMO

Esta dissertação tem como objetivo discutir a caracterização estatística e modelagem das respostas em frequência de canais de linhas de energia elétrica e de canais concatenados de rede de energia elétrica e sem fio (canais híbridos de rede de energia elétrica e sem fio) compreendendo a faixa de frequência de 1.7 até 100 MHz. A caracterização e modelagem baseiam-se em análises estatísticas realizadas em conjuntos de dados constituídos por estimativas de respostas em frequência de canal medidos, as quais foram adquiridas através de uma campanha de medições realizada em várias residências brasileiras. A este respeito, um método aprimorado de modelagem estatística é proposto para obtenção dos modelos estatísticos baseados no pressuposto de que as respostas em frequência dos canais são processos aleatórios não correlacionados e, como consequência, as componentes de magnitude e fase dessas respostas de canal constituem dois processos aleatórios independentes. Ao adotar quatro critérios estatísticos, são apresentadas as melhores distribuições estatísticas que modelam as funções de magnitude e fase das estimativas de resposta em frequência dos canais. Além disso, uma técnica de interpolação baseada em splines cúbicas é aplicada com o intuito de oferecer formas de onda representativas dos parâmetros das melhores distribuições estatísticas, no domínio do tempo contínuo, com um baixo número de coeficientes. Por fim, os algoritmos, utilizados para implementar o método aprimorado de modelagem estatística, são detalhados. No que se refere aos canais de rede de energia elétrica, a modelagem estatística encontrada anteriormente na literatura pode não ser adequada para a modelagem dos canais de rede de energia elétrica residenciais brasileiros. Como resultado, um modelo estatístico para o canal de rede de energia elétrica residencial brasileiro é introduzido. Em relação ao canal híbrido de rede de energia elétrica e sem fio, um modelo estatístico é introduzido.

Palavras-chave: Caracterização estatística. Comunicação híbrida. Comunicação via rede de energia elétrica. Comunicação sem fio. Metodologia de modelagem.

ABSTRACT

This thesis aims to discuss the statistical characterization and modeling of channel frequency responses of power line channels and the series concatenation of power line and wireless channels (hybrid power line - wireless channels), comprising the frequency band from 1.7 up to 100 MHz. The characterization and modeling rely on statistical analyses based on data sets constituted by measured channel frequency responses estimates, which were acquired through a measurement campaign carried out in several Brazilian residences. In this regard, an enhanced statistical modeling method is proposed to obtain the statistical models based on the assumption that channel frequency responses are uncorrelated random process and, as a consequence, the magnitude and phase components of these channel frequency responses constitute two independent random processes. By adopting four statistical criteria, it is shown the best statistical distributions that models the magnitude and phase functions of channel frequency response estimates. Moreover, an interpolation technique based on cubic Splines is applied, offering representative waveform of the parameters of the best statistical distributions in the continuous-time domain with a low number of coefficients. Furthermore, the algorithms used to implement the enhanced statistical modeling method are described. Concerning to the power line channels, it is shown that the previous statistical modeling, found in the literature, may not be suitable for modeling the Brazilian in-home power line channels. As a result, an statistical model for Brazilian in-home power line channel is introduced. Regarding the hybrid power line - wireless channels, an statistical model is introduced.

Key-words: statistical characterization, hybrid communication, power line communication, wireless communication, modeling methodology.

LIST OF FIGURES

Figure 1 – The block diagram of a PLC system.	23
Figure 2 – The block diagram of a hybrid PLC-WLC system.	26
Figure 3 – Measurement setup for the <i>short-path</i> (2-m) and <i>long-path</i> (6-m) versions of the hybrid PLC-WLC channels.	27
Figure 4 – Five consecutive and valid CFR Magnitudes of the measured in-home PLC channel.	40
Figure 5 – The relative frequency associated with the chosen statistical distribution that best models the CFR magnitude in accord with the adopted criteria.	41
Figure 6 – The log-likelihood ratio for the following statistical distributions: Beta, Birnbaum-Saunders, and Log-normal.	42
Figure 7 – The relative frequency of the magnitude of the valid CFR estimates at the sample $k = 1067$ ($k\Delta f = 52.1$ MHz) and the modeling based on the Beta distribution.	42
Figure 8 – The relative frequency of the magnitude of the valid CFR estimates at the sample $k = 1600$ ($k\Delta f = 78.1$ MHz) and the modeling based on the Beta distribution.	43
Figure 9 – The MSE values for the parameters from PLC scenario: (a) α parameter, (b) β parameter.	44
Figure 10 – The result of the interpolation technique based on cubic Splines applied to obtain $\alpha(f) = \zeta_1(f)$ for the Beta distribution ($\alpha(k\Delta f)$ are the original values of the parameter and $\hat{\alpha}(f)$ is the interpolated curve). . .	45
Figure 11 – The result of the interpolation technique based on cubic Splines applied to obtain $\alpha(f) = \zeta_1(f)$ for the Beta distribution ($\alpha(k\Delta f)$ are the original values of the parameter and $\hat{\alpha}(f)$ is the interpolated curve). . .	45
Figure 12 – The result of the interpolation technique based on cubic Splines applied to obtain $\beta(f) = \zeta_2(f)$ for the Beta distribution ($\beta(k\Delta f)$ are the original values of the parameter and $\hat{\beta}(f)$ is the interpolated curve). . .	46
Figure 13 – The relative frequency associated with the chosen statistical distribution that best models CFR phase in accord with the adopted criteria. .	46
Figure 14 – The relative frequency of the phase of the valid CFR estimates at the sample $k = 1067$ ($k\Delta f = 52.1$ MHz) using the Uniform distribution. . .	47
Figure 15 – The relative frequency of the phase of the valid CFR estimates at the sample $k = 1600$ ($k\Delta f = 78.1$ MHz) using the Uniform distribution. . .	47
Figure 16 – Five consecutive and valid CFR Magnitudes of the measured in-home PLC channel.	48

Figure 17 – The relative frequency associated with the chosen statistical distribution that best models the CFR magnitude in accord with the adopted criteria.	48
Figure 18 – The log-likelihood ratio for the following statistical distributions: Log-normal, Gamma.	49
Figure 19 – The relative frequency of the magnitude of the valid CFR estimates at the sample $k = 1040$ ($k\Delta f = 50.78$ MHz) and the modeling based on the Log-normal distribution.	49
Figure 20 – The relative frequency of the magnitude of the valid CFR estimates at the sample $k = 1650$ ($k\Delta f = 80.57$ MHz) and the modeling based on the Log-normal distribution.	50
Figure 21 – The MSE values for the parameters from <i>short-path</i> scenario: (a) μ parameter, (b) σ parameter.	51
Figure 22 – The result of the interpolation technique based on cubic Splines applied to obtain $\mu(f) = \zeta_1(f)$ for the Log-normal distribution ($\mu(k\Delta f)$ are the original values of the parameter and $\hat{\mu}(f)$ is the interpolated curve). . .	52
Figure 23 – The result of the interpolation technique based on cubic Splines applied to obtain $\sigma(f) = \zeta_2(f)$ for the Log-normal distribution ($\sigma(k\Delta f)$ are the original values of the parameter and $\hat{\sigma}(f)$ is the interpolated curve). . .	52
Figure 24 – The relative frequency associated with the chosen statistical distribution that best models CFR phase in accord with the adopted criteria. .	53
Figure 25 – The relative frequency of the phase of the valid CFR estimates at the sample $k = 1040$ ($k\Delta f = 50.78$ MHz) using the Uniform distribution. .	53
Figure 26 – The relative frequency of the phase of the valid CFR estimates at the sample $k = 1650$ ($k\Delta f = 80.57$ MHz) using the Uniform distribution. .	54
Figure 27 – Five consecutive and valid CFR magnitudes of the measured in-home PLC-WLC <i>long-path</i> channel.	54
Figure 28 – The relative frequency associated with the chosen statistical distribution that best models the CFR magnitude in accord with the adopted criteria.	55
Figure 29 – The log-likelihood ratio for the following statistical distributions: Log-normal, Gamma.	55
Figure 30 – The relative frequency of the magnitude of the valid CFR estimates at the sample $k = 1060$ ($k\Delta f = 51.76$ MHz) and the modeling based on the Log-normal distribution.	56
Figure 31 – The relative frequency of the magnitude of the valid CFR estimates at the sample $k = 1600$ ($k\Delta f = 78.1$ MHz) and the modeling based on the Log-normal distribution.	56

Figure 32 – The MSE values for the parameters from PLC-WLC <i>long-path</i> scenario: (a) μ parameter, (b) σ parameter.	58
Figure 33 – The result of the interpolation technique based on cubic Splines applied to obtain $\mu(f) = \zeta_1(f)$ for the Log-normal distribution ($\mu(k\Delta f)$ are the original values of the parameter and $\hat{\mu}(f)$ is the interpolated curve). . .	59
Figure 34 – The result of the interpolation technique based on cubic Splines applied to obtain $\sigma(f) = \zeta_2(f)$ for the Log-normal distribution ($\sigma(k\Delta f)$ are the original values of the parameter and $\hat{\sigma}(f)$ is the interpolated curve). . .	59
Figure 35 – The relative frequency associated with the chosen statistical distribu- tion that best models CFR phase in accord with the adopted criteria. . .	60
Figure 36 – The relative frequency of the phase of the valid CFR estimates at the sample $k = 1060$ ($k\Delta f = 51.76$ MHz) using the Uniform distribution. . .	60
Figure 37 – The relative frequency of the phase of the valid CFR estimates at the sample $k = 1600$ ($k\Delta f = 78.1$ MHz) using the Uniform distribution. . .	61
Figure 38 – Block diagram of the PLC measurement setup.	70
Figure 39 – Block diagram of the hybrid PLC-wireless measurement setup.	71

LIST OF TABLES

Table 1 – Characteristics of the measured residences.	71
Table 2 – $\alpha(f)$ parameter: Coefficients of the cubic Splines for $L = 19$ nonuniform subbands.	72
Table 3 – $\beta(f)$ parameter: Coefficients of the cubic Splines for $L = 19$ nonuniform subbands.	73
Table 4 – $\mu(f)$ parameter: Coefficients of the cubic Splines for $L = 15$ nonuniform subbands.	74
Table 5 – $\sigma(f)$ parameter: Coefficients of the cubic Splines for the $L = 15$ nonuniform subbands.	75
Table 6 – $\mu(f)$ parameter: Coefficients of the cubic Splines for $L = 15$ nonuniform subbands.	76
Table 7 – $\sigma(f)$ parameter: Coefficients of the cubic Splines for the $L = 15$ nonuniform subbands.	77

ACRONYMS

AIC	Akaike information criterion
ACA	average channel attenuation
ACG	average channel gain
BIC	Bayesian information criterion
BPSK	binary phase shift keying
CFR	channel frequency response
CIR	channel impulse responses
CB	coherence bandwidth
CT	coherence time
CP	cyclic prefix
DFT	discrete Fourier transform
EDC	Efficient determination criterion
HS-OFDM	hermitian-symmetric orthogonal frequency-division multiplexing
IoT	Internet of Things
LPTV	linear periodically time varying
LTI	linear time-invariant
LPWAN	Low Power Wide Area Networks
MLE	Maximum Likelihood Estimation
MSE	mean squared error
PLC	power line communication
RF	radio frequency
r.va.	random variable
r.v.	random vector
RMS-DS	root mean squared delay spread
SG	smart grid

UWB Ultra-wide-band

WLC wireless communication

WLAN wireless local area network

CONTENTS

1	INTRODUCTION	16
1.1	OBJECTIVES	20
1.2	THESIS ORGANIZATION	20
1.3	SUMMARY	21
2	PROBLEM FORMULATION	22
2.1	PLC CHANNEL	23
2.2	HYBRID PLC-WLC CHANNEL	25
2.3	INVESTIGATION QUESTIONS	27
2.4	SUMMARY	28
3	THE ENHANCED STATISTICAL MODELING METHOD .	29
3.1	FINDING THE BEST STATISTICAL DISTRIBUTIONS	30
3.2	INTERPOLATING THE PARAMETERS VALUES	32
3.3	SUMMARY	34
4	NUMERICAL RESULTS	37
4.1	SIMULATIONS DESCRIPTIONS	37
4.2	UNCORRELATED CFR MODEL OF PLC CHANNELS	40
4.3	UNCORRELATED CFR MODEL OF HYBRID PLC-WLC <i>SHORT- PATH</i> CHANNELS	46
4.4	UNCORRELATED CFR MODEL OF HYBRID PLC-WLC <i>LONG- PATH</i> CHANNELS	53
4.5	SUMMARY	58
5	CONCLUSIONS	62
5.1	FUTURE WORKS	63
	REFERENCES	64
	APPENDIX A – Measurement Campaign	70
	APPENDIX B – In-home PLC channels in the frequency band delimited by 1.7 and 100 MHz: Tables of the values of cubic splines used to model the parameter of the Beta Distribution.	72

APPENDIX C – In-home hybrid PLC-WLC <i>short-path</i> channels in the frequency band delimited by 1.7 and 100 MHz: Tables of the values of cubic splines used to model the parameters of the Log-Normal Distribution.	74
APPENDIX D – In-home hybrid PLC-WLC <i>long-path</i> channels in the frequency band delimited by 1.7 and 100 MHz: Tables of the values of cubic splines used to model the parameters of the Log-Normal Distribution.	76
APPENDIX E – List of Publications	78

1 INTRODUCTION

Power line communication (PLC) systems have been investigated by academic and industry sectors worldwide over the past decades. Recently, these systems have become attractive solutions for data communication once they can be deployed over the existing electric power systems infrastructure. As a matter of fact, the ubiquitousness of electric power systems is the main advantage associated with the use of PLC technologies. Based on this very important characteristic, PLC systems can assist the deployment of smart grid (SG), the Internet of Things (IoT), smart city, and Industry 4.0 technologies. On the other hand, one may say that the wireless communications constitute a more established alternative for this purpose due to its low-cost and suitability for fulfilling the needs and demands of these technologies. However, it is widely recognized that SG, IoT, smart city and Industry 4.0 will be supported by a heterogeneous set of telecommunication technologies, as no single solution fits all scenarios [1,2]. For the given reasons, PLC and unlicensed wireless communications are considered as the two leading data communication technologies for SG applications and IoT [3–5].

Some researches have pointed out that the deployment and operational costs related to the PLC systems can be low [4, 6] and it constitutes a relevant advantage in favor of these data communication systems; however, electric power grids were originally conceived and designed for generating, transmitting and delivering or distributing energy to consumers or prosumers and, as a consequence, the propagation of signals carrying information through power lines may suffer severe attenuation and/or frequency-selective fading due to the use of non-ideal and unshielded conductors, the existence of impedance mismatching, and dynamics of loads and equipments connected to electric power grids. Also, it is important to highlight that signals carrying information over power line can be corrupted by the high power impulsive noise presences associated with the dynamics of electric power systems and the use of electromagnetically unshielded power lines. In addition, the diversity of topologies and distances of electric power grids may result in very disparate behaviors that demand powerful PLC systems for dealing with this problems; power lines work as antennas and, as consequence, interference with other telecommunication systems operating in the same frequency band may result in significant radio frequency (RF) interference; and the remarkable increase of connections of new types of loads make the electric power grids a challenging media for data communication purposes. Moreover, it is important to pay attention to the voltage level (low, medium and high-voltage), the type of environment, such as indoor (vehicle, residences and building) and outdoor (metropolitan and rural areas), among other issues.

As a common sense in the telecommunication field, it is well-established that the measurement, characterization and modeling of PLC channels are mandatory tasks to be *a priori* accomplished for fostering advances in PLC systems because they yield important

information for driving the designers of telecommunication devices. Due to the complexity and diversity of electric power systems, it is well-accepted by the PLC community that PLC channels can be, in terms of voltage level, organized in the low-voltage (indoor or outdoor) [7], medium-voltage (outdoor and underground) [8] and high-voltage (outdoor) [9]. It is important to emphasize that this organization is aligned with the electric power systems field. Also, it deserves attention the fact that the underground medium-voltage electric power grids are more distinct because of the surrounding environment [10].

Focusing on the electric power grids located in indoor facilities, research efforts toward the characterization and modeling of PLC channels may be organized in terms of the type of facilities as follows: residential or commercial buildings, known as in-home or in-building PLC [11, 12] and in-vehicles (i.e., cars [13], ships [14], and aircrafts [15–17]). Regarding the frequency band of operation, the PLC community does not follow the communications community once the concept of the narrowband-PLC systems is associated with data communication through the frequency band delimited by 0 and 500 kHz [18, 19], while the concept of the broadband-PLC systems refers to the use of the frequency band from 1.705 up to 100 MHz [12, 20], depending on the telecommunications regulation, for data communication purpose. For instance, in Brazil, broadband-PLC systems are allowed to operate in the frequency band delimited by 1.7 and 50 MHz [21]. Some contributions point out that the frequency band between 0 and 500 MHz may be used by future generation of PLC systems [22, 23]. In this context, several improvements are being investigated, such as those obtained by cooperative communication [24–28].

Still addressing the indoor electric power grids and focusing on the in-home environments, several contributions related to research efforts for PLC channels characterizations carried out in distinct countries can be highlighted. For instance, [29] discussed in-home PLC channels in Spain that are related to channel attenuation and additive noise in the frequency band between 1.705 and 30 MHz, while [30] considered other features, such as delay spread, average channel gain (ACG) and coherence bandwidth (CB). Also, [31] discussed the normal/log-normal nature of delay spread and ACG. In [20, 32], the in-home PLC channels in some urban and suburban United States (US) residences were characterized in terms of ACG and root mean squared delay spread (RMS-DS), considering the frequency band ranging from 2 up to 30 MHz. In [12], a characterization of in-home PLC channels was performed in some urban and suburban France residences, describing values of CB and time-delay parameters, considering the frequency band ranging from 30 kHz up to 100 MHz. Recently, [33] has analyzed the channel frequency response (CFR), average channel attenuation (ACA), RMS-DS, CB, and coherence time (CT) of Brazilian in-home PLC channels when the frequency band ranges from 1.7 up to 100 MHz. Analyzing the aforementioned works and contributions, we notice that several works had adopted as true that the Log-normal distribution for modeling the CFR magnitude; however, the lack of confidence on it [31] brings our attention to the necessity of further investigation of CFR

of in-home PLC channels.

Concerning wireless communication (WLC), it is important to point out the high dependence on line-of-sight propagation, the increasing signal attenuation along with both distance and carrier frequency, the susceptibility to interference among two or more telecommunication systems operating in the same frequency band, the scarcity of spectrum, and vulnerability to non-authorized access, among other things, constitute a relevant set of problems. Also, the transmitted signal through the air suffers three different propagation effects: reflection, scattering and diffraction [34]. Remarkable problems in WLC are associated with the distortions introduced by the aforementioned propagation effects and co-channel interference, which is primarily generated from uncoordinated transmissions [5].

WLC channel characterization and modeling has been attracting high attention since they can highly reduce the time of developing WLC systems. The WLC system support several different technologies and includes, among others, the wireless local area network (WLAN), comprising five distinct frequency bands: 900 MHz, 2.4 GHz, 3.6 GHz, 5 GHz, and 60 GHz [35]; the cellular data service, using the main frequency range around 900 MHz, 1.8 GHz and 1.9 GHz [36]; the Low Power Wide Area Networks (LPWAN), which bridges the frequency gap between WLAN and cellular technologies, commonly used on IoT applications [37]. As the number of users and service stations has significantly increased in the last decades, more research efforts to correctly characterize and model WLC channel have been carried out. Channel characterization and modeling in such situations can give valuable insights such as predicting the communication quality of a WLC system when high data traffic and or large number of users are demanding the same frequency bandwidth. Among the well established WLC channel models in the literature we can mention: the COST 2100 channel model [38], that provides statically close-to-true descriptions of wireless channels both for indoor scenarios, regarding 3.6 and 5.3 GHz frequency bands, and outdoor scenarios, covering the 400 MHz frequency band; the IEEE 802.15.4a channel model [39], concerning models for diverse frequency ranges and environments, such as indoor and outdoor Ultra-wide-band (UWB) channels covering the frequency range from 2 up to 6 GHz; the Hiperlan/2 channel model [40], covering wireless models in different indoor scenarios for the frequency band of 5 GHz. Regarding the single-input single-output modeling of WLC channels, it is worth stating that the frequency band up to 6 GHz has been very well investigated for characterization and modeling purpose, while the research efforts related related to multiple-input multiple-output is somehow well-established. Currently, a great deal of attention is toward the frequency band related to 5 GHz and beyond.

In a nutshell, it is important to emphasize that PLC and WLC media present distinct characteristics that can be jointly exploited for improving the telecommunication

systems performance in terms of reliability, data-rate, physical layer security, coverage, and flexibility in the physical and link layers [4,5,41–44]. In this regard, a hybrid approach exploiting the existing diversity between PLC and WLC communication systems was initially introduced in order to overcome the problems experienced in both isolated systems. Essentially, it assumes that the PLC and WLC channels are concatenated in series such that PLC and WLC devices operate in the same frequency band. This type of hybrid data communication system emerged at the very beginning of the XX Century [45] but the advances related to WLC system during the following decades drastically reduced the interests in this kind of data communication. Only at the beginning of the XXI Century, precisely one century after its initial investigation, [46] revisited and investigated this kind of channels. As it was initially proposed, it made use of unshielded power lines to propagate and irradiate the transmitted signal by a PLC device. In other words, it assumes that the power line acts as an antenna. As a result, the power lines radiate signals and, conversely, wireless signals, generated by a WLC device, are inductively injected into the power lines. Currently, there is a great deal of attention in parallel and cascade usages of PLC and WLC channels to provide either reliability or high data rate. The former approach result in the so-called the hybrid PLC/WLC system while the later is coined the hybrid PLC-WLC system. The hybrid PLC/WLC system have also been investigated as an alternative to improve data communication performance [3, 41–43, 47–49] since it can take advantage of both electric power grids and air to improve data rate and reliability between source and destination nodes under several circumstances, see [4] for details. In such data communication systems, electric power grids and wireless media are used simultaneously in a cooperative perspective to maximize the available channel resources and, as a consequence, to fulfill data communication constraints.

At this time, it is important to emphasize that there are several works for characterizing PLC channels but PLC channel modeling is still an open problem, once the behavior of electric power grids over narrowband (frequency band from 0 up to 500 kHz) and broadband (frequency band from 1.7 up to 100 MHz) are different in terms of signal propagation and additive noise influence due to the complexity of electric power systems (e.g., load dynamics, topologies and voltage levels). Therefore, channel modeling is still an open problem related to PLC systems. Regarding WLC channels, the huge research efforts carried out worldwide have introduced representative models that are well-established in the literature [38–40]. Furthermore, when the discussion is toward to hybrid PLC-WLC channels, which is defined as the series concatenation of PLC and WLC channels, there is a complete lack of contribution regarding their modeling in the literature. In other words, the investigation of channel models for PLC channels and hybrid PLC-WLC channels is an important research endeavor demanding attention. In this regard, this dissertation strives to cover this gap and to expand the knowledge on these channels by extracting and modeling the benefits of PLC and hybrid PLC-WLC channels for data communication in

the frequency band delimited by 1.7 and 100 MHz.

1.1 OBJECTIVES

Aiming to pay attention to PLC and hybrid PLC-WLC channels for data communication, this thesis seek to provide statistical characterization and modeling of CFRs of Brazilian in-home PLC and hybrid PLC-WLC channels, in order to support future efforts for simulating and designing in-home data communication systems. In this context, an enhanced statistical modeling method, which emerged from the drawbacks associated with the methodology presented in [22, 50], is proposed. Furthermore, the statistical characterization and modeling results, based on data sets of measured CFRs of in-home PLC and hybrid PLC-WLC channels, are detailed. The mentioned data sets were acquired during a measurement campaign performed in several Brazilian residences, see more informations about the measurement campaign in [33, 46, 51, 52]. In this contribution, the frequency band is set to be from 1.7 up to 100 MHz, once it covers broadband PLC systems that can offer data rates in the order of 1 – 2 Gbps [33, 53]. Also, it is a frequency band that comprises Brazilian, European and US telecommunication regulations for PLC systems. Overall, the main objectives of this thesis may be organized as follows:

- To introduce the enhanced statistical modeling method, based on the method presented in [22, 50], that is capable of searching for the best statistical distribution to model the CFR of in-home PLC and hybrid PLC-WLC channels. It treats the magnitude and phase components of CFRs as random processes. Based on the fact that the proposed enhanced statistical modeling method is designed in the discrete-time domain, it encompasses a procedure for interpolating the parameters values of the chosen statistical distributions, by dividing the desired frequency band into subbands and using the cubic Spline interpolation technique to come up with a concise representation (i.e., finite and low number of parameters) of the parameters of this random process in the continuous-frequency domain. Also, the algorithms that implements the enhanced statistical modeling method is detailed.
- To provide statistical analyses of measured Brazilian in-home PLC and hybrid PLC-WLC channels, which were acquired by a measurement campaign carried out several residences and took into account the frequency band between 1.7 and 100 MHz. To present the models of such channels and to compare the attained results with the ones found in the literature regarding PLC channels. To introduce, for the first time, models of the CFRs of hybrid PLC-WLC channels.

1.2 THESIS ORGANIZATION

The remainder of this document is structured as follows:

- Chapter 2 covers the mathematical formulation necessary for dealing with the modeling of PLC channels, based on the assumption that the magnitude and phase responses of a CFR can be modeled as two random processes in the discrete-time domain. In sequel, the modeling of the CFRs of hybrid PLC-WLC channels is formulated likewise.
- Chapter 3 describes the proposed enhanced statistical modeling method, based on the method presented in [22, 50], to obtain the CFR model of PLC and hybrid PLC-WLC channels, based on its magnitude and phase responses. The enhanced statistical modeling method also presents a procedure to interpolate the parameters of the statistical distributions that is capable of modeling randomness of magnitude and phase components of CFRs in the discrete and continuous-time domains.
- Chapter 4 discusses statistical analyses and numerical results of the proposed enhanced statistical modeling method, over a data set of CFRs estimates, acquired through a measurement campaign carried out in several Brazilian residences. Also, it offers comparison among the results found in the literature and the ones presented on this thesis.
- Chapter 5 summarizes the main contributions and findings achieved in this thesis. Also, it outlines future research endeavors and new problems that came out to attention during the time spent with the investigation of these challenging and interesting channels.

1.3 SUMMARY

This chapter has presented a brief introduction of this thesis, addressing important aspects of PLC and hybrid PLC-WLC systems. Also, the main objectives and the organization of this work have been summarized.

2 PROBLEM FORMULATION

The independent use of electric power grids and wireless media for data communication purpose has been pursued since long time ago. However, the need for maximizing their usage and fulfilling the astonishing and growing demands for connectivity among human beings and machines has brought attention to the drawbacks and limitations of these media. Attempting to address these issues, the investigation of the combined use of electric power grids and wireless media for data communication has started a few years ago.

Currently, an increasing number of works are investigating, characterizing, and modeling hybrid PLC and WLC channels for improving the performance of in-home broadband communication systems [29, 32, 33, 46, 51]. The motivation behind these research effort refers to the need for increasing the reliability, data rate, flexibility and coverage of data communication systems that must fulfill the needs and demands related to the IoT, Smart Grids and Industry 4.0. The majority of the aforementioned works adopts well-known channel models in which PLC and hybrid PLC and WLC CFRs are flat and its channel impulse responses (CIR) are modeled as discrete-time and stationary random process. Nevertheless, surveys about electric power grid measurements available in the literature have shown that more investigations have to be carried out to come up with representative PLC channel models. In fact, the evolving characteristic and the diversity of loads connected to the electric power systems emphasizes the need for carrying out worldwide measurement campaigns and characterization of electric power systems, mainly in the medium and low-voltage levels.

Aiming to fulfill this gap, [33, 46, 51] discussed measurement campaign and characterization of Brazilian in-home PLC and hybrid PLC-WLC channels over the frequency band from 1.7 up to 100 MHz. Based on a extensive measurement campaign carried out in seven Brazilian residences, the characterization of these type of channels were performed over a data set constituted by several PLC and hybrid PLC-WLC channels estimates together with additive noise measurements. A contribution to be added to those presented in [33, 46] is to provide statistical models of the CFR, in order to feed the specifications that researchers need for carrying out more analyses of the data communication systems.

In this regard, this chapter approaches the problem formulation for modeling the CFRs of the in-home PLC and hybrid PLC-WLC channels, covering the frequency band delimited by 0 and B Hz . First, a formulation of the broadband PLC system is considered with the objective of deriving a concise model for the frequency response of inhome PLC channels. In the sequel, a formulation for the hybrid PLC-WLC system, taking into account the findings reported in [46], is presented to come up with the statistical model of CFR of PLC-WLC channels, which encompasses the two data communication media

(PLC and WLC).

This chapter is organized as follows: Section 2.1 outlines the problem formulation for the inhome PLC channel. In the sequel, Section 2.2 presents the problem formulation the hybrid PLC-WLC channels. Section 2.3 exposes the investigation questions regarding the formulations presented in Sections 2.1 and 2.2. Section 2.4 addresses a brief summary on this chapter.

2.1 PLC CHANNEL

Fig. 1 shows the block diagram of a PLC system which is supposed to transmit information carrying signals through an electric power circuit in the frequency band delimited by 0 and B Hz (i.e., baseband data communication). This electric power circuit is supposed to be linear and time-varying system. According to this figure, the received signal is expressed as

$$Y_P(t) = \tilde{Y}_P(t) + V_P(t) = \int_{-\infty}^{+\infty} h_P(t, \tau) X(\tau) d\tau + V_P(t), \quad (2.1)$$

where $X(t) \in \mathbb{R}$ is the transmitted signal modeled as a wide sense stationary stochastic process; $h_P(t, \tau) \in \mathbb{R}$ is the time varying CIR, related to an impulse applied on the PLC channel at the instant τ , modeling the propagation of the transmitted signal through the electric power circuit; $V_P(t) \in \mathbb{R}$ is the additive noise that is modeled as a wide sense stationary random process, $\tilde{Y}_P(t) \in \mathbb{R}$ and $Y_P(t) \in \mathbb{R}$ denote wide sense stationary random processes called the free-of-noise received signal and the received signal, respectively.

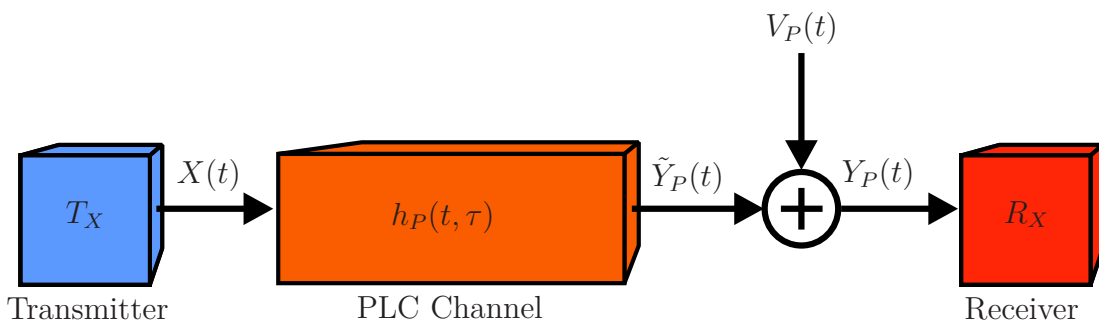


Figure 1: The block diagram of a PLC system.

Due to the linear periodically time varying (LPTV) behavior of PLC channels, which is related to the loads dynamics and the fact that electric power systems transmit or deliver energy at 50 or 60 Hz, $h_P(t, \tau)$ can be considered as a cyclostationary stochastic random process with a period equal to a half of the mains frequency [54]. Based on the knowledge of the coherence time, $T_c \in \mathbb{R}_+$, of the PLC channels, the mains cycle (50 Hz or 60 Hz) can be divided into microslots of time interval duration equal to $T_m \in \mathbb{R}_+ | T_m < T_c$ and, as a consequence, the PLC channels can be modeled as linear time-invariant (LTI)

during the time interval duration of one microslot. In other words, the channel impulse response of a PLC channel at the i^{th} microslot can be expressed as

$$h_i(t), \forall t \in [iT_m, (i+1)T_m] \mid T_m < T_c. \quad (2.2)$$

From now on, we drop the index i for facilitating further deductions. Based on this adoption, the discrete-time representation of the CIR of the PLC channel in a microslot is given by

$$h[n] = h_P(t)|_{t=nT_s}, n = 0, 1, \dots, L_h - 1, \quad (2.3)$$

where L_h is the length of the LTI PLC channel, $T_s = 1/f_s$ is the sampling period and $f_s = 2B$ Hz is the sampling frequency. Usually, the value of L_h contribute to the adoption of an hermitian-symmetric orthogonal frequency-division multiplexing (HS-OFDM) scheme for channel estimation because the number of subcarriers of an HS-OFDM symbol ($2N$) is chosen to ensure that $2N \gg L_h$. Moreover, $B/N < B_c$, in which B_c is the coherence bandwidth of the PLC channels. In order to work with $2N$ subcarriers in the HS-OFDM scheme for performing CFR estimation, the zero-padding have to be applied to $\{h[n]\}$. In vectorial terms, let $\mathbf{h} = [h_0 h_1 \dots h_{L_h-1}]^T$, such as $h_n = h[n]$, then we can obtain an $2N$ -length vector (i.e., $N \in \mathbb{N} \mid B/N < B_c$) that represents the extended version of the vector \mathbf{h} when the zero-padding approach is taken into account. As a consequence, the vectorial representation of the CFR associated with the extended version of the vector \mathbf{h} is expressed as

$$\mathbf{H} = \mathbf{W}_{2N} \begin{bmatrix} \mathbf{I}_{L_h} \\ \mathbf{0}_{(2N-L_h) \times L_h} \end{bmatrix} \mathbf{h}, \quad (2.4)$$

where $\mathbf{W}_{2N} \in \mathbb{C}^{2N \times 2N}$ denotes the $2N \times 2N$ -size discrete Fourier transform (DFT) matrix, $\mathbf{I}_{L_h} \in \mathbb{R}^{L_h \times L_h}$ denotes an $L_h \times L_h$ -size identity matrix, and $\mathbf{0}_{(2N-L_h) \times L_h}$ is an $(2N-L_h) \times L_h$ null matrix. The k^{th} element of the vector $\mathbf{H} = [H_0 H_1 \dots H_{2N-1}]^T \in \mathbb{C}^{2N \times 1}$ may be expressed in polar form $H_k = |H_k| \exp(j\Theta_k)$, in which $|\cdot|$ denotes the absolute value and Θ_k is the phase value of H_k . Since the CIR of the PLC channel is real-valued, it means that CFR posses the hermitian symmetry property and, as a consequence, only the first half of samples of the CFR have to be analyzed. The vectors $|\mathbf{H}| \triangleq [|H_0| |H_1| \dots |H_{N-1}|]^T$ and $\Theta \triangleq [\Theta_0 \Theta_1 \dots \Theta_{N-1}]^T$ are two distinct random processes that represent, respectively, the magnitude and phase of the first half of the vector \mathbf{H} . The modeling of CFR based on these two vectors is very useful for data communication purpose once that the knowledge of the magnitude and the squared magnitude (i.e., $|\mathbf{H}|^2 \triangleq [|H_0|^2 |H_1|^2 \dots |H_{N-1}|^2]^T$) of the CFR allows deriving closed-form expression of theoretical channel capacity, energy harvesting, physical layer security, among other things. Also, the knowledge of phase allows the derivation of delay spread and group delay. It is important to emphasize that the nature of PLC channels indicates that the vectors $|\mathbf{H}|$ and Θ are non-stationary and correlated random processes.

Since the vector \mathbf{H} is a random vector (r.v.) that can be represented by the two distinct r.v.s (i.e., $|\mathbf{H}|$ and Θ), a generic r.v. $\mathbf{X} \in \{|\mathbf{H}|, \Theta\}$ is adopted. Therefore, we assume that the k^{th} random variable (r.va.) belonging to both random processes (i.e., the element $|H_k|$ or Θ_k) can be modeled by an statistical distribution owing a set of parameters represented by $\mathcal{C}_{X_k} = \{\zeta_1[k], \dots, \zeta_U[k]\}$, which is constituted by $U \in \mathbb{N}_+$ parameters. Note that $\zeta_u[k] \in \mathbb{R}$ is the u^{th} parameter associated with the chosen statistical distribution offering the best description of the k^{th} element of the r.v. \mathbf{X} (i.e., $|\mathbf{H}|$ or Θ).

2.2 HYBRID PLC-WLC CHANNEL

Fig. 2 shows the block diagram of the employment of hybridism concept in a data communication system, in which PLC and WLC channels are employed in cascade without an intermediate data communication node between them.. As a matter of fact, PLC devices are connected to electric power grids through a coupling circuit while the WLC devices are connected to the air through an antenna. The PLC and WLC devices directly communicate with each other since both of them occupy the frequency band delimited by 0 and B Hz.

According to [46], as the signal transmitted by a PLC device is irradiated from unshielded power lines, a WLC device can be wirelessly connected to a PLC system, which is supposed to work with PLC devices physically connected to power lines. Similarly to Section 2.1, the received signals at the input of the hybrid PLC-WLC channels, which is supposed to be a linear stochastic system, are expressed as

$$Y_{PW}(t) = \int_{-\infty}^{+\infty} h_{PW}(t, \tau) X(\tau) d\tau + V_{PW}(t), \quad (2.5)$$

for the signal propagation from the PLC device to the WLC device (i.e., PLC \rightarrow WLC direction), and

$$Y_{WP}(t) = \int_{-\infty}^{+\infty} h_{WP}(t, \tau) X(\tau) d\tau + V_{WP}(t), \quad (2.6)$$

for the reverse path, which is defined by the signal propagation from the WLC device to the PLC device (i.e., WLC \rightarrow PLC direction). In (2.5)-(2.6), $X(t) \in \mathbb{R}$ is the transmitted signal modeled as a wide sense stationary stochastic process; $h_{PW}(t, \tau) \in \mathbb{R}$ and $h_{WP}(t, \tau) \in \mathbb{R}$ denote the CIRs when an impulse at the instant τ is applied to the PLC \rightarrow WLC and WLC \rightarrow PLC directions, respectively; $V_{PW}(t) \in \mathbb{R}$ and $V_{WP}(t) \in \mathbb{R}$ are, respectively, the additive noise components and are modeled as two different wide sense stationary random processes found at the input of the transmitting transceivers, when the PLC \rightarrow WLC and WLC \rightarrow PLC directions, respectively, take place; $Y_{PW}(t) \in \mathbb{R}$ and $Y_{WP}(t) \in \mathbb{R}$ are wide sense stationary random processes denoting the received signals, respectively, in the PLC \rightarrow WLC and WLC \rightarrow PLC directions.

It is important to highlight that the symmetry of the hybrid PLC-WLC channel magnitude response is verified when the transmitter and the receiver have the same access

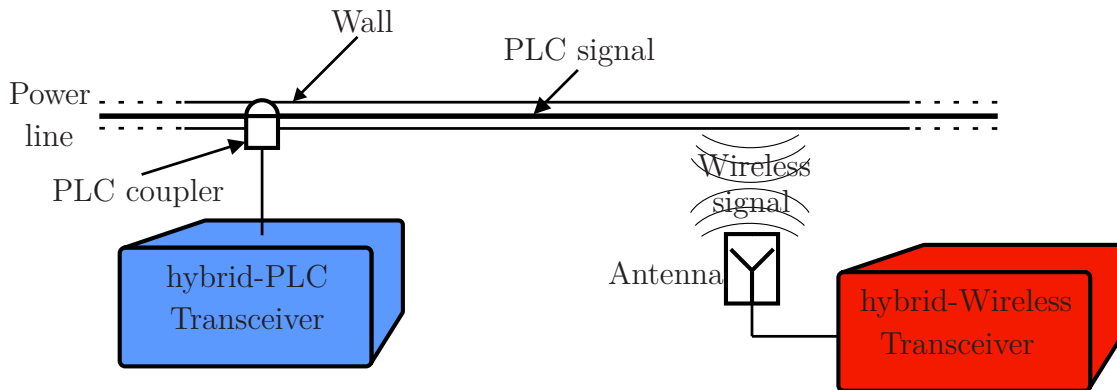


Figure 2: The block diagram of a hybrid PLC-WLC system.

impedance, see [46]. In other words, the CFR of the hybrid PLC-WLC channel remains the same independent from the data transmission direction. Mathematically, $h_{PW}(t, \tau) = h_{WP}(t, \tau)$ agrees with the results presented in [53], which focuses only on PLC channels. Due to the specific characteristics of each media (e.g., power line and air), the symmetry property does not hold true for the additive noises $V_{PW}(t)$ and $V_{WP}(t)$ [46]. As a matter of fact the additive noise in a power line is constituted by several components that are generated by dynamic of load connected to electric power grids. It is well-known as man-made-noise and present a power spectral density that exponentially decay as frequency changes from 0 Hz to 30 MHz. On the other hand, the noise in the air considering the frequency band between 0 and 100 MHz owns a almost constant power spectral density with some peaks that are associated with narrowband channels dedicated to AM and FM stations, among others. The findings reported in [46,51,52] are very interesting to motivate this kind of data communication systems for fulfilling the scarcity of spectrum for dealing with the astonishing increase of data exchanges among entities in smart grids, the IoT and industry 4.0 applications. Advances in this field may facilitate the work of researchers and hybrid PLC-WLC systems designers under the availability and representative of hybrid PLC-WLC channels.

In [46] was proposed the following organization for modeling the hybrid PLC-WLC channels:

- *short-path* channel: On this scenario, the WLC Transceiver may be randomly positioned within a 2 m radius circle, centered at the outlet in which the PLC Transceiver was connected.
- *long-path* channel: On this scenario, the WLC Transceiver was randomly placed into a area defined as a swept circle, having an outer and inner radius of 6 m and 2 m, respectively, centered at the outlet in which the PLC Transceiver was connected.

Fig. 3 shows the coverage region related to the *short-path* and *long-path* channels.

According to [46,51,52], these channels are different because the attenuation of the signal remarkably increases with the distance of the WLC device from the power line.

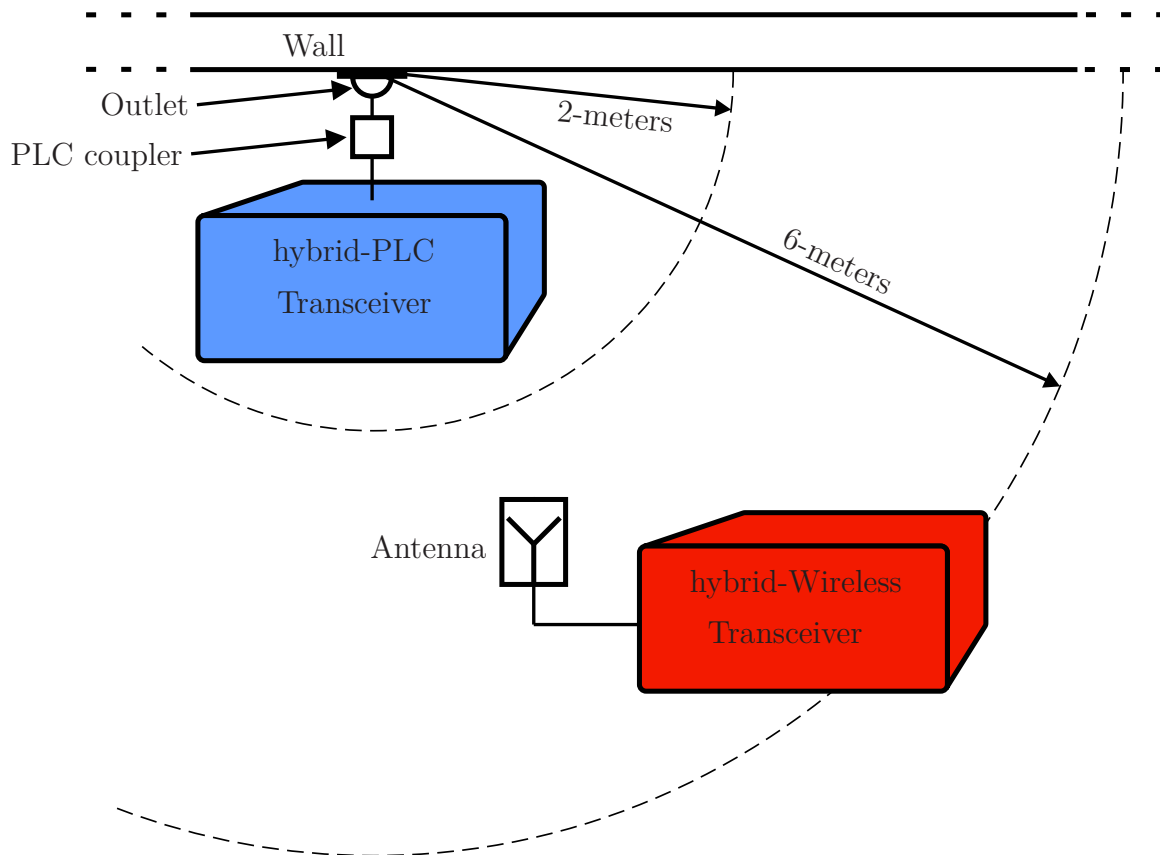


Figure 3: Measurement setup for the *short-path* (2-m) and *long-path* (6-m) versions of the hybrid PLC-WLC channels.

Similar to PLC systems, the hybrid PLC-WLC system operates in the baseband. Therefore the deduction adopted in Subsection 2.1 is directly applied to the channel impulse responses of the PLC-WLC channels considering both *short-path* and *long-path* scenarios. As a result, the vectorial representation of channel frequency response of the hybrid PLC-WLC channel is denoted by the vector $\mathbf{X} \in \{|\mathbf{H}|, \Theta\}$.

2.3 INVESTIGATION QUESTIONS

Given the aforementioned formulation, the following research questions arise regarding the modeling of CFRs of in-home PLC and hybrid PLC-WLC channels within a time interval corresponding to one microslot:

- *What kind of statistical distributions are suitable for modeling the random variables that constitute the vectors $|\mathbf{H}|$ and Θ under the availability of measured data set obtained from a measurement campaign carried out in Brazilian residences?*

- *Could we state that the random vectors $|\mathbf{H}|$ and Θ related to the measured PLC and hybrid PLC-WLC channels in Brazilian residences are stationary random processes?*
- *Which level of correlations exist among the elements of vectors $|\mathbf{H}|$ and Θ ? How to address this feature of these random processes to come up with a generator of channel frequency responses of in-home PLC and hybrid PLC-WLC channels?*

The first and second research questions are covered in this dissertation, while the third research question is left for being investigated in a future work. The investigation of the first two research questions is very interesting from the data communication perspective because it can offer models for allowing researchers to investigate channel capacity, cooperative communication, energy harvesting, physical layer security, among other things.

Chapters 3 and 4 try to answer the first two research questions.

2.4 SUMMARY

This chapter has focused on the formulation of the problems addressed in this thesis.

3 THE ENHANCED STATISTICAL MODELING METHOD

In accordance with the literature, it is well-established that channel modeling of PLC channels can be accomplished by using the following approaches:

- bottom-up: This approach allows obtaining the CFR of PLC channels starting from the properties of the components in the electric power grids, such as topology, type of power lines, branches and loads. It clearly describes the existing relationship between the CFR of PLC channels and the characteristics of constituting components of the electric power grids. Following this approach, CFR can be obtained by either using the network matrix formulation [55] or the theory of transmission lines that considers the effects of multiple transmissions and reflections [56]. Both techniques require complete knowledge of electric power grids and their components, which is a very difficult task to be accomplished due to the complexity of electric power grids. In addition, it is important to point out that the characterization of their components may not be easily available and their interactions with other components in such very complex systems may demand an astonishing efforts to be addressed.
- top-down: This approach considers the PLC channel as a black box and provides the multipath propagation channel model by using an echo model in the time domain [57]. Also, it can make use of a parametric model in the frequency domain [58] with parameters estimated from a data set obtained during measurement campaigns. Based on a data set availability, this kind of channel model can be easily accomplished. Different from the bottom-up approach, the top-down approach is not capable of describing the physics behind the signal propagation through the electric power grids.

It is important to point out that the top-down approach can be applied to perform statistical characterization and modeling of both PLC and hybrid PLC-WLC channels based on measurement campaign for estimating the CFR of the channels, while the bottom-up approach is more easier to be applied to PLC channels in comparison to the hybrid PLC-WLC channels. The use of the bottom-up approach in hybrid PLC-WLC channels relies on the electromagnetic theory and other aspects related to the air that are not easy to represent mathematically. Based on this discussion and previous works in the literature reporting the usefulness of the top-down approach [59], this chapter focuses on an statistical modeling of the PLC and hybrid PLC-WLC channels based on the top-down approach.

This chapter proposes a enhanced statistical modeling method to obtain the statistical model of the elements of the r.v. \mathbf{X} , on the frequency band covering the band-

width between 0 and B Hz. This enhanced statistical modeling method can be seen as an improved version of the method introduced in [22, 50] for performing the statistical modeling of the access impedances in in-home electric circuit. According to [22, 50], several polynomials are used to represent the waveforms of the parameters associated with the statistical distribution offering the best modeling of a random vector. A problem found in the statistical modeling method organized in [22, 50] was the edge effects at the boundaries of the intervals chosen to be presented by a unique polynomial when several consecutive frequency bands are taken into account. Due to the characteristic of access impedances in a given frequency band (e.g., $f \in [0, B)$), the statistical modeling method presented in [22, 50] can be easily extended for modeling the CFR of PLC and hybrid PLC-WLC channels; however, the edge effects between the polynomials covering consecutive frequency bands needs to be better addressed.

In order to introduce an enhanced version of the statistical modeling method introduced in [22, 50], this chapter applies splines to come up with the waveforms that represent the parameters of statistical distribution covering the whole frequency bandwidth, e.g., $f \in [0, B)$. Based on [22, 50], the enhanced statistical modeling method, may be organized into four steps. The first step covers the use of several statistical distribution, which are well-known in the telecommunication field as well as others that fulfill the support of the elements of the r.v. \mathbf{X} . The second step consists in applying well-established statistical criteria that are capable of informing the statistical distribution offering the best modeling. The third step focuses on a heuristic decision-making approach that choose the statistical distribution offering the best modeling. The last step refers to the use of spline techniques to obtain the waveforms of the parameters associated with the chosen statistical distribution in the frequency domain.

This chapter is organized as follows: Section 3.1 addresses the part of the proposed enhanced statistical modeling method that is responsible for finding the best statistical distribution to model each element of the r.v. \mathbf{X} . Section 3.2 derives the procedure to interpolate the parameters of the chosen statistical distributions by using the Spline technique. Section 3.3 presents a summary about this chapter.

3.1 FINDING THE BEST STATISTICAL DISTRIBUTIONS

Aiming to address the first two research questions exposed in Chapter 2, the statistical models of the magnitude and phase of a CFR related to PLC and PLC-WLC channels are devised. In this regard, let us assume that each element of the r.v. $\mathbf{X} \in \{|\mathbf{H}|, \Theta\}$ are independent distributed random variables. In other words, the joint distribution of the r.v. \mathbf{X} is the product of the individual distributions of all elements of this vector. Also, all elements of the r.v. \mathbf{X} are modeled by same the statistical distribution. The only and possible difference are the values of the parameters associated with the statistical

distribution applied to model the elements of the r.v. \mathbf{X} . This is an interesting approach to come up with simple statistical models for the r.v. \mathbf{X} that can be useful for performing theoretical analysis related to channel capacity, physical layer security, energy harvesting and cooperative communication, among others.

Based on the aforementioned assumptions, previous discussions and the use of a data set of CFR estimates, which were obtained from a measurement campaign, the statistical modeling may be interpreted as the search for statistical distributions offering the best fits to the majority of the elements of \mathbf{X} . As previously stated, it is important to emphasize that all elements of \mathbf{X} will be modeled with the same statistical distribution; however, with a different set of parameter values. It means that the type of statistical distribution together with its parameters are the modeling information for each element of the r.v. \mathbf{X} . In other words, the model is the chosen statistical distribution together with its parameter values for all elements of \mathbf{X} . Overall, the process of finding the best statistical models for the majority of the elements of the r.v. \mathbf{X} can be organized in three steps, detailed as follows:

- **Step #1:** Assume that the r.v. \mathbf{X} represents $|\mathbf{H}|$ or Θ . In sequel, model all elements of the r.v. \mathbf{X} with each statistical distributions belonging to a set of statistical distributions that addresses the characteristics of the elements of this r.v.. It is important to highlight that $|\mathbf{H}| \in \mathbb{R}_+^{N \times 1} | 0 \leq |H_k| \leq 1$ and $\Theta \in \mathbb{R}_+^{N \times 1} | 0 \leq \Theta_k \leq 2\pi$ determine the suitability of a set of statistical distributions for modeling the two types of the r.v. \mathbf{X} (i.e., $|\mathbf{H}|$ and Θ). Given the supports of the elements of the r.v. \mathbf{X} ($|\mathbf{H}|$ or Θ), it is clear that only statistical distributions covering positive values may apply.
- **Step #2:** Appraise the set of statistical distributions, for each element of the r.v. \mathbf{X} in order to select the best statistical distribution. For decision-making, apply the majority vote rule [60] in the values obtained by using the four statistical criteria: Maximum Likelihood Estimation (MLE), Akaike information criterion (AIC), Bayesian information criterion (BIC), and Efficient determination criterion (EDC) [16,61,62]. By considering MLE criterion, the best statistical modeling is the distribution that achieves the maximum value, whereas for the AIC, BIC, and EDC information criteria, the best modeling is the statistical distribution achieving the minimum value. It is important to emphasize that these criteria are well-established in the statistical literature because they offer quantitative and unbiased comparisons among distinct statistical distributions applied to model the elements of a r.v..
- **Step #3:** Find the statistical distribution yielding the best statistical model for the majority of the elements of the r.v. \mathbf{X} . It is important to note that the said distribution must achieve a minimum percentage ratio over the best results evaluated

on the MLE criteria, for the elements in which the distribution is not the best model, to be considered a valid model over the desired frequency band. This statistical distribution is then chosen as the statistical distribution for all elements of the r.v. \mathbf{X} . The set of parameters (i.e., $\mathcal{C}_{X_k} = \{\zeta_1[k], \dots, \zeta_U[k]\}$) associated with the chosen statistical distributions for the k^{th} element of the r.v. \mathbf{X} is obtained.

Algorithm 1 implements the aforementioned three steps of the enhanced statistical modeling method.

In order to visualize when an statistical distribution yields the best results in terms of the MLE criterion, the log-likelihood ratio expressed as

$$\rho_{MLE}[k] \triangleq \frac{\max_{\mathcal{A}} MLE(A, k)}{MLE(A, k)}, \quad (3.1)$$

is a useful parameter to be taken into account. Note that $MLE(A, k)$ is the value of the log-likelihood associated with the statistical distribution (A) belonging to the set of the chosen statistical distributions \mathcal{A} at the frequency tone k , while $\max_{\mathcal{A}} MLE(\mathcal{A})$ is the value of the log-likelihood related to the statistical distribution yielding the best statistical model. Note that the best results are achieved when $\rho_{MLE}(k) \rightarrow 1$. In addition, considering the continuous-time domain, then the log-likelihood ratio may be represented by

$$\rho_{MLE}(f) \triangleq \frac{\max_{\mathcal{A}} MLE(A, f)}{MLE(A, f)}. \quad (3.2)$$

3.2 INTERPOLATING THE PARAMETERS VALUES

In addition to finding the best statistical distribution that fits the elements of the r.v. \mathbf{X} , it is important to come up with the statistical model of the $H(f) = |H(f)| \exp[j\theta(f)]$, which is the continuous-time Fourier transform of the impulse responses of PLC or hybrid PLC-WLC channels in the continuous-time domain, $h(t)$, that is supposed to be time-invariant during a time interval shorter than T_c .

To do so, the use of a technique capable of yielding a suitable interpolation with a reduced number of parameters and without presenting edge effects, such as that ones reported in [50] is a very convenient solution. The standard interpolation technique based on the digital signal processing theory can be applied to obtain $H(e^{j\omega}) | -\infty < \omega < \infty$ from the vector \mathbf{H} but it demands a large number of parameters because all elements of the vector \mathbf{H} have to be considered for performing the interpolation [63]. Note that $H(e^{j\omega})$ is the discrete-time Fourier transform of the channel impulse response in the discrete-time domain, $h[n]$. At this time, it is important to emphasize that $h(t) \leftrightarrow H(f) = H(j\Omega)|_{\Omega=2\pi f}$ may be easily obtained from $H(e^{j\omega})$, see [63] for details. Based on the fact that the aim is to yield statistical models for the CFRs of PLC and hybrid PLC-WLC channels, the use

of a reduced set of parameters for performing the interpolation is valuable to facilitate the work of other researchers. In this context, the use of the Spline-based interpolation techniques emerges. In fact, this kind of technique can be applied to interpolate the values of the parameters of the statistical distribution chosen for each element of the r.v. \mathbf{X} .

Regarding the chosen statistical distribution, we can assume that $\zeta_u(\omega) = F_u(\omega; F_u(0), F_u(2\pi/N), \dots, F_u(2\pi(N-1)/N))$ in which $\omega \in [0, 2\pi)$ and $F_u(2\pi k/N) = \zeta_u[k], k = 0, 1, \dots, N-1$, represents the waveform associated with the u -th parameters belonging to the set $\{\zeta_u[0], \zeta_u[1], \dots, \zeta_u[N-1]\}$, which are obtained from the chosen statistical distributions of all elements of the r.v. \mathbf{X} . Note that its discrete-frequency representation is given by $\zeta_u[k] = F_u(\omega; F_u(0), F_u(2\pi/N), \dots, F_u(2\pi(N-1)/N))|_{\omega=2\pi k/N} = F_u[k; \zeta_u[0], \zeta_u[1], \dots, \zeta_u[N-1]], k = 0, 1, \dots, N-1$. In this context, this interpolation problem may be solved by finding an approximation polynomial $P_u(\omega)$ for the function $F_u(\omega)$ within the defined class of functions such that it can result in as close as possible values at the points $\omega_k = 2\pi k/N$ (i.e., $F_u(\omega_k) \approx P_u(\omega_k)$) for $k = 0, 1, \dots, N-1$.

The Lagrange Interpolation is the direct solution to obtain $P_u(\omega)$; however, the degree of the interpolating Lagrange polynomial is strictly related to the amount of points (nodes) $\omega_k = 2\pi k/N$, which makes the problems with high number of input data difficult to solve. Another interpolation technique that could be applied was discussed in [22, 50] but its efficiency may be limited because the edge effects occurrences in the boundaries between two polynomials, which are supposed to interpolate the values of the parameters in two consecutive frequency subbands. According to the literature, the use of Splines is very interesting approach to deal with this interpolating problem. Similar to [22, 50], the Spline-based interpolation technique divides the frequency band into $L_B \in \mathbb{N}$ nonuniform subbands, individually constructs the interpolating polynomial in the l -th subband, $P_{u,l}(\omega), l = 1, \dots, L_B$. In addition, it groups the resulting interpolating polynomials to obtain $P_u(\omega)$. A remarkable characteristic of the Splines is its capacity of avoiding the Runge's phenomenon.

It is well-known that there are several interpolation techniques based on Splines; however, this contribution makes a choice in favor of the cubic Splines [64] once that their characteristics of working with nonuniform frequency subbands, producing smoother curves, interpolating the boundaries of the subbands, and generating a continuous curve over the chosen frequency band are quite interesting for dealing the current problem.

Based on the aforementioned discussion, the Splines-based interpolation technique is covered by the fourth step of the enhanced statistical modeling method. Essentially, this step consists in the use of the cubic Splines over the parameters values of the chosen statistical distribution for interpolating purpose. A detailed description of the fourth step is as follows:

- **Step #4:** Interpolate the parameters in the previous step using the cubic Spline interpolation approximation for obtaining $\mathcal{C}_\omega = \{\zeta_1(\omega), \dots, \zeta_U(\omega)\}$. This procedure consists on dividing the desired frequency band into L subbands delimited by $\omega_{l,\text{lower}}$ and $\omega_{l,\text{upper}}$ bounds, and evaluating a third-degree polynomial that describes the l^{th} subband. Note that all subbands address $\omega \in [0, 2\pi)$ and the coefficients of the l^{th} polynomial are obtained for each subband following the procedure discussed in [65, 66].

The implementation of the fourth step of the enhanced statistical modeling method is detailed in Algorithm 2, which is based on [65, 66].

3.3 SUMMARY

This chapter has presented an enhanced statistical modeling method for CFR of PLC and hybrid PLC-WLC channels. In addition, the algorithms necessary for implementing it have been detailed.

Algorithm 1: Finding the best statistical distributions of the elements of the random vector $\mathbf{X} \in \{|\mathbf{H}|, \Theta\}$

- $\mathbf{M}_{\theta_m} \in \mathbb{R}^{N \times M \times P}$: it is the three-dimensional matrix of P unknown parameters from M distinct probability distributions associated with the elements of the random vector \mathbf{X} .
- $\mathbf{M}_H \in \mathbb{R}^{N \times M}$: it is the MLE matrix associated with the M probability distributions.
- $\mathbf{M}_A \in \mathbb{R}^{N \times M}$: it is the AIC matrix associated with the M probability distributions.
- $\mathbf{M}_B \in \mathbb{R}^{N \times M}$: it is the BIC matrix associated with the M probability distributions.
- $\mathbf{M}_E \in \mathbb{R}^{N \times M}$: it is the EDC matrix associated with the M probability distributions.
- $f(x, \theta_m)$: it is a parametric probability density function of a r.v. $X = x \in \mathbb{R}$, in which $\theta_m \in \mathbb{R}^{L \times 1}$ is the m^{th} parameter vector belonging to the matrix \mathbf{M}_θ .
- $\mathbf{v}_{\mathcal{P}^{k*}} \in \mathbb{N}^{N \times 1}$: it is the vector of chosen statistical distribution.
- $\mathbf{M}_{\theta^{k*}} \in \mathbb{N}^{N \times P}$: it is the matrix of parameters associated with the chosen statistical distribution.

Input:

$\mathbf{M}_X \in \mathbb{R}^{N \times L}$, in which $\mathbf{X} \in \{|\mathbf{H}|, \Theta\}$: it is the matrix constituted by L distinct \mathbf{X} vectors

$\mathcal{P} = \{\mathcal{P}_1, \dots, \mathcal{P}_M\}$: it is the set of M probability distributions

Output:

\mathcal{P}^{k*} = index of best evaluated distribution for magnitude, based on the chosen criteria

$\mathbf{M}_\theta \in \mathbb{R}^{U \times N}$ = the matrix of parameters associated with the best probability distributions

begin

Select the best distribution to model the r.v. \mathbf{X}

for $k = 1$ to N do

for $m = 1$ to M do

Step #1 Obtain the vector θ for the m^{th} probability distribution belonging to \mathcal{P} yielding the maximum MLE value:

$$M_{\theta_m}(k, m, :) = \arg \max_{\theta_m} \left(\sum_{l=1}^L \ln f \left(\sqrt{M_{\mathbf{X}}(k, l)}, \theta_m \right) \right)$$

Step #2 Evaluate the MLE, AIC, BIC and EDC

$$M_L(k, m) = \sum_{l=1}^L \ln f \left(\sqrt{M_{\mathbf{X}}(k, l)}, M_{\theta_m}(k, m, :) \right)$$

$$M_A(k, m) = -2M_L(k, m) + 2L$$

$$M_B(k, m) = -2M_L(k, m) + L \log_{10} N$$

$$M_E(k, m) = -2M_L(k, m) + 0.2L\sqrt{N}$$

end

Step #2 Choose the probability distribution based on the majority voting criterion (priority is given to MLE value)

$$[\mathbf{v}_{\mathcal{P}^{k*}}(k), M_{\theta^{k*}}(k, :)] = \text{majority_vote}(M_L(k, :), M_A(k, :), M_B(k, :), M_E(k, :))$$

end

Step #3 Select the statistical distribution with more occurrences

$$\mathcal{P}^{k*} = \text{choose_most_frequent}(\mathbf{v}_{\mathcal{P}^{k*}})$$

\mathcal{P}^{k*} becomes the chosen statistical distribution to all elements of r.v. \mathbf{X}

Parameters of the chosen statistical distributions are retrieved

for $k = 1$ to N do

$$M_\theta(:, k) = M_{\theta_m}(k, \mathcal{P}^{k*}, :)$$

end

end

Algorithm 2: Interpolation procedure to obtain $\alpha_l(\omega), l = 1, \dots, L$

- $l \in \mathbb{N} | l = 1, \dots, L$: it is the labels of the interpolation subbands
- $\omega_{l,\text{lower}} \in \mathbb{R}$: it is the lower bound of the interpolation subband
- $\omega_{l,\text{upper}} \in \mathbb{R}$: it is the upper bound of the interpolation subband
- $P_{u,l}(\omega) = \{a_{u,l}\omega^3 + b_{u,l}\omega^2 + c_{u,l}\omega + d_{u,l} | a_{u,l}, b_{u,l}, c_{u,l}, d_{u,l}, \omega \in \mathbb{R}, \omega_{l,\text{lower}} \leq \omega \leq \omega_{l,\text{upper}}\}$
- $\beta_l(\omega) \in \mathbb{R}$: it is the function of ω at the l^{th} subband mapped to $[0, 1]$
- $m_{l,\text{lower}(\omega)} \in \mathbb{R}$: it is the tangent evaluated at $\omega_{l,\text{lower}}$
- $m_{l,\text{upper}(\omega)} \in \mathbb{R}$: it is the tangent evaluated at $\omega_{l,\text{upper}}$

Input:

$\mathbf{v} \in \mathbb{R}^{(L+1) \times 1}$: it is the vector constituted by the bounds of the L interpolation subbands.

$\mathbf{M}_\theta \in \mathbb{R}^{U \times N}$: it is the matrix of parameters associated with the best probability distributions.

Output:

$\mathbf{M}_P \in \mathbb{R}^{4U \times L}$: it is the matrix constituted by the coefficients of polynomials $P_{u,l}(\omega)$ fitting the L interpolation subbands. U denotes the number of coefficients.

Step #4 Perform the interpolation

begin

for $u = 1$ **to** U **do**

for $l = 1$ **to** L **do**

lower and upper bounds:

$$\omega_{l,\text{lower}} = v_l$$

$$\omega_{l,\text{upper}} = v_{l+1}$$

Mapping ω to the interval $[0, 1]$:

$$\beta_l(\omega) = \frac{\omega - \omega_{l,\text{lower}}}{\omega_{l,\text{upper}} - \omega_{l,\text{lower}}}$$

evaluate the tangents $m_{l,\text{lower}}(\omega)$ and $m_{l,\text{upper}}(\omega)$:

$$m_{l,\text{lower}}(\omega) = \frac{1}{2} \left(\frac{M_\theta(u, \omega_{l,\text{upper}}) - M_\theta(u, \omega_{l,\text{lower}})}{\omega_{l,\text{upper}} - \omega_{l,\text{lower}}} \right) + \frac{1}{2} \left(\frac{M_\theta(u, \omega_{l,\text{lower}}) - M_\theta(u, v_{l-1})}{\omega_{l,\text{lower}} - v_{l-1}} \right)$$

$$m_{l,\text{upper}}(\omega) = \frac{1}{2} \left(\frac{M_\theta(u, v_{l+2}) - M_\theta(u, \omega_{l,\text{upper}})}{v_{l+2} - \omega_{l,\text{upper}}} \right) + \frac{1}{2} \left(\frac{M_\theta(u, \omega_{l,\text{upper}}) - M_\theta(u, \omega_{l,\text{lower}})}{\omega_{l,\text{upper}} - \omega_{l,\text{lower}}} \right)$$

Evaluate the 3rd-order polynomial for the l th interpolated subband $[\omega_{l,\text{lower}}, \omega_{l,\text{upper}}]$:

$$P_{u,l}(\omega) = (2\beta_l(\omega)^3 - 3\beta_l(\omega)^2 + 1)M_\theta(u, \omega_{l,\text{lower}}) + (\beta_l(\omega)^3 - 2\beta_l(\omega)^2 + \beta_l(\omega))(\omega_{l,\text{upper}} - \omega_{l,\text{lower}})m_{l,\text{lower}}(\omega) + (-2\beta_l(\omega)^3 + 3\beta_l(\omega)^2)M_\theta(u, \omega_{l,\text{upper}}) + (\beta_l(\omega)^3 - \beta_l(\omega)^2)(\omega_{l,\text{upper}} - \omega_{l,\text{lower}})m_{l,\text{upper}}(\omega)$$

Store the Coefficients of $P_{u,l}(\omega)$:

$$M_P(1 + 4(u - 1), l) = a_{u,l}$$

$$M_P(2 + 4(u - 1), l) = b_{u,l}$$

$$M_P(3 + 4(u - 1), l) = c_{u,l}$$

$$M_P(4 + 4(u - 1), l) = d_{u,l}$$

end

end

end

4 NUMERICAL RESULTS

This chapter focuses on the statistical analyses covered by the proposed technique in Chapter 3 to numerically introduce random process models for the measured CFRs of in-home PLC and hybrid PLC-WLC channels. In this context, a systematic presentation of these analyses is as follows: Section 4.1 describes details about the data sets used in the numerical analyses and the adoptions for carrying out the numerical analyses. Section 4.2 addresses the results of CFR modeling of PLC channels. Section 4.3 focuses on CFR modeling of hybrid PLC-WLC channels in the *short-path* scenario while Section 4.4 discusses the results related to hybrid PLC-WLC channels in the *long-path* scenario. Section 4.5 addresses a brief summary on this chapter.

4.1 SIMULATIONS DESCRIPTIONS

The statistical analyses are performed by means of two data sets constituted by CFR estimates of in-home PLC and hybrid PLC-WLC channels, which were acquired through a measurement campaign detailed in [33] and [46], and summarized in Appendix A. These data sets cover the frequency band between 1.7 and 100 MHz. Regarding the PLC portion of the measurement campaign, a total of 245 different combinations of outlets pairs were measured, allowing the acquisition of 148,037 different CFR estimates, with approximately 604 consecutive CFR estimates for each individual measure. The methodology applied to obtain the CFR estimates is the one discussed in [67] and it relies on a measurement setup based on the HS-OFDM scheme [68, 69]. Note that the HS-OFDM scheme is a kind of sounding technique for estimating CFR in the discrete-time domain when the data communication channel is in the baseband. This scheme estimates CFR of in-home PLC channels by encompassing offset correction [70], timing synchronization [71], CFR estimation [67], and enhancement of CFR estimates [72, 73]. After applying the aforementioned techniques, the average of $L_1 \in \mathbb{N}_+$ consecutive CFR estimates is obtained, respecting the coherence time of the PLC channel, and then stored as a valid CFR of PLC channel estimate. This last step is applied aiming to reduce the noise influence on the CFR estimates. It is important to emphasize that the measurement setup covers signal generation and acquisition boards, rugged computers and coupling devices [50, 74].

Considering the hybrid PLC-WLC portion of the measurement campaign, 293 different combinations of locations for both hybrid-PLC and hybrid-Wireless transceivers were evaluated. As a result, a total of 175,428 different CFR estimates were acquired, with approximately 600 consecutive CFR estimates for each individual channel acquisition. Two different cases were considered during the measurement campaign, named *short-path channel* and *long-path channel*, respectively. Regarding the *short-path channel*, the

WLC transceiver was randomly positioned within a 2 m radius circle centered at the outlet in which the PLC transceiver was connected, this scenario was responsible for estimating around 136,683 CFRs in 200 different combinations of locations for both PLC and WLC transceivers. On the other hand, in the *long-path* channel scenario, the WLC transceiver was randomly placed into an area defined as a swept circle, having an outer and inner radius of 6 m and 2 m, respectively, centered in the outlet in which the PLC transceiver was connected. This case allowed to obtain 38,745 CFR estimates in 93 different combinations of locations for both PLC and WLC transceivers. Similarly to the PLC measurement campaign described before, the channel estimation methodology applied to obtain the CFR estimates was the one discussed in [67]. The measurement setup was also similar, composed of signal generation and acquisition boards, rugged computers, a coupling device [50] for the PLC transceiver and an antenna for the WLC transceiver. Once more, the HS-OFDM scheme [68,69] was used for estimating the CFR of in-home hybrid PLC-WLC channels. Finally, after applying the aforementioned scheme, averages of $L_2 \in \mathbb{N}_+$ and of $L_3 \in \mathbb{N}_+$ consecutive CFR estimates were obtained, for the *short-path* and *long-path* channels respectively, respecting the coherence time of hybrid PLC-WLC channels in their corresponding scenarios. The obtained estimates were stored as valid CFRs of hybrid PLC-WLC channels. Similar to the PLC channel, this last step was applied for reducing the noise influence on the CFR estimates.

It is important to emphasize that one CFR estimate is obtained during a time interval corresponding to one HS-OFDM symbol period (T_{sym}) duration and, as a consequence, it assumes that the time interval duration of the HS-OFDM symbol must be shorter than the coherence time of the PLC or hybrid PLC-WLC channel. Based on the set of parameters of the estimation technique, an enhanced channel estimate is obtained every $T_{\text{sym}} = (2N + L_{cp})T_s = 23.04 \mu\text{s}$, where $N = 2048$ is the number of binary phase shift keying (BPSK) modulated subcarriers of the HS-OFDM symbol, $L_{cp} = 512$ samples is the length of the so-called cyclic prefix (CP), $f_s = 200 \text{ MHz}$ is the sampling rate and $T_s = 1/f_s = 5 \text{ ns}$ is the sampling period. According to [75], $600 \mu\text{s}$ is the minimum time period within which the in-home PLC channel can be considered time invariant in Spain, while [33] pointed out $950 \mu\text{s}$ for the Brazilian in-home PLC channels. In addition, [46] shows that $156 \mu\text{s}$ and $39.5 \mu\text{s}$ are the minimum time period within which the in-home hybrid PLC-WLC *short-path* and *long-path* channels, respectively, can be considered time invariant.

Regardless of the location and communication media, the time interval duration of each CFR estimation (T_{sym}) complies with the coherence time and, as a consequence, we can take it as an advantage to reduce the noise impulsiveness influence on the CFR estimates, with exception of the *long-path* channel case in the hybrid PLC-WLC scenario because of its short coherent time. The attenuation of noise influence is accomplished by taking the average of $L_1 = 10$, $L_2 = 5$ and $L_3 = 1$ consecutive CFR estimates within the

coherence time of PLC channel, PLC-WLC *short-path* and PLC-WLC *long-path* channels, respectively.

Moreover, the assumed value of N and the chosen frequency band (1.7–100) MHz, results in CFR estimates with a corresponding frequency resolution of $\Delta f = 48.83$ kHz, which is shorter than the coherence bandwidth of Brazilian and Spanish in-home PLC channels [33, 75] as well as shorter than the coherence bandwidth of Brazilian in-home hybrid PLC-WLC channels [46]. Being shorter than the coherence bandwidth means that each sample of a valid CFR estimates is representative for carrying out the statistical analyses. Furthermore, for sake of clearness, all numerical results are presented in the continuous-time domain rather than the discrete-time one.

In order to perform the statistical analyses of the valid CFR of PLC and hybrid PLC-WLC channels, the following statistical distributions were adopted: Beta, Birnbaum-Saunders, Gamma, Logistic, Log-normal, Normal, Rayleigh, Rician, t Location-Scale, and Uniform. These statistical distributions cover the well-established ones in the telecommunication field and apply to model a random variable belonging to \mathbb{R}_+ . Regarding the valid CFR phase, the Beta, Logistic, Normal, t Location-Scale and Uniform distributions were considered. As described in Chapter 3, once the best statistical distribution for modeling the valid CFR magnitudes and phases are chosen, the parameters defining the statistical distributions are used for performing the interpolation by using the cubic Splines and, as a consequence, generating a continuous waveform in the frequency domain. This procedure is performed individually over each parameter of the statistical distributions along the frequency domain. In order to apply the interpolation technique based on the cubic Splines, L_b samples of the CFR estimates, which are related to frequencies located in the frequency band (1.7 – 100 MHz), were heuristically chosen as frontiers/edges of the subbands, resulting in $L = L_b - 1$ subbands, to be interpolated by the cubic Splines. This heuristic approach was adopted because it could result in subband bandwidth in which the use of the third-order (cubic) Splines is satisfactory. Note that the number of subbands was carefully chosen by adopting a procedure consisting in the generation of nonuniform (random) spacing among L_b edges, which were initially linearly spaced along the desired frequency band. Based on previous quantitative investigation of the number of edges/frontiers, $L_b \in \mathbb{N} | L_b = 10, 11, 12, \dots 50$ was chosen as the number of edges/frontiers. In order to quantitatively evaluate the suitability of the approximation carried out over the chosen number of subbands, the mean squared error (MSE) value was considered. In accordance with the literature, MSE can be given by

$$MSE = \frac{1}{N} \sum_{k=0}^{N-1} (\zeta_u(2\pi k/N) - \zeta_u[k])^2, \quad (4.1)$$

in which $\zeta_u(2\pi k/N) = \zeta_u(\omega)|_{\omega=2\pi k/N}$ and $\zeta_u[k]$ are the parameters value outputted by **Step #3** (see Section 3.1). For presenting the results related to the choice of subbands,

a Monte Carlo simulation composed of 3000 sample for each value of L_b was carried out for generating the expected value of the MSE. The number of subbands is chosen based on the MSE value. Finally, but not the least, the feasibility of the number of subbands is associated with the computational complexity for obtaining all polynomials.

4.2 UNCORRELATED CFR MODEL OF PLC CHANNELS

In this section, the statistical modeling of the valid CFRs data set related to in-home PLC channels, which were acquired through the measurement campaign, described in [33], is presented. For illustrative purpose, Fig. 4 portrays five valid and consecutive estimates of the CFR magnitude. Each valid CFR estimate was obtained by averaging L_1 consecutive CFR estimates of the PLC channel associated with an in-home electric power circuit, which was measured during the measurement campaign. Note that the PLC channel attenuation ranges from approximately -30 dB up to 0 dB. In addition, these plots shows that in-home PLC channels present a small time-varying behavior during a time interval shorter than 1 ms once each valid CFR estimate covers a time interval equal to $\Delta T = L_1 T_{\text{sym}} \approx 230.4 \mu\text{s}$ and, as a consequence, $5\Delta T = 1.15$ ms.

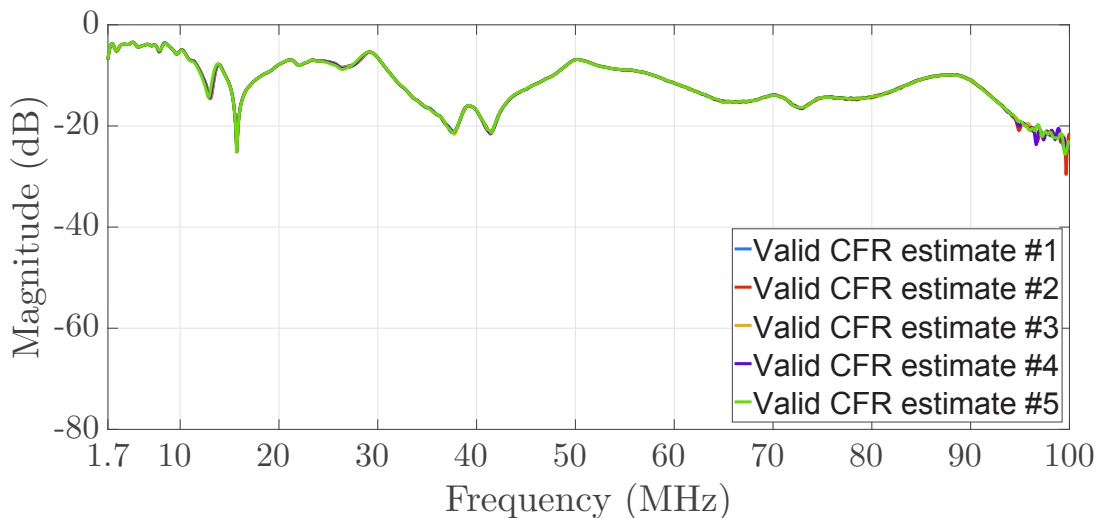


Figure 4: Five consecutive and valid CFR Magnitudes of the measured in-home PLC channel.

Fig. 5 illustrates the relative frequency of statistical distributions that had modeled, in accordance with the adopted criteria, the magnitude of the whole data set of valid CFR estimates. It is noted that there is not only a single distribution that models the majority of the magnitudes, but three different statistical distributions that stand out as possible candidates to model the CFR magnitudes, among the chosen statistical distributions. As a matter of fact, in 35% of the CFR estimates data set the Beta distribution resulted in the best model, in 30% of it the Birnbaum-Saunders distribution offered the best modeling and in 24% of it the Log-normal distribution yielded the best modeling.

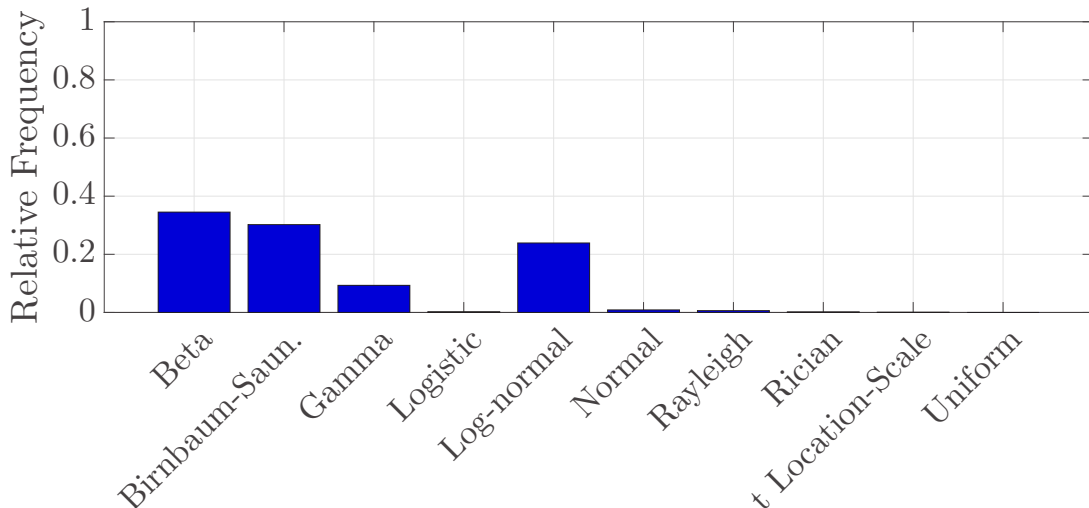


Figure 5: The relative frequency associated with the chosen statistical distribution that best models the CFR magnitude in accord with the adopted criteria.

In order to evaluate which of the three statistical distributions is the best choice for modeling the magnitude of the CFR estimates, we use the log-likelihood ratio $\rho_{MLE}(f)$ (3.2) as defined in subsection 3.1, where the set of statistical distribution is denote by $\mathcal{A} \in \{\text{Beta, Birnbaum-Saunders, Gamma, Logistic, Log-normal, Normal, Rayleigh, Rician, } t \text{ Location-Scale, Uniform}\}$. It is important to emphasize that the choice of $\rho_{MLE}(f)$ is for illustrating the results in continuous-time domain. Fig. 6 shows the values of $\rho_{MLE}(f)$ for the three best statistical distributions candidates to model the magnitude of the valid CFR estimates. The threshold value 1.2, corresponding to a deviation of 20% from the best achievable result, was heuristically chosen as the upper bound, indicated by a red dashed line, under which the statistical distribution can be considered good enough to model the CFR of in-home PLC channels. Note that the vertical axis was limited to the range between 0 and 5.0 to facilitate the visualization and the comparison among the log-likelihood ratio ($\rho_{MLE}(f)$) curves. These curves emphasize the suitability of the Beta distribution to model the samples of the magnitude of the valid CFR estimates. Overall, the results showed in Fig. 5 and Fig. 6 strongly suggest the use of the Beta distribution to model the magnitude of the valid CFR estimates of the measured in-home Brazilian PLC channels. In other words, the magnitude of the valid CFR estimates of in-home PLC channels can be modeled by using only one statistical distribution (i.e., the Beta distribution).

The statistical analysis of the magnitude of the valid CFR estimates shows that the parameters of the Beta distribution assume different values as frequency changes. If $\mathcal{C}_k = \{\zeta_1[k], \zeta_2[k]\}$ is the set of parameters for the statistical distribution modeling the magnitude of the valid CFR estimates of in-home PLC channels, where $k = 0, 1, \dots, N - 1$, $\zeta_1[k] = \alpha[k]$ and $\zeta_2[k] = \beta[k]$, are the two shape parameters ($U = 2$) of the Beta distribution associated with the k -th sample of the valid CFR in the discrete-time domain.

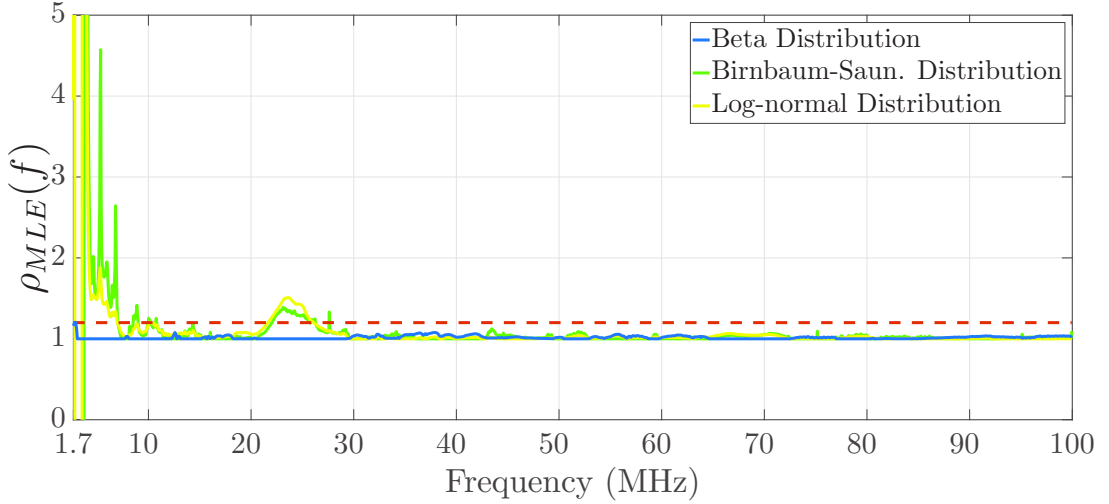


Figure 6: The log-likelihood ratio for the following statistical distributions: Beta, Birnbaum-Saunders, and Log-normal.

Then, Fig. 7 and Fig. 8 portrays the statistical models for two different values of frequency: $f = 52.1$ MHz ($k = 1067 \rightarrow f = 1067\Delta f$) and $f = 78.1$ MHz ($k = 1600 \rightarrow f = 1600\Delta f$), respectively. The parameters of the Beta distribution are $\alpha(1067\Delta f) = \zeta_1[1067] = 0.717$ and $\beta(1067\Delta f) = \zeta_2[1067] = 10.435$; $\alpha(1600\Delta f) = \zeta_1[1600] = 0.780$ and $\beta(1600\Delta f) = \zeta_2[1600] = 17.772$ for $f = 52.1$ MHz and $f = 78.1$ MHz, respectively.

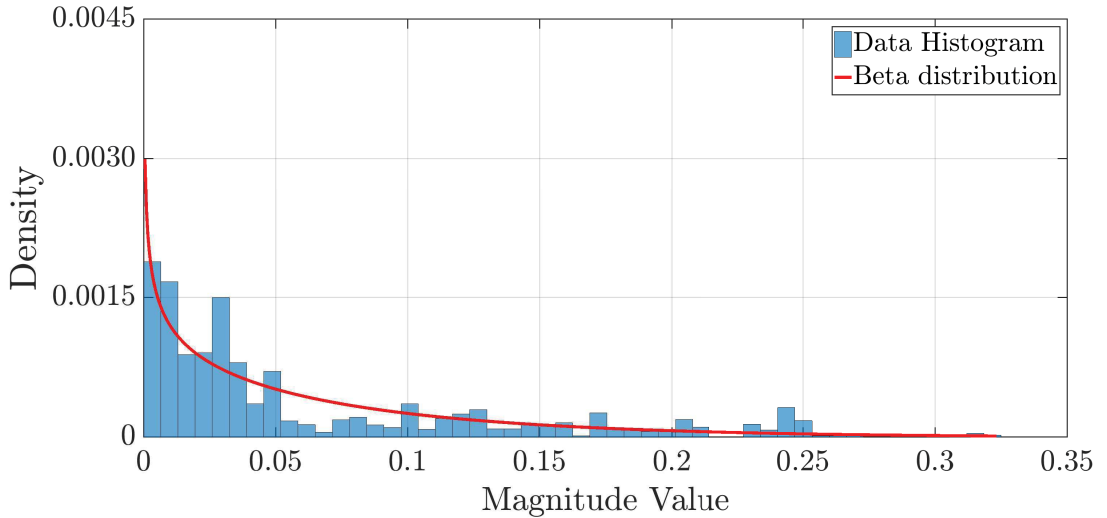


Figure 7: The relative frequency of the magnitude of the valid CFR estimates at the sample $k = 1067$ ($k\Delta f = 52.1$ MHz) and the modeling based on the Beta distribution.

Fig. 9 illustrates the MSE results in terms of the number of subbands for the in-home PLC channels. According to this plot, independent of the chosen criterion to select the non-uniformity of the subbands, the MSE value does not change significantly as the number of subbands becomes higher than 19. Due to a trade off between the precision of the interpolation and complexity of the computation, $L = 19$ was chosen as the number of subbands. By interpolating the parameters values $\alpha[k]$ and $\beta[k]$ of the Beta distributions

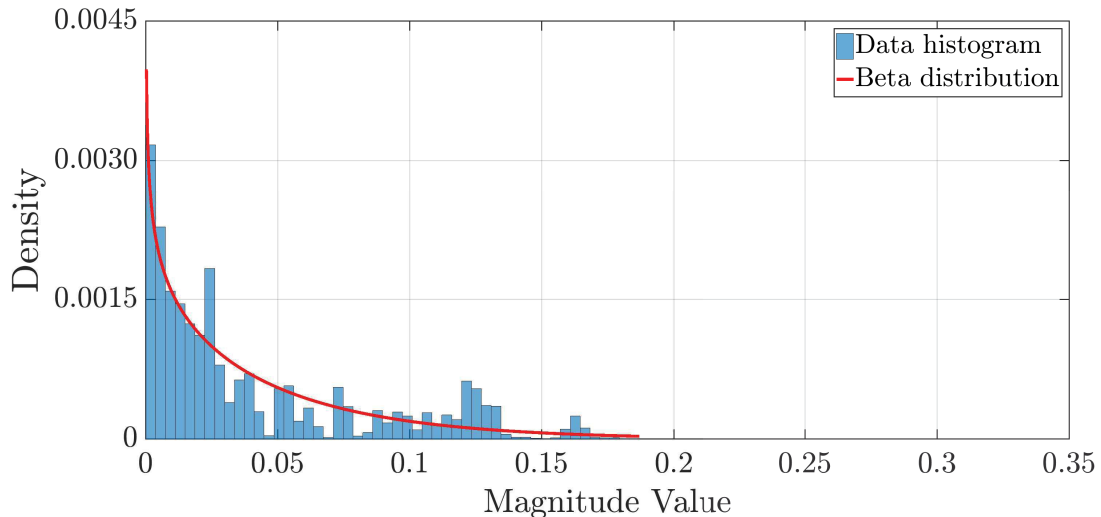
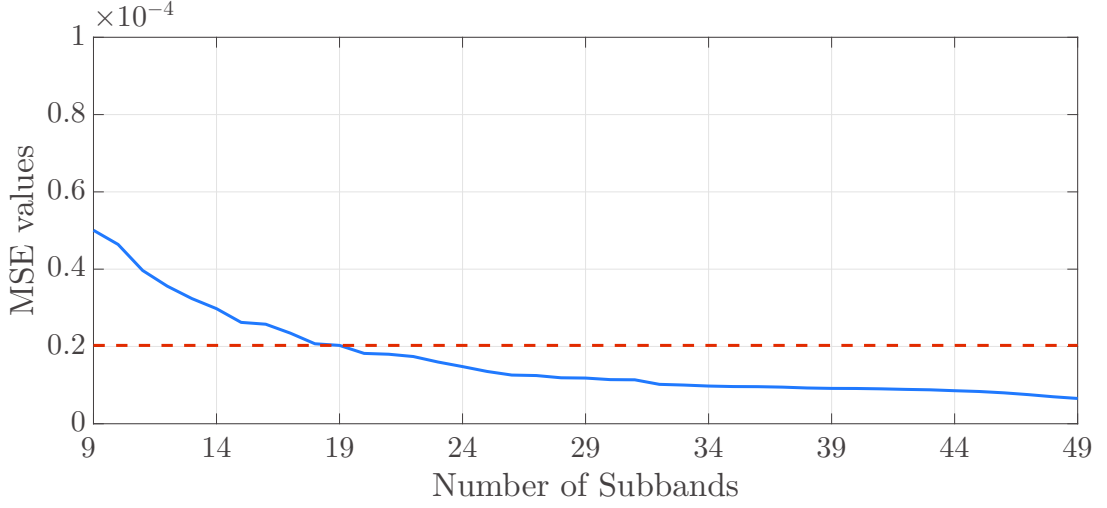


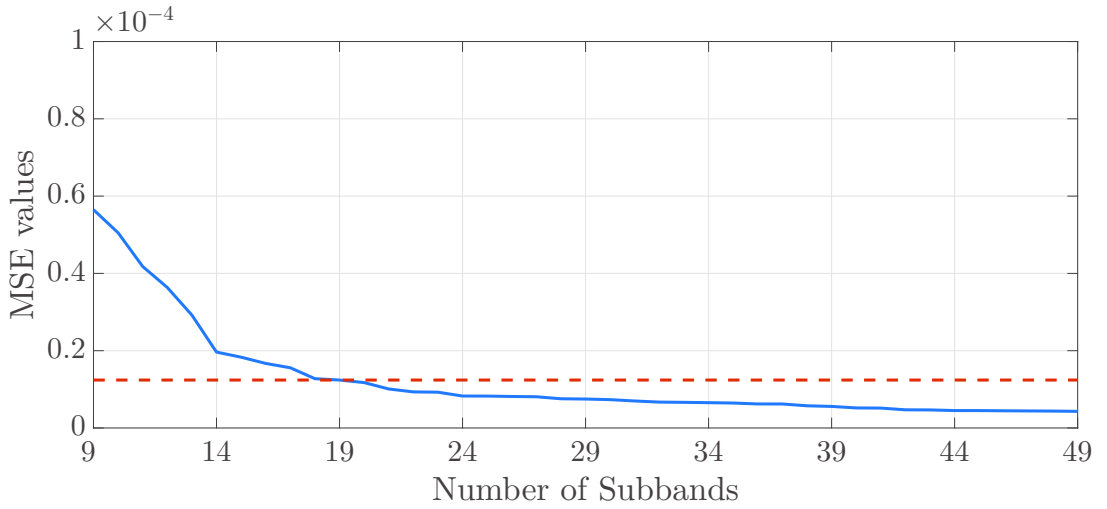
Figure 8: The relative frequency of the magnitude of the valid CFR estimates at the sample $k = 1600$ ($k\Delta f = 78.1$ MHz) and the modeling based on the Beta distribution.

using $L = 19$ subbands and the Algorithm 2, the continuous curves of parameters $\hat{\alpha}(\omega)$ and $\hat{\beta}(\omega)$ are yielded. Finally, the curves $\hat{\alpha}(f)$ and $\hat{\beta}(f)$ are easily obtained because $\omega \in [0, \pi]$ directly corresponds to the frequency band between 0 and 100 MHz. Figs. 10 and 12 illustrates the curves for the parameters $\alpha(f)$ and $\beta(f)$, which are obtained by applying frequency domain interpolation technique detailed in [63] and the curves obtained by using the cubic Spline interpolation with $L = 19$ subbands. For the sake of comparison Fig. 11 shows the curves for parameter $\alpha(f)$ obtained, by applying the frequency domain interpolation technique detailed in [63] and by using the interpolation technique discussed in [50] applied over $L = 19$ subbands denoted by 20 equally spaced interval bounds, over the desired frequency bandwidth. On this figure is possible to notice the presence of edge effects that occurs in the boundaries between two polynomials, which are interpolating the values of the parameters in two consecutive frequency subbands. Note that Table 2, in Appendix B, lists the cubic Spline coefficients for modeling the parameter $\alpha(f)$ of the valid CFR magnitude while Table 3, also in Appendix B, lists the cubic Spline coefficients for modeling the parameter $\beta(f)$. As a result, the Beta distribution and its coefficients waveform $\hat{\alpha}(f)$ and $\hat{\beta}(f)$ define the random process representing the magnitude of the CFR of the in-home PLC channel.

Fig. 13 portrays the relative frequency of statistical distributions that had modeled, in accordance with the adopted criteria, the phase of the whole set of valid CFR estimates. Note that 100% of the data set is best modeled by the Uniform distribution. On this scenario, differently from the statistical modeling of the CFR magnitude, the statistical modeling of the phase of the valid CFR estimates illustrates that each sample of it can be modeled by the same set of parameters of the Uniform distribution. In other words, $\Theta_k \in [0, 2\pi]$ denotes the interval of values that the phase of the valid CFR estimates can assume and it defines the support for the Uniform distribution.



(a)



(b)

Figure 9: The MSE values for the parameters from PLC scenario: (a) α parameter, (b) β parameter.

Fig. 14 and Fig. 15 portrays the statistical models regarding the frequencies $f = 52.1$ MHz ($k = 1067 \rightarrow f = 1067\Delta f$) and $f = 78.1$ MHz ($k = 1600 \rightarrow f = 1600\Delta f$), respectively. Independent of the frequency values, the phase model of the valid CFR estimates remains the same. As a result, by using the Uniform distribution defined in the interval $[0, 2\pi]$, the random process representing the phase of the CFR of the in-home PLC channel is yielded.

In summary, the use of the proposed enhanced statistical modeling method, see Chapter 3, for modeling the CFR of in-home PLC channels showed that its magnitude can be modeled by the Beta distribution, with parameters value changing as the frequency varies. As a result, the magnitude function of CFR of in-home PLC channels is a non-stationary random process. This result is different from previous works that had suggested the Log-normal or Rayleigh distributions, with fixed parameters values, to model this

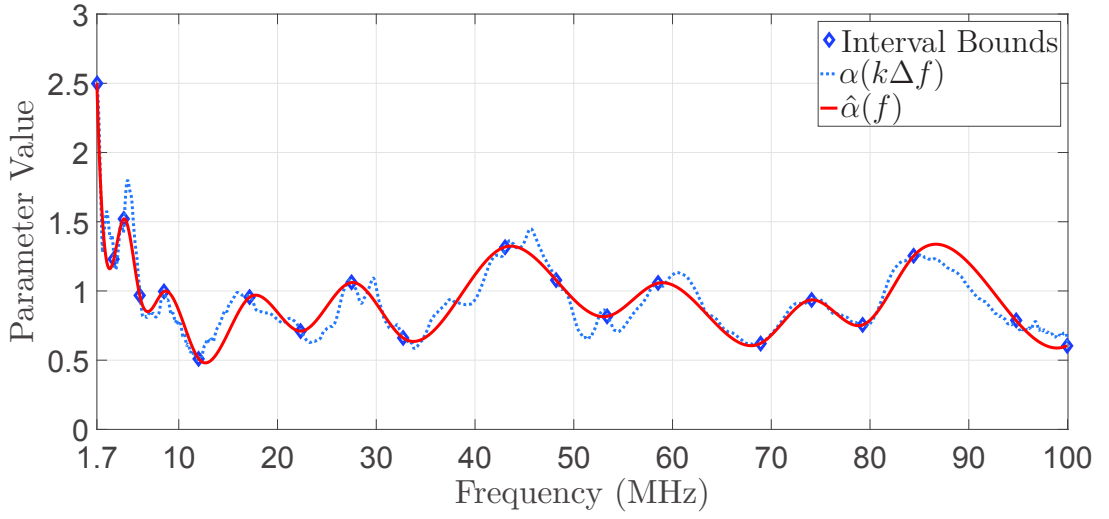


Figure 10: The result of the interpolation technique based on cubic Splines applied to obtain $\alpha(f) = \zeta_1(f)$ for the Beta distribution ($\alpha(k\Delta f)$ are the original values of the parameter and $\hat{\alpha}(f)$ is the interpolated curve).

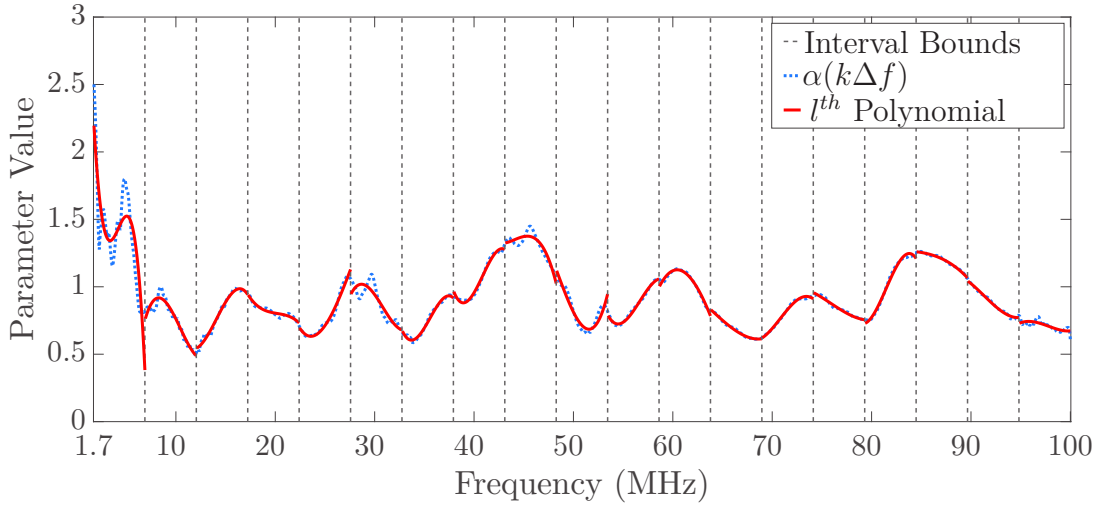


Figure 11: The result of the interpolation technique based on cubic Splines applied to obtain $\alpha(f) = \zeta_1(f)$ for the Beta distribution ($\alpha(k\Delta f)$ are the original values of the parameter and $\hat{\alpha}(f)$ is the interpolated curve).

magnitude, see [20,76]. In other words, the attained results for the Brazilian in-home PLC channels shows that previous statistical modeling may not be suitable for the Brazilian residences. The statistical analyses has also verified that the phase component of in-home PLC channels can be modeled by the Uniform distribution with fixed parameters as frequency varies, thus denoting that the phase function of CFR of in-home PLC channels is a stationary random process.

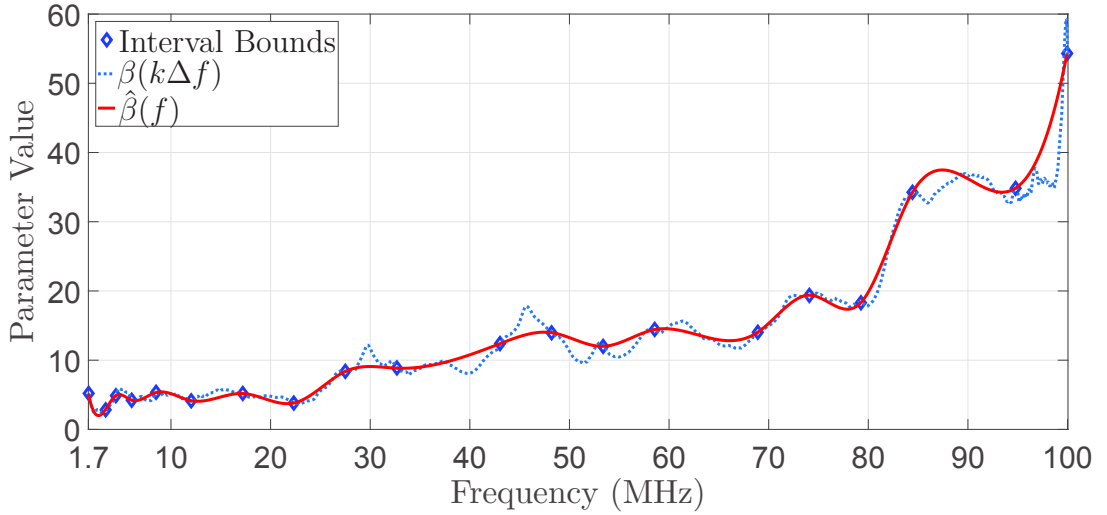


Figure 12: The result of the interpolation technique based on cubic Splines applied to obtain $\beta(f) = \zeta_2(f)$ for the Beta distribution ($\beta(k\Delta f)$ are the original values of the parameter and $\hat{\beta}(f)$ is the interpolated curve).

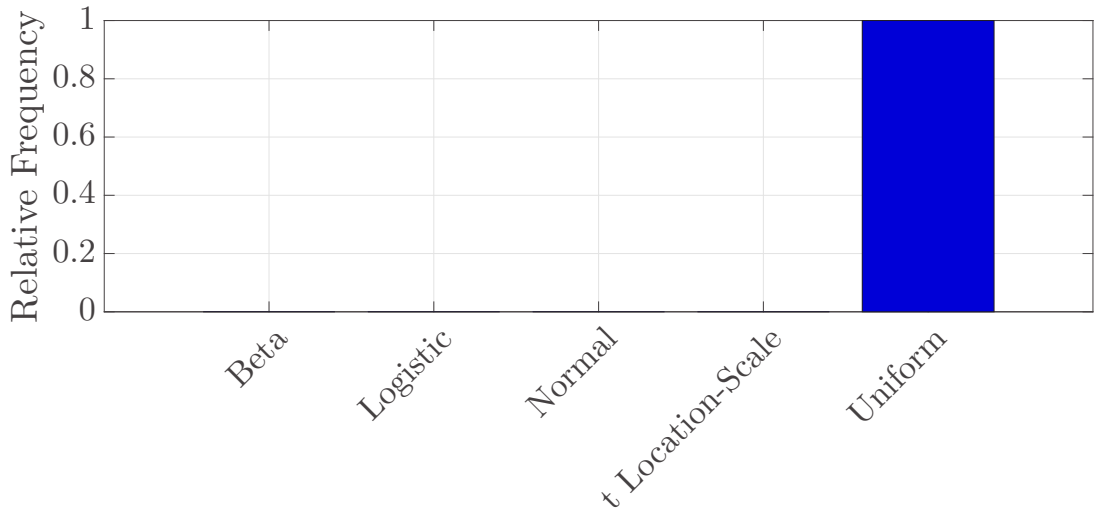


Figure 13: The relative frequency associated with the chosen statistical distribution that best models CFR phase in accord with the adopted criteria.

4.3 UNCORRELATED CFR MODEL OF HYBRID PLC-WLC *SHORT-PATH* CHANNELS

This section outlines the modeling of the valid CFRs data set related to in-home hybrid PLC-WLC *short-path* channels, which were acquired through the measurement campaign described in [46]. Fig. 16 portrays five valid and consecutive estimates of the CFR magnitude. Each valid CFR estimate was obtained by averaging L_2 consecutive CFR estimates of the hybrid PLC-WLC *short-path*. Note that the channel attenuation ranges from approximately -40 dB up to -10 dB and, in addition, a small time-varying behavior during a time interval shorter than $550\mu\text{s}$ is observed, once each valid CFR estimate covers a time interval equal to $\Delta T = L_2 T_{sym} \approx 115.2\mu\text{s}$ and, as a consequence,

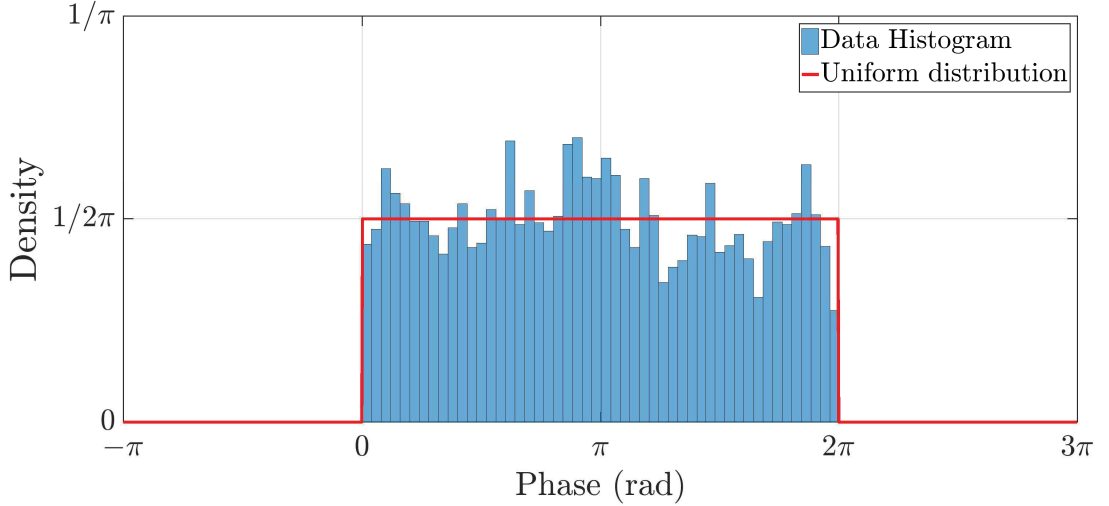


Figure 14: The relative frequency of the phase of the valid CFR estimates at the sample $k = 1067$ ($k\Delta f = 52.1$ MHz) using the Uniform distribution.

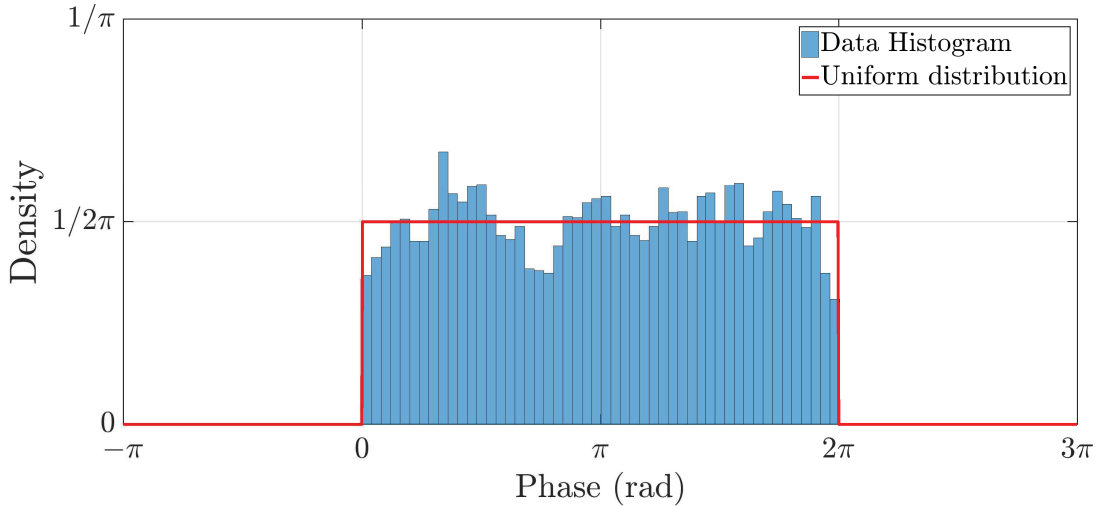


Figure 15: The relative frequency of the phase of the valid CFR estimates at the sample $k = 1600$ ($k\Delta f = 78.1$ MHz) using the Uniform distribution.

$$5\Delta T = 576\mu\text{s}.$$

Fig. 17 illustrates the relative frequency of statistical distributions that had modeled the magnitude of the hybrid PLC-WLC *short-path* CFR estimates. On these plots, it is noticeable a statistical distribution that models the majority of the magnitudes, once that in 54% of the CFR estimates the Log-normal distribution resulted in the best model. However, another different statistical distribution stand out as possible candidate to model the CFR magnitudes, since in 30% of the CFR estimates, the Gamma distribution offered the best modeling.

Similarly to subsection 4.2, the log-likelihood ratio $\rho_{MLE}(f)$ (3.2) was used in order to evaluate which of the two distributions is the best choice to model the magnitude component of the CFR estimates. Fig. 18 shows the values of $\rho_{MLE}(f)$ for the two best

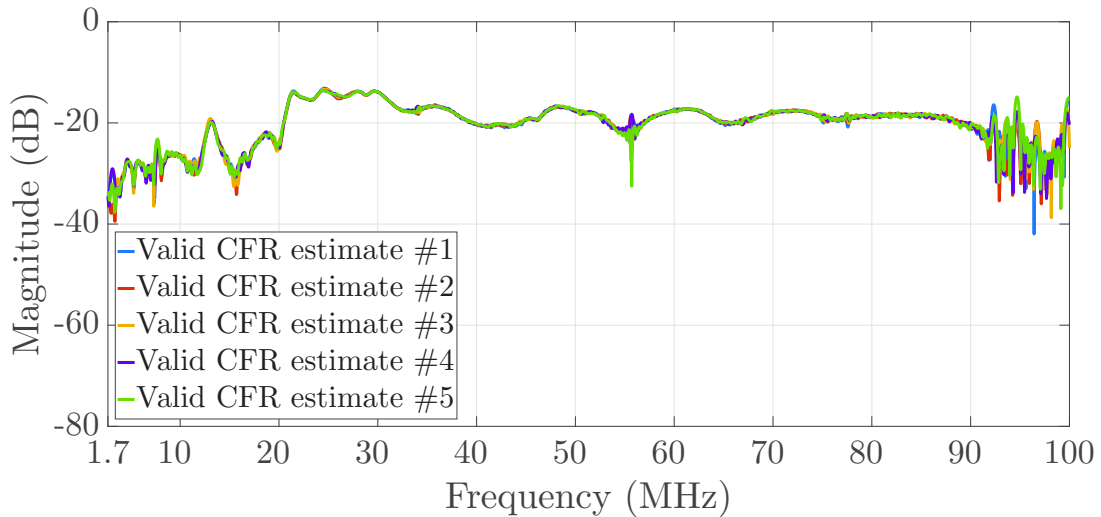


Figure 16: Five consecutive and valid CFR Magnitudes of the measured in-home PLC channel.

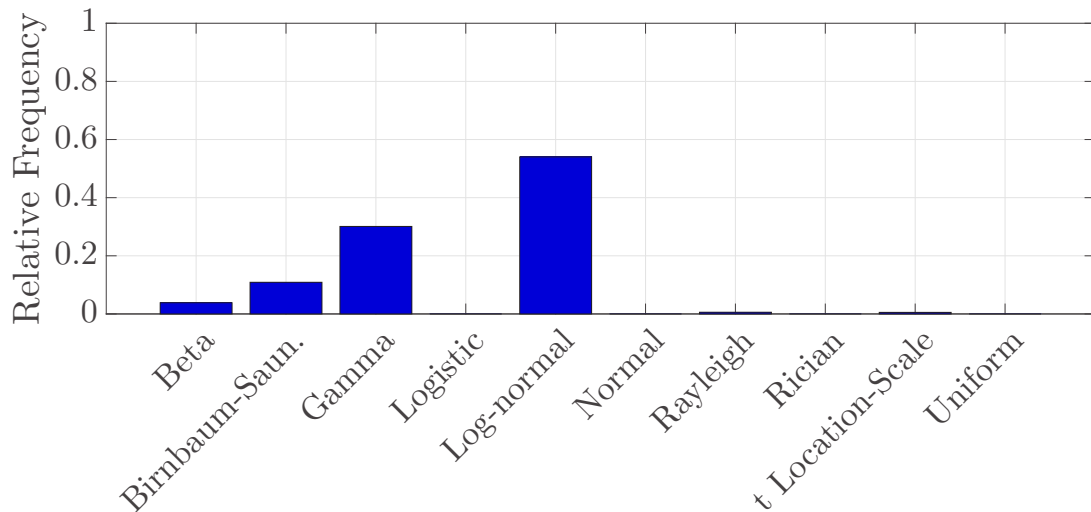


Figure 17: The relative frequency associated with the chosen statistical distribution that best models the CFR magnitude in accord with the adopted criteria.

statistical distributions candidates to model the magnitude of the valid CFR estimates. Once again a red dashed line was used to indicate the threshold value of 1.2, under which the statistical distribution can be considered good enough to model the magnitude of CFR. These curves emphasize that both Log-normal and Gamma distributions achieved the minimum ratio over the MLE criteria, in this scenario, the Log-normal distribution was chosen due to its greater occurrence as the best model for the PLC-WLC *short-path* CFR magnitudes, as portrayed in Fig. 17. In other words, the magnitude of the valid CFR estimates of in-home hybrid PLC-WLC *short-path* channels is modeled by using only one statistical distribution (i.e., the Log-normal distribution).

The statistical analysis of the magnitude of the valid PLC-WLC *short-path* CFR estimates showed that the parameters of the Log-normal distribution assume different

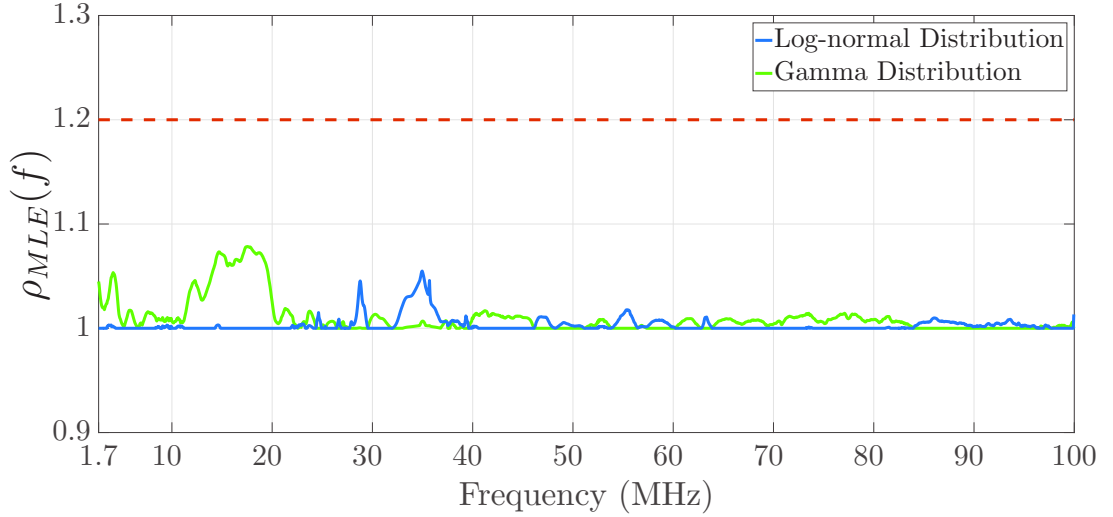


Figure 18: The log-likelihood ratio for the following statistical distributions: Log-normal, Gamma.

values as frequency changes. If $\mathcal{C}_k = \{\zeta_1[k], \zeta_2[k]\}$ is the set of parameters for the statistical distribution modeling the magnitude of the valid CFR estimates of PLC-WLC *short-path* channels, where $k = 0, 1, \dots, N - 1$, $\zeta_1[k] = \mu[k]$ and $\zeta_2[k] = \sigma[k]$, are the two parameters ($U = 2$) of the Log-normal distribution, named mean and standard deviation respectively, associated with the k -th sample of the valid CFR. Then, Fig. 19 and Fig. 20 illustrates the statistical models for two different values of frequency: $f = 50.78$ MHz ($k = 1040 \rightarrow f = 1040\Delta f$) and $f = 80.57$ MHz ($k = 1650 \rightarrow f = 1650\Delta f$), respectively. The parameters of the Log-normal distribution are $\mu(1040\Delta f) = \zeta_1[1040] = -4.0117$ and $\sigma(1040\Delta f) = \zeta_2[1040] = 0.5903$; $\mu(1650\Delta f) = \zeta_1[1650] = -5.034$ and $\sigma(1650\Delta f) = \zeta_2[1650] = 0.82$ for $f = 50.78$ MHz and $f = 80.57$ MHz, respectively.

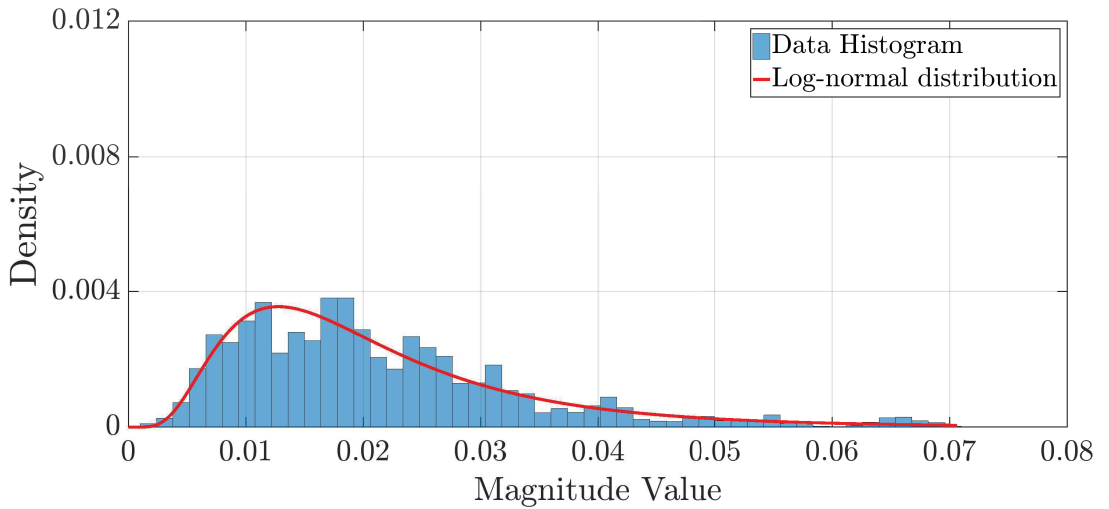


Figure 19: The relative frequency of the magnitude of the valid CFR estimates at the sample $k = 1040$ ($k\Delta f = 50.78$ MHz) and the modeling based on the Log-normal distribution.

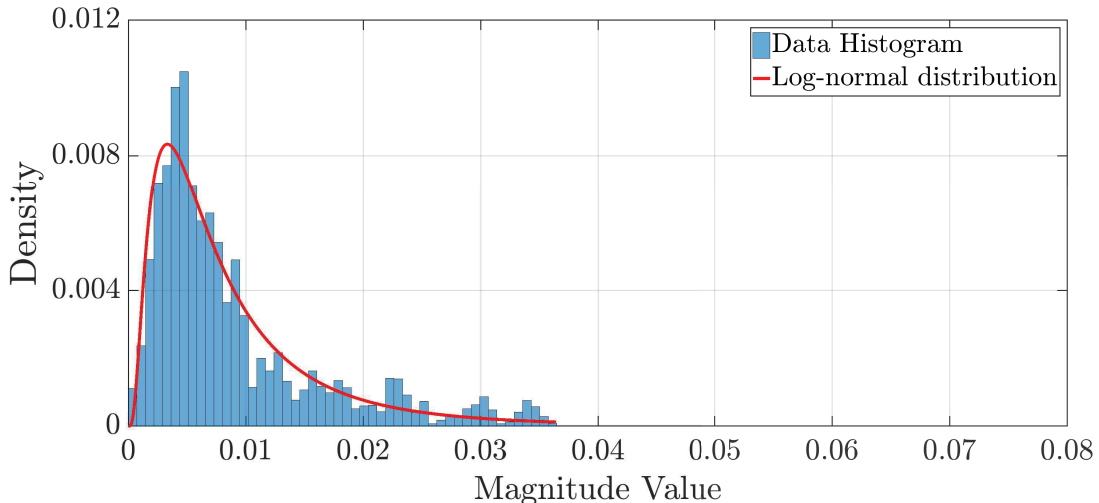
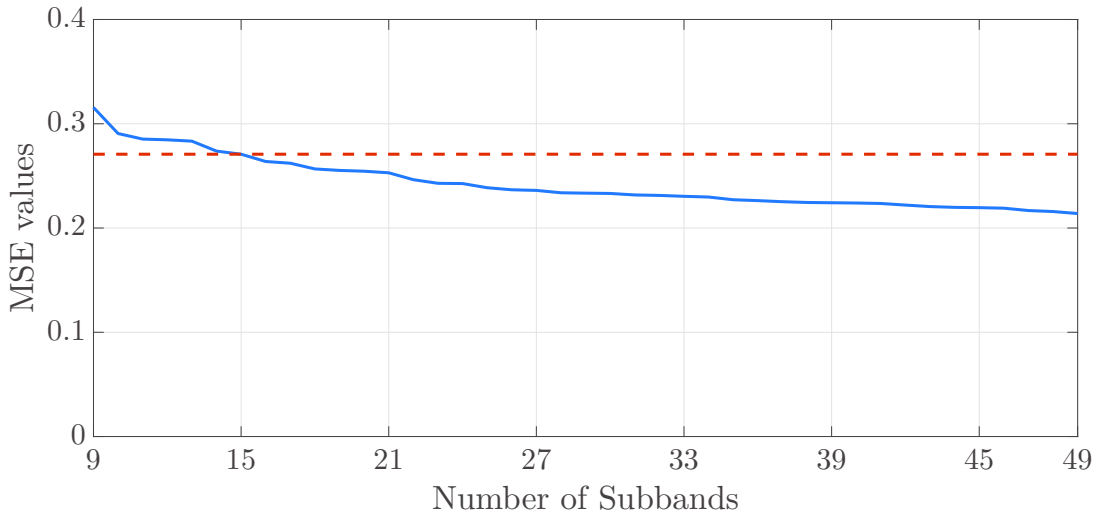


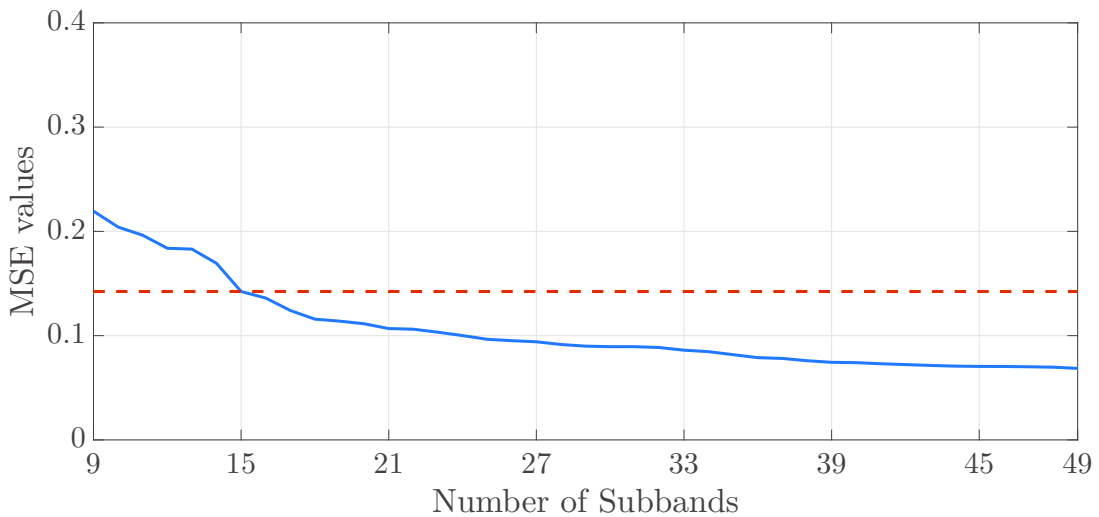
Figure 20: The relative frequency of the magnitude of the valid CFR estimates at the sample $k = 1650$ ($k\Delta f = 80.57$ MHz) and the modeling based on the Log-normal distribution.

Fig. 21 illustrates the MSE results in terms of the number of subbands for the in-home hybrid PLC-WLC *short-path* channels. On these plots is possible to notice that independently of the chosen criterion to select the non-uniformity of the subbands, the MSE value does not change significantly as the number of subbands becomes higher than 15 and due to a trade off between the precision of the interpolation and the complexity of computing it, $L = 15$ was chosen as the number of subbands. By interpolating the parameters values $\mu[k]$ and $\sigma[k]$ of the Log-normal distributions associated with the model of the CFR of the hybrid PLC-WLC *short-path* channel using $L = 15$ subbands and the Algorithm 2, the continuous curves of parameters $\hat{\mu}(\omega)$ and $\hat{\sigma}(\omega)$ are yielded. Finally, the curves $\hat{\mu}(f)$ and $\hat{\sigma}(f)$ are easily obtained once $\omega \in [0, \pi)$ directly corresponds to the frequency band between 0 and 100 MHz. Figs. 22 and 23 portrays the curves for the parameters $\mu(f)$ and $\sigma(f)$, which are obtained by applying frequency domain interpolation technique detailed in [63] and the curves obtained by using the cubic Spline interpolation with $L = 15$ subbands. Similar to previous subsections, Table 4 in Appendix C lists the cubic Spline coefficients for modeling the parameter $\mu(f)$, of the valid CFR magnitude while Table 5, in Appendix C as well, covers the cubic Spline coefficients for modeling the parameter $\sigma(f)$. Overall, it is important to point out that the Log-normal distribution and its coefficients waveform $\hat{\mu}(f)$ and $\hat{\sigma}(f)$ define the random process representing the magnitude of the CFR of the in-home hybrid PLC-WLC *short-path* channel.

Fig. 24 portrays the relative frequency of statistical distributions that had modeled, in accord with the adopted criteria, the phase of the whole set of valid hybrid PLC-WLC *short-path* CFR estimates. Similarly to the PLC CFR estimates, on this scenario 100% of the data set was best modeled by the Uniform distribution and the statistical modeling of the phase of the valid CFR estimates have shown that each sample of it can be modeled



(a)



(b)

Figure 21: The MSE values for the parameters from *short-path* scenario: (a) μ parameter, (b) σ parameter.

by the same set of parameters of the Uniform distribution. In other words, $\Theta_k \in [0, 2\pi]$ denotes the interval of values that the phase of the valid PLC-WLC *short-path* CFR estimates can assume and it defines the support for the Uniform distribution.

Fig. 25 and Fig. 26 shows the statistical models regarding the frequencies $f = 50.78$ MHz ($k = 1040 \rightarrow f = 1040\Delta f$) and $f = 80.57$ MHz ($k = 1650 \rightarrow f = 1650\Delta f$), respectively. Independent of the frequency values, the phase model of the valid CFR estimates remains the same. As a result, by using the Uniform distribution defined in the interval $[0, 2\pi]$, the random process representing the phase of the in-home hybrid PLC-WLC *short-path* channel is obtained.

In a nutshell, the use of the proposed enhanced statistical modeling method for modeling the CFR of in-home hybrid PLC-WLC *short-path* channels showed that the

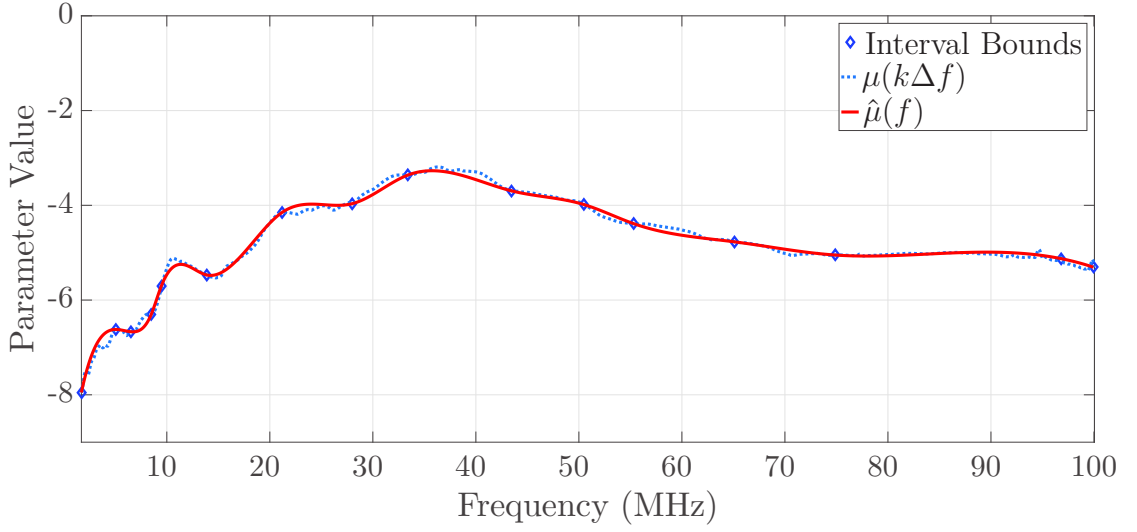


Figure 22: The result of the interpolation technique based on cubic Splines applied to obtain $\mu(f) = \zeta_1(f)$ for the Log-normal distribution ($\mu(k\Delta f)$ are the original values of the parameter and $\hat{\mu}(f)$ is the interpolated curve).

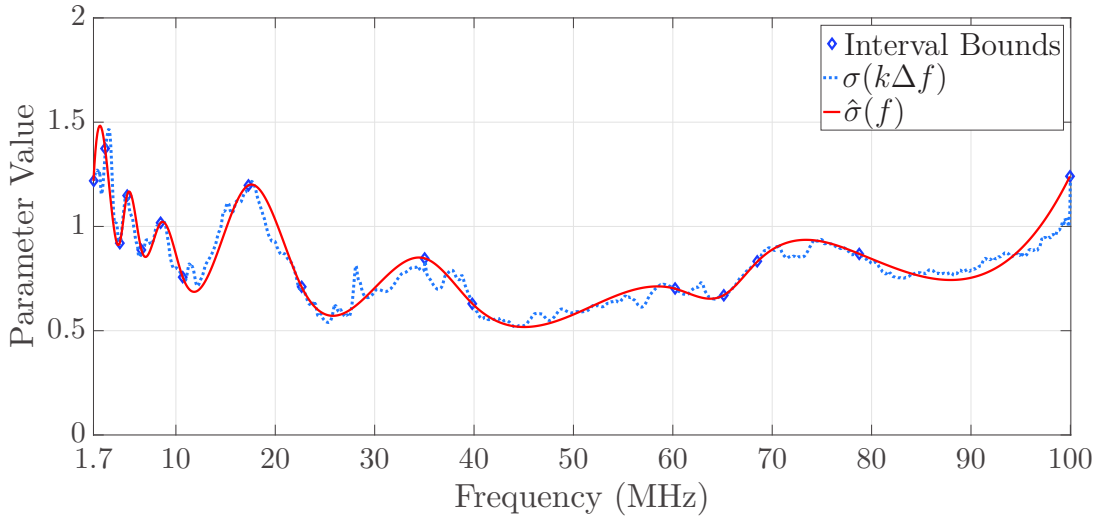


Figure 23: The result of the interpolation technique based on cubic Splines applied to obtain $\sigma(f) = \zeta_2(f)$ for the Log-normal distribution ($\sigma(k\Delta f)$ are the original values of the parameter and $\hat{\sigma}(f)$ is the interpolated curve).

magnitude component of them is a nonstationary random process, that can be modeled by the Log-normal distribution. The statistical analyses has also verified that, similarly to the PLC channel, the phase component of in-home hybrid PLC-WLC *short-path* channels can be modeled by the Uniform distribution with fixed parameters as frequency varies, thus denoting that the phase function of CFR of in-home hybrid PLC-WLC *short-path* channels is a stationary random process.

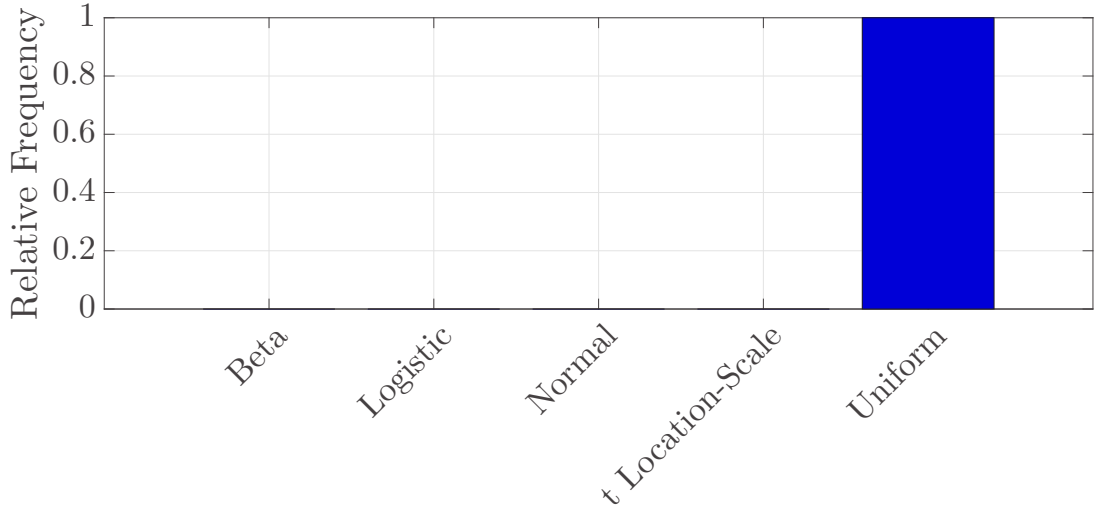


Figure 24: The relative frequency associated with the chosen statistical distribution that best models CFR phase in accord with the adopted criteria.

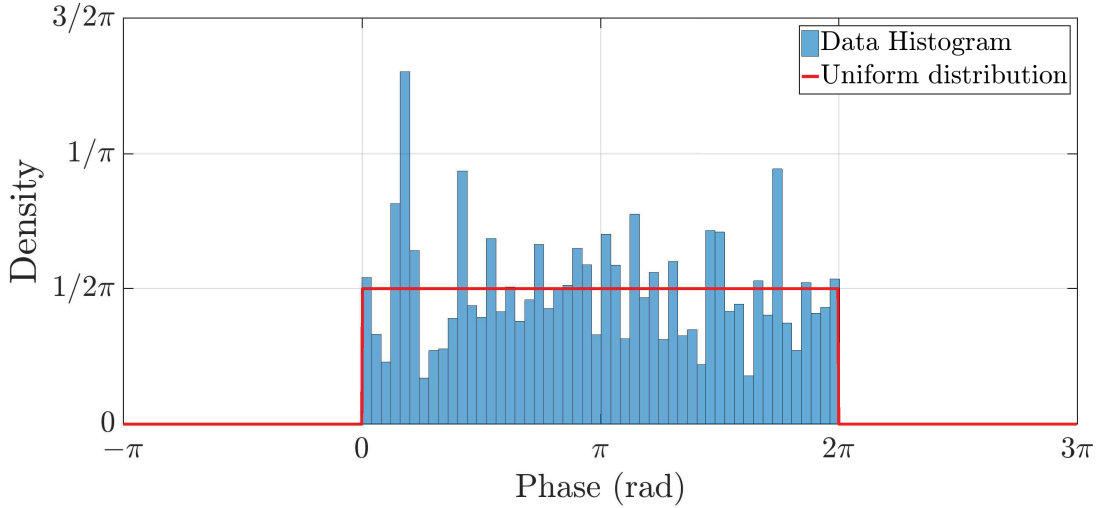


Figure 25: The relative frequency of the phase of the valid CFR estimates at the sample $k = 1040$ ($k\Delta f = 50.78$ MHz) using the Uniform distribution.

4.4 UNCORRELATED CFR MODEL OF HYBRID PLC-WLC *LONG-PATH* CHANNELS

This section highlights the modeling of the CFRs data set related to PLC-WLC *long-path* channels, which were acquired through the measurement campaign described in [46]. Fig. 27 shows 5 valid and consecutive estimates of the CFR magnitude. On this scenario the average operation was not used on the CFR estimates, since the coherence time of the PLC-WLC *long-path* channels was not long enough to contain the duration of at least two symbol periods (T_{sym}). Note that the channel attenuation ranges from approximately -45 dB up to 15 dB and that the plots cover a time interval equal to $\Delta T_{sym} \approx 23.04\mu s$ and, as a consequence, $5\Delta T = 115.2\mu s$.

Fig. 28 illustrates the relative frequency of statistical distributions that had mo-

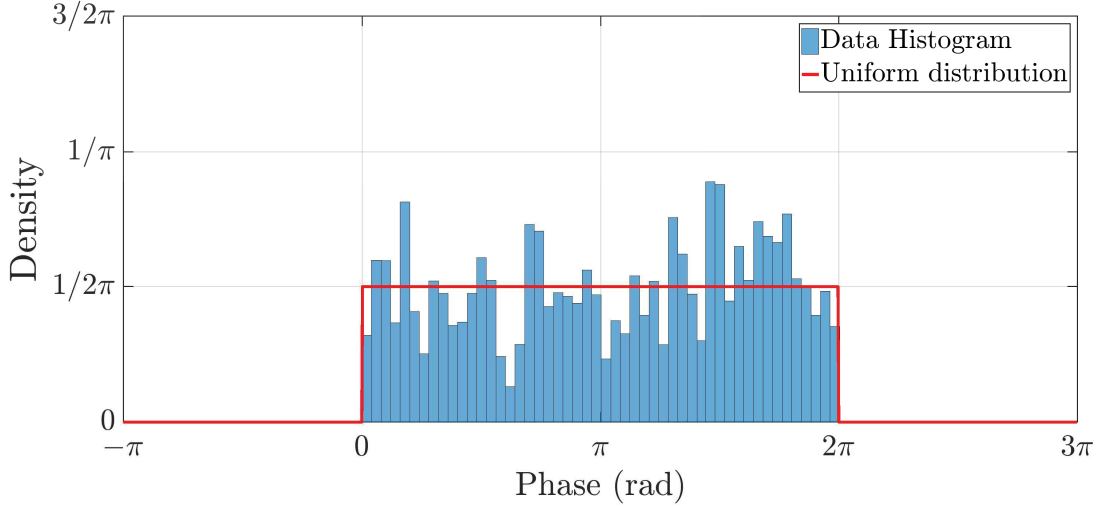


Figure 26: The relative frequency of the phase of the valid CFR estimates at the sample $k = 1650$ ($k\Delta f = 80.57$ MHz) using the Uniform distribution.

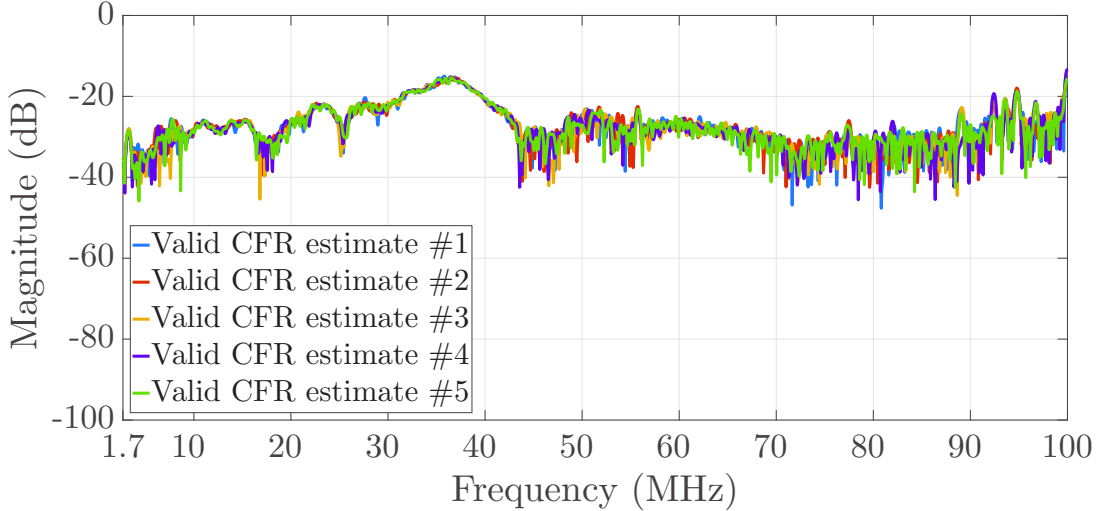


Figure 27: Five consecutive and valid CFR magnitudes of the measured in-home PLC-WLC *long-path* channel.

deled, in accord with the adopted criteria, the magnitude of the whole set of valid CFR estimates. Similarly to the results acquired on the PLC-WLC *short-path* channels, a single statistical distribution have modeled the majority of the magnitudes, but another different statistical distribution stood out as possible candidate to model the CFR magnitudes. As a matter of fact, in 51% of the CFR estimates the Log-normal distribution resulted in the best model and in 38% of it the Gamma distribution offered the best modeling.

Once again the log-likelihood ratio $\rho_{MLE}(f)$ (3.2) presented in the subsection 3.1 was used in order to evaluate which of the two distributions is the best choice to model the magnitude component of the CFR estimates. Fig. 29 portrays the values of $\rho_{MLE}(f)$ for the two best statistical distributions candidates to model the magnitude of the valid CFR estimates. The threshold value of 1.2 was again indicated as a red dashed line, under

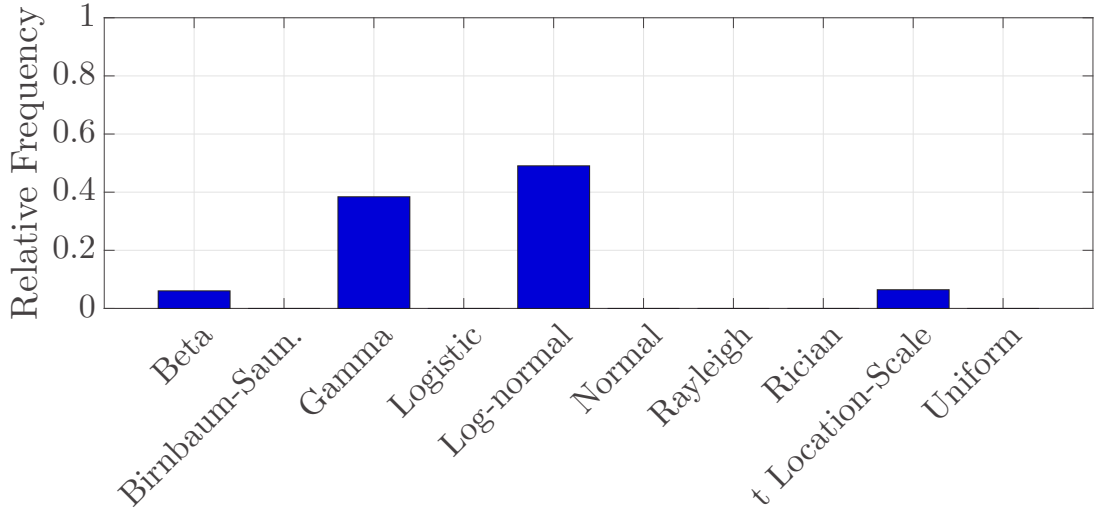


Figure 28: The relative frequency associated with the chosen statistical distribution that best models the CFR magnitude in accord with the adopted criteria.

which the statistical distribution can be considered good enough to model the CFR. These curves emphasize that only the Log-normal distributions achieved the minimum ratio over the MLE criteria. Overall, the results presented in Fig. 28 and Fig. 29 illustrates that the Log-normal distribution is the best option to model the magnitude of the valid CFR estimates of the measured in-home hybrid PLC-WLC *long-path* channels. In other words, the magnitude of the valid CFR estimates of in-home hybrid PLC-WLC *long-path* channels can be modeled by using only one statistical distribution (i.e., the Log-normal distribution).

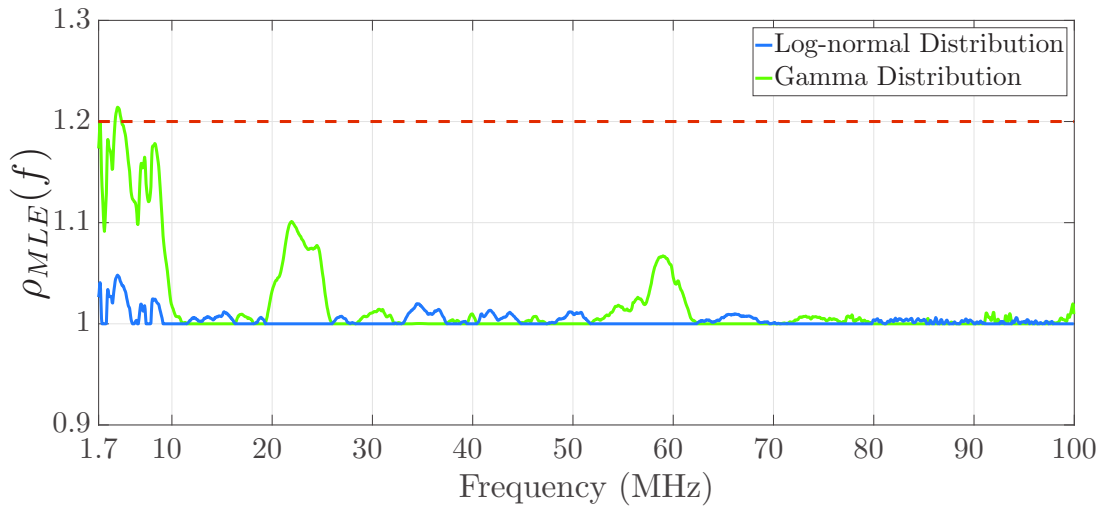


Figure 29: The log-likelihood ratio for the following statistical distributions: Log-normal, Gamma.

The statistical analysis of the magnitude of the valid CFR estimates shows that the parameters of the Log-normal distribution assume different values as frequency changes. If $\mathcal{C}_k = \{\zeta_1[k], \zeta_2[k]\}$ is the set of parameters for the statistical distribution modeling

the magnitude of the valid CFR estimates of PLC-WLC *short-path* channels, where $k = 0, 1, \dots, N - 1$, $\zeta_1[k] = \mu[k]$ and $\zeta_2[k] = \sigma[k]$, are the two parameters ($U = 2$) of the Log-normal distribution, named mean and standard deviation respectively, associated with the k -th sample of the valid CFR. Then, Fig. 30 and Fig. 31 illustrates the statistical models for two different values of frequency: $f = 51.76$ MHz ($k = 1060 \rightarrow f = 1060\Delta f$) and $f = 78.1$ MHz ($k = 1600 \rightarrow f = 1600\Delta f$), respectively. The parameters of the Log-normal distribution are $\mu(1060\Delta f) = \zeta_1[1060] = -6.0759$ and $\sigma(1060\Delta f) = \zeta_2[1040] = 0.8118$; $\mu(1600\Delta f) = \zeta_1[1600] = -6.8347$ and $\sigma(1600\Delta f) = \zeta_2[1600] = 0.8407$ for $f = 51.76$ MHz and $f = 78.1$ MHz, respectively.

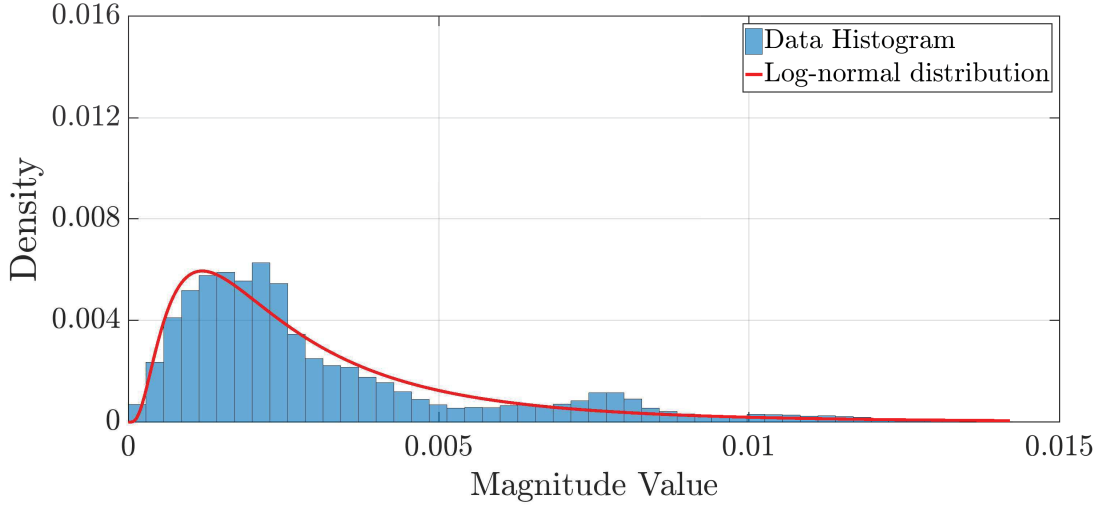


Figure 30: The relative frequency of the magnitude of the valid CFR estimates at the sample $k = 1060$ ($k\Delta f = 51.76$ MHz) and the modeling based on the Log-normal distribution.

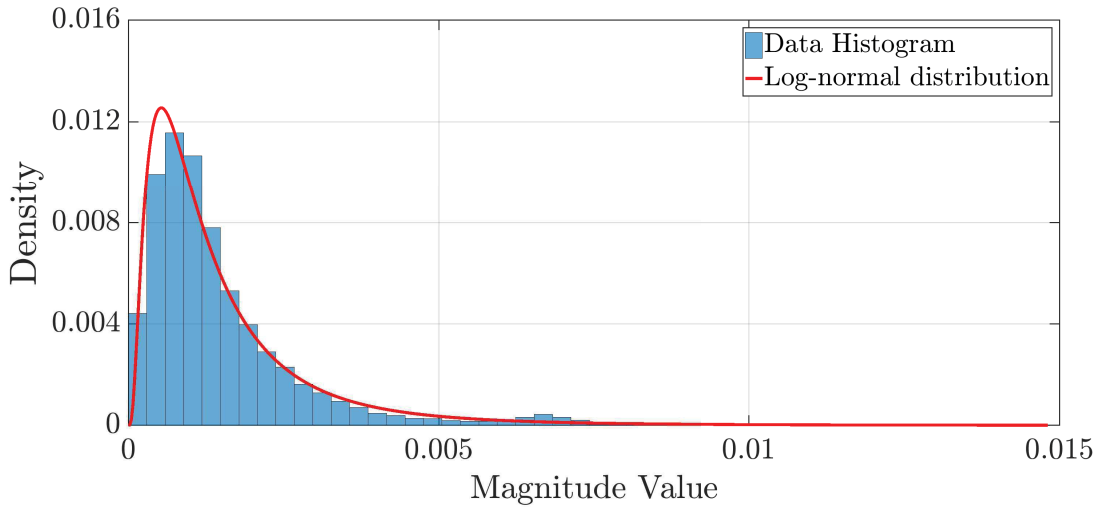


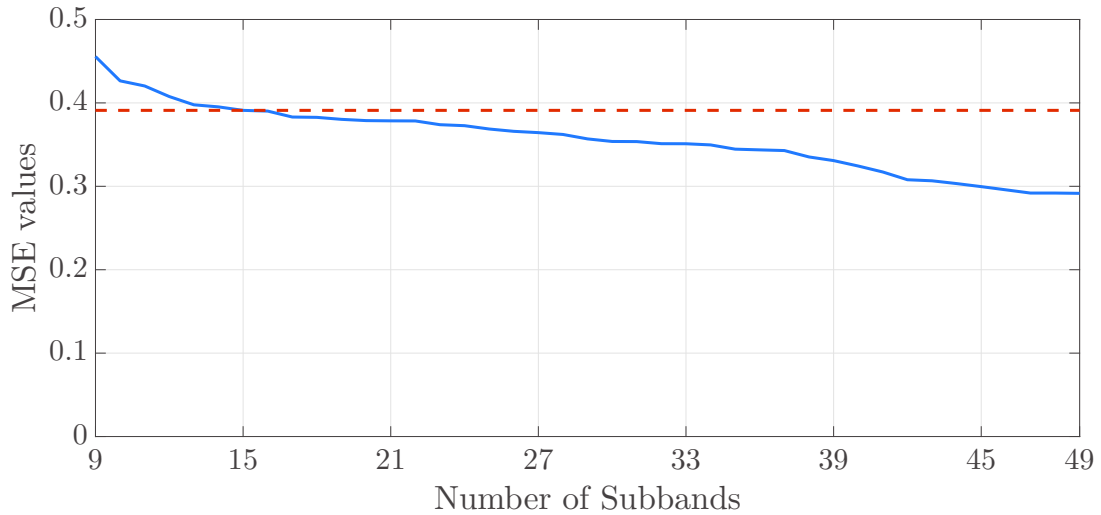
Figure 31: The relative frequency of the magnitude of the valid CFR estimates at the sample $k = 1600$ ($k\Delta f = 78.1$ MHz) and the modeling based on the Log-normal distribution.

Fig. 32 portrays the MSE results in terms of the number of subbands for the in-home PLC-WLC *long-path* channels. According to this plot, independent of the chosen criterion to select the non-uniformity of the subbands, the MSE value does not change significantly as the number of subbands becomes higher than 15. Due to a trade off between the precision of the interpolation and complexity of computing it, $L = 15$ was chosen as the number of subbands. By interpolating the parameters values $\mu(k\Delta f)$ and $\sigma(k\Delta f)$ of the Log-normal distributions associated with the model of PLC-WLC *long-path* CFR using $L = 15$ subbands and the Algorithm 2, the continuous curves of parameters $\hat{\mu}(\omega)$ and $\hat{\sigma}(\omega)$ are yielded. Finally, the curves $\hat{\mu}(f)$ and $\hat{\sigma}(f)$ are easily obtained because $\omega \in [0, \pi)$ directly corresponds to the frequency band between 0 and 100 MHz. Figs. 33 and 34 shows the curves for the parameters $\mu(f)$ and $\sigma(f)$, which are obtained by applying frequency domain interpolation technique detailed in [63] and the curves obtained by using the cubic Spline interpolation with $L = 15$ subbands. Furthermore, Table 6 (see Appendix D) lists the cubic Spline coefficients for modeling the parameter $\mu(f)$, of the valid CFR magnitude. Similarly, Table 7 (see Appendix D) lists the cubic Spline coefficients for modeling the parameter $\sigma(f)$. As a result, the coefficients values, the waveforms $\hat{\mu}(f)$ and $\hat{\sigma}(f)$, and the Log-normal distribution define the random process representing the magnitude of the CFR of the in-home PLC-WLC *long-path* channel.

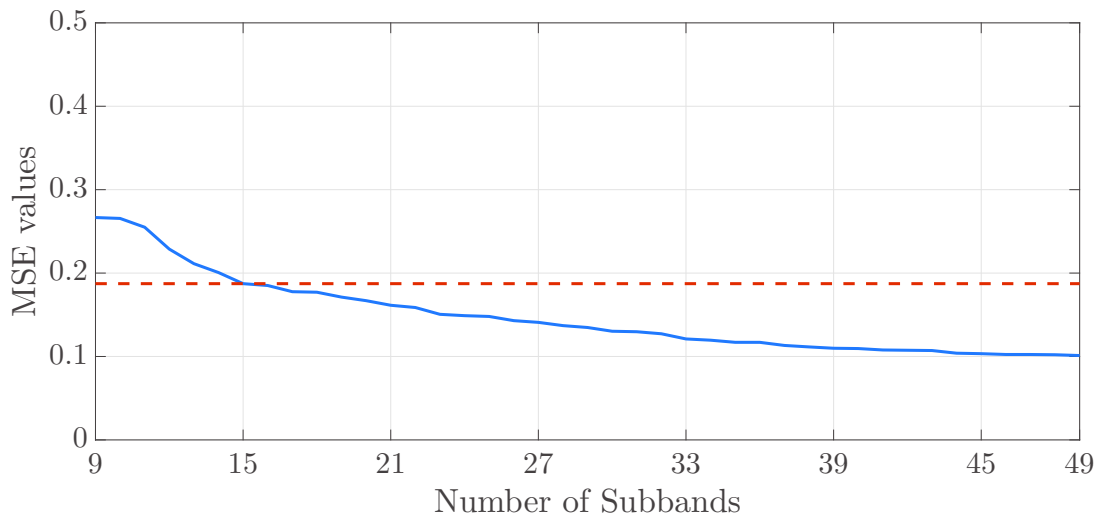
Fig. 35 shows the relative frequency of statistical distributions that had modeled, in accord with the adopted criteria, the phase of the whole set of valid CFR estimates. Note that 100% of the data set is best modeled by the Uniform distribution. On this scenario, differently from the statistical modeling of the CFR magnitude, the statistical modeling of the phase of the valid CFR estimates shows that each sample of it can be modeled by the same set of parameters of the Uniform distribution. In other words, $\Theta_k \in [0, 2\pi]$ denotes the interval of values that the phase of the valid CFR estimates can assume and it defines the support for the Uniform distribution.

Fig. 36 and Fig. 37 illustrates the statistical models regarding the frequencies $f = 51.76$ MHz ($k = 1060 \rightarrow f = 1060\Delta f$) and $f = 78.1$ MHz ($k = 1600 \rightarrow f = 1600\Delta f$), respectively. Independent of the frequency values, the phase model of the valid CFR estimates remains the same. As a result, by using the Uniform distribution defined in the interval $[0, 2\pi]$, the random process representing the phase of the in-home PLC-WLC *long-path* channel is yielded.

Overall, the use of the proposed enhanced statistical modeling method for modeling the CFR of in-home PLC-WLC *long-path* channels showed that the magnitude component of the in-home PLC-WLC *long-path* channel can be modeled by the Log-normal distribution, with parameters value changing as the frequency varies, resulting in a non-stationary random process. The statistical analyses has also verified that the phase component of in-home PLC-WLC *short-path* channels is a stationary random process,



(a)



(b)

Figure 32: The MSE values for the parameters from PLC-WLC *long-path* scenario: (a) μ parameter, (b) σ parameter.

that can be modeled by the Uniform distribution.

4.5 SUMMARY

This chapter has presented statistical analyses of CFRs of PLC and hybrid PLC-WLC channels, acquired through a measurement campaign. These analyses were performed by employing the enhanced statistical modeling method described in Chapter 3. The statistical distributions offering the best models for the random processes $|\mathbf{H}|$ and Θ , which represent magnitude and phase components of the CFR, respectively, were detailed for both PLC and hybrid PLC-WLC scenarios in the frequency band from 1.7 up to 100 MHz.

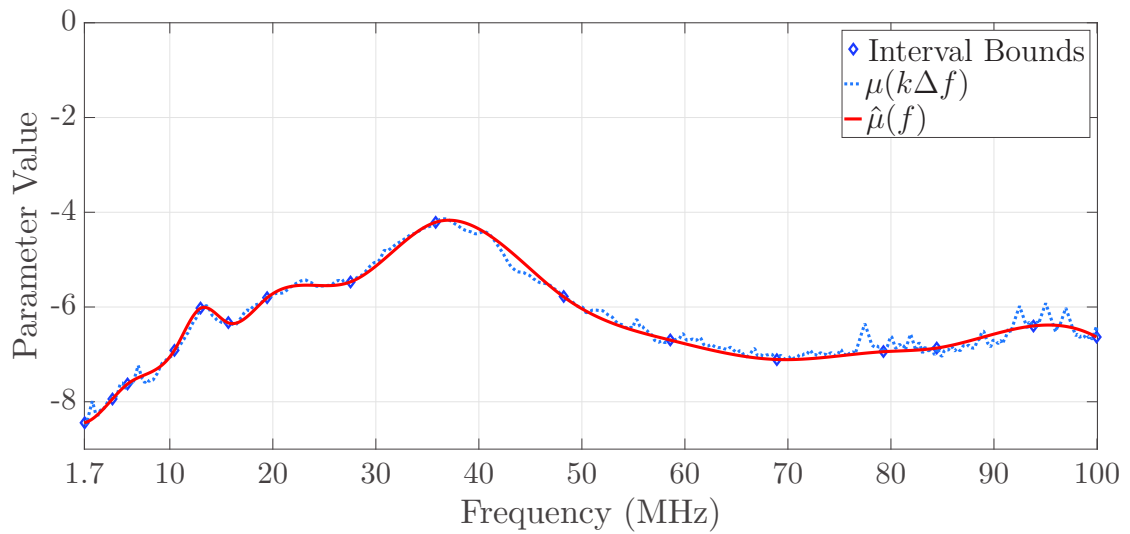


Figure 33: The result of the interpolation technique based on cubic Splines applied to obtain $\mu(f) = \zeta_1(f)$ for the Log-normal distribution ($\mu(k\Delta f)$ are the original values of the parameter and $\hat{\mu}(f)$ is the interpolated curve).

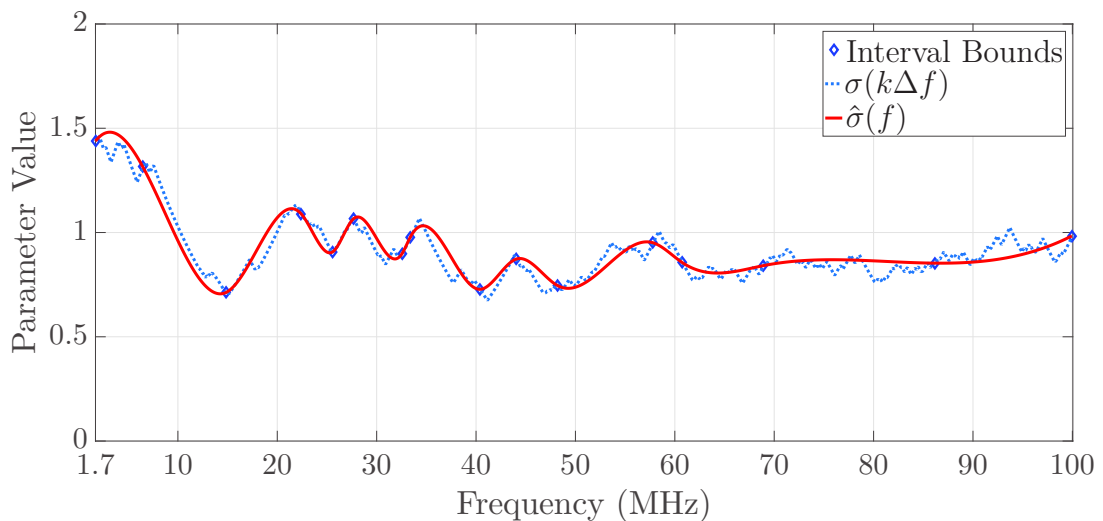


Figure 34: The result of the interpolation technique based on cubic Splines applied to obtain $\sigma(f) = \zeta_2(f)$ for the Log-normal distribution ($\sigma(k\Delta f)$ are the original values of the parameter and $\hat{\sigma}(f)$ is the interpolated curve).

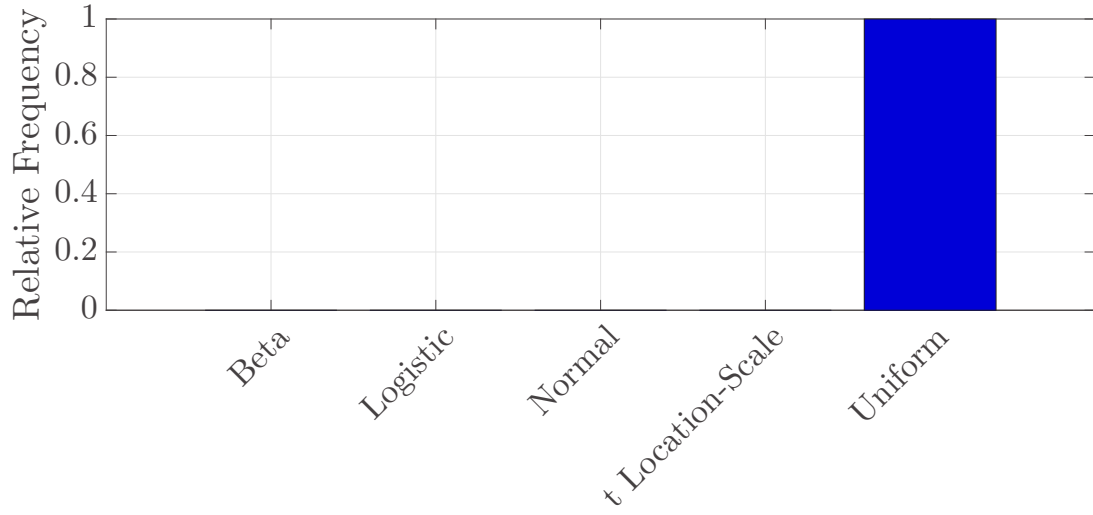


Figure 35: The relative frequency associated with the chosen statistical distribution that best models CFR phase in accord with the adopted criteria.

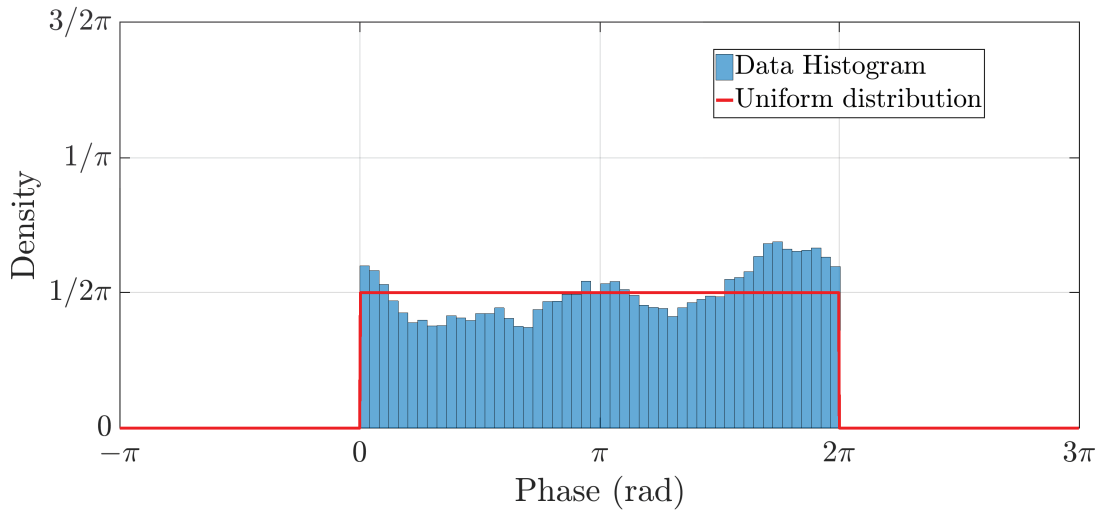


Figure 36: The relative frequency of the phase of the valid CFR estimates at the sample $k = 1060$ ($k\Delta f = 51.76$ MHz) using the Uniform distribution.

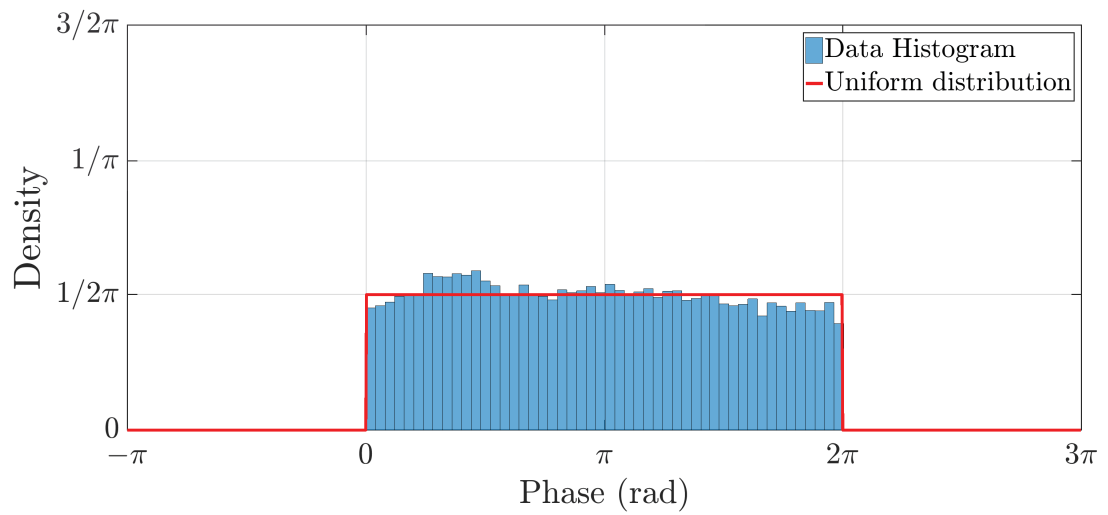


Figure 37: The relative frequency of the phase of the valid CFR estimates at the sample $k = 1600$ ($k\Delta f = 78.1$ MHz) using the Uniform distribution.

5 CONCLUSIONS

This work has presented statistical characterizations and modelings of the CFR estimates of Brazilian in-home PLC and hybrid PLC-WLC channels, constituting an important result to support future efforts in simulating and designing in-home broadband communication systems. The statistical characterization and modeling have been based on numerical analyses of two data sets of measured CFR estimates, covering the frequency band between 1.7 and 100 MHz, which were acquired from a measurement campaign performed in seven typical Brazilian residences.

Chapter 2 has introduced the problem formulation, in which the main assumption is that the magnitude and phase of the CFR estimates are two random processes, with uncorrelated samples, denoted by two r.v.s ($|\mathbf{H}|$ and Θ , respectively). The adopted road map is based on the fact that these random processes can be individually modeled by statistical distributions and the parameters values of these distribution can be obtained along the frequency domain. Moreover, some investigation questions were brought to attention regarding the statistical distributions that could model the magnitude and phase processes for the PLC, PLC-WLC *short-path* and PLC-WLC *long-path* scenarios, separately, and the behavior of such statistical distributions in the frequency band, in other words, if the magnitude and phase random processes could be considered stationary.

Furthermore, Chapter 3 has introduced the enhanced statistical modeling method, which emerged from the drawback found in the method presented in [22, 50], for modeling the magnitude and phase of CFR estimates acquired from a data set. The enhanced statistical modeling method was organized into four steps. The first three steps cover the search for the most suitable statistical distribution among a predetermined set of candidates statistical distributions based on four chosen criteria (MLE, AIC, BIC and EDC). The fourth step focuses on the interpolation of the parameters of the chosen statistical distributions, in the frequency domain, through the use of the cubic Spline interpolation technique, resulting in a table of reduced number of polynomials coefficients, for each parameter being interpolated. The enhanced statistical modeling method was designed to generate uncorrelated CFR magnitude and phase response. Moreover, Chapter 3 ended by describing two algorithms for implementing the first three steps and the fourth step, respectively.

Chapter 4 has covered the numerical results and statistical analyses. After applying the enhanced statistical modeling method on a data set of CFR estimates, acquired through a measurement campaign carried out in several Brazilian residences, the uncorrelated statistical models for the magnitude and phase responses of the PLC, hybrid PLC-WLC *short-path*, and hybrid PLC-WLC *long-path* scenarios were obtained. The magnitude of the CFR estimates has been observed to be a non-stationary random pro-

cess, modeled by the Beta distribution for the in-home PLC channel, a result that disagrees with some previous models adopted by the literature. Moreover, numerical results have shown that the magnitude response of CFRs for both in-home hybrid PLC-WLC *short-path* and *long-path* channels are best modeled by the Log-normal distribution. The number of subbands used to generate the interpolated curve of the parameters values, through the cubic spline interpolation, was carefully chosen by adopting a procedure combining a Monte Carlo simulation of MSE values for allowing a decision about the number of subbands to be adopted when computational complexity for obtaining the polynomials is taken into account. Regarding the PLC channel scenario, the cubic spline interpolation required a total of nineteen third order polynomials in order to interpolate the parameters of the Beta distribution over the desired frequency band. As to the hybrid PLC-WLC *short-path* and *long-path* scenarios, the cubic spline interpolation required a total of fifteen third order polynomials, for each case, in order to interpolate the parameters of the Log-normal distributions over the desired frequency band. The polynomials coefficients were presented in six different tables located in the Appendix section. Regarding of the phase response of CFRs, all three different scenarios presented in this thesis (i.e., PLC channel, hybrid PLC-WLC *short-path* channel and hybrid PLC-WLC *long-path* channel) have been observed to be stationary random processes, with samples modeled by the Uniform distribution defined in the interval represented by $[0, 2\pi]$, regardless of the frequency value.

5.1 FUTURE WORKS

A list of future works is as follows:

- To investigate the insertion of correlation among consecutive samples of the CFR magnitude and phase components, in order to generate models for PLC and hybrid PLC-WLC channels that can be used to perform data communication through these channels.
- To extend the enhanced statistical modeling method to handle channel modeled as cyclostationary random processes.
- To apply the enhanced statistical modeling method in other data communication channels (i.e., broadband and narrowband outdoors and narrowband indoor).

REFERENCES

- [1] S. Galli, A. Scaglione, and Z. Wang, “For the grid and through the grid: The role of power line communications in the smart grid,” *Proceedings of the IEEE*, vol. 99, no. 6, pp. 998–1027, Jun. 2011.
- [2] S. Verma and P. Rana, “Wireless communication application in smart grid: An overview,” in *Proc. 2014 Innovative Applications of Computational Intelligence on Power, Energy and Controls with their impact on Humanity (CIPECH)*, Nov 2014, pp. 310–314.
- [3] M. Sayed and N. Al-Dhahir, “Narrowband-PLC/wireless diversity for smart grid communications,” in *Proc. IEEE Global Commun. Conf.*, Dec. 2014, pp. 2966–2971.
- [4] L. de M. B. A. Dib, V. Fernandes, M. de L. Filomeno, and M. V. Ribeiro, “Hybrid PLC/wireless communication for smart grids and Internet of Things applications,” *IEEE Internet Things J.*, vol. 5, no. 2, pp. 655–667, Apr. 2018.
- [5] M. Sayed, G. Sebaali, B. L. Evans, and N. Al-Dhahir, “Efficient diversity technique for hybrid narrowband-powerline/wireless smart grid communications,” in *Proc. IEEE Int. Conf. Smart Grid Commun.*, Nov. 2015, pp. 1–6.
- [6] H. Hrasnica, A. Haidine, and R. Lehnert, *Broadband PowerLine Communications Network Design*. John Wiley & Sons, 2004.
- [7] M. Y. Zhai, “Transmission characteristics of low-voltage distribution networks in China under the smart grids environment,” *IEEE Trans. Power Del.*, vol. 26, no. 1, pp. 173–180, Jan. 2011.
- [8] A. G. Lazaropoulos and P. G. Cottis, “Transmission characteristics of overhead medium-voltage power-line communication channels,” *IEEE Trans. Power Del.*, vol. 24, no. 3, pp. 1164–1173, Jul. 2009.
- [9] M. Zajc, N. Suljanovic, A. Mujcic, and J. Tasic, “High voltage power line constraints for high speed communications,” in *Proc. IEEE Mediterranean Electrotechnical Conf.*, vol. 1, May 2004, pp. 285–288.
- [10] R. Aquilue, M. Ribo, J. R. Regue, J. L. Pijoan, and G. Sanchez, “Scattering parameters-based channel characterization and modeling for underground medium-voltage power-line communications,” *IEEE Trans. Power Del.*, vol. 24, no. 3, pp. 1122–1131, Jul. 2009.
- [11] P. Amirshahi and M. Kavehrad, “High-frequency characteristics of overhead multi-conductor power lines for broadband communications,” *IEEE J. Sel. Areas Commun.*, vol. 24, no. 7, pp. 1292–1303, Jul. 2006.
- [12] M. Tlich, A. Zeddani, F. Moulin, and F. Gauthier, “Indoor power-line communications channel characterization up to 100 mhz-part ii: time-frequency analysis,” *IEEE Trans. Power Del.*, vol. 23, no. 3, pp. 1402–1409, Jul. 2008.
- [13] A. B. Vallejo-Mora, J. J. Sanchez-Martinez, F. J. Canete, J. A. Cortes, and L. Diez, “Analysis of in-vehicle power line channel response,” *IEEE Latin America Transactions*, vol. 9, no. 4, pp. 445–450, Jul. 2011.

- [14] S. Barmada, L. Bellanti, M. Raugi, and M. Tucci, “Analysis of power-line communication channels in ships,” *IEEE Trans. Veh. Technol.*, vol. 59, no. 7, pp. 3161–3170, Sep. 2010.
- [15] C. H. Jones, “Communications over aircraft power lines,” in *Proc. IEEE Int. Symp. on Power Line Commun. Appl.*, 2006, pp. 149–154.
- [16] A. Camponogara, “Measurement and characterization of aircraft PLC channels,” Master’s thesis, Federal University of Juiz de Fora, Aug. 2016.
- [17] A. Camponogara, T. R. Oliveira, W. A. Finamore, F. P. V. Campos, and M. V. Ribeiro, “Aircraft PLC channels characterization: Initial discussion,” in *Proc. XXXIV Simpósio Brasileiro de Telecomunicações*, Sep. 2016, pp. 839–842.
- [18] H. Gassara, F. Rouissi, and A. Ghazel, “Statistical characterization of the indoor low-voltage narrowband power line communication channel,” *IEEE Trans. Electromagn. Compat.*, vol. 56, no. 1, pp. 123–131, Jul. 2014.
- [19] A. I. Chrysochos, T. A. Papadopoulos, A. ElSamadouny, G. K. Papagiannis, and N. Al-Dhahir, “Optimized MIMO-OFDM design for narrowband-PLC applications in medium-voltage smart distribution grids,” *Electric Power Systems Research*, vol. 140, pp. 253–262, Feb. 2016.
- [20] S. Galli, “A novel approach to the statistical modeling of wireline channels,” *IEEE Trans. Commun.*, vol. 59, no. 5, pp. 1332–1345, May 2011.
- [21] *Brazilian resolution for PLC*, ANATEL Std. 527, 2009.
- [22] L. G. S. Costa, “Non-adaptive and adaptive coupling circuits for power line communication system,” Ph.D. dissertation, Federal University of Juiz de Fora, Sep. 2017.
- [23] A. Mascco, F. Gauthier, M. Tlich, P. Pagani, and A. Zeddani, “Two models for the stationary noise measured on indoor PLC lines up to 500 mhz,” in *Proc. Fourth Workshop on Power Line Communications (Applications in Networking and Smart Grid)*, Sep. 2010, pp. 22–25.
- [24] M. d. L. Filomeno, G. R. Colen, L. G. de Oliveira, and M. V. Ribeiro, “Two-stage single-relay channel model for in-home broadband plc systems,” *IEEE Systems Journal*, pp. 1–11, 2018.
- [25] M. S. P. Facina, H. A. Latchman, H. V. Poor, and M. V. Ribeiro, “Cooperative in-home power line communication: analyses based on a measurement campaign,” *IEEE Trans. Commun.*, vol. 64, no. 2, pp. 778–789, Feb. 2016.
- [26] M. S. P. Facina, “Cooperative in-home power line communication: analyses based on a measurement campaign,” Master’s thesis, Federal University of Juiz de Fora, May 2015.
- [27] J. Valencia, T. R. Oliveira, and M. V. Ribeiro, “Cooperative power line communication: Analysis of brazilian in-home channels,” in *Proc. 18th IEEE International Symposium on Power Line Communications and Its Applications*, Mar. 2014, pp. 301–305.

- [28] R. M. Oliveira, M. S. P. Facina, M. V. Ribeiro, and A. B. Vieira, "Performance evaluation of in-home broadband PLC systems using a cooperative mac protocol," *Computer Networks*, vol. 95, pp. 62–76, Dec. 2015.
- [29] F. J. Canete, L. Diez, J. A. Cortes, and J. T. Entrambasaguas, "Broadband modelling of indoor power-line channels," *IEEE Trans. Consum. Electron.*, vol. 48, no. 1, pp. 175–183, Feb. 2002.
- [30] F. J. Canete, J. A. Cortes, L. Diez, and J. T. Entrambasaguas, "A channel model proposal for indoor power line communications," *IEEE Commun. Mag.*, vol. 49, no. 12, pp. 166–174, Dec. 2011.
- [31] J. A. Cortes, F. J. Canete, L. Díez, and J. L. G. Moreno, "On the statistical properties of indoor power line channels: measurements and models," in *Proc. IEEE Int. Symp. on Power Line Commun. Appl.*, Apr. 2011, pp. 271–276.
- [32] S. Galli, "A simplified model for the indoor power line channel," in *Proc. IEEE Int. Symp. on Power Line Commun. Appl.*, Mar. 2009, pp. 13–19.
- [33] T. R. Oliveira, A. A. M. Picorone, S. L. Netto, and M. V. Ribeiro, "Characterization of Brazilian in-home power line channels for data communication," *Electric Power Systems Research*, vol. 150, pp. 188–197, Sep. 2017.
- [34] S. Güzelgöz, "Characterizing wireless and powerline communication channels with applications to smart grid networks," Ph.D. dissertation, University of South Florida, Apr. 2011.
- [35] "Ieee standard for information technology–telecommunications and information exchange between systems local and metropolitan area networks–specific requirements - part 11: Wireless lan medium access control (mac) and physical layer (phy) specifications," *IEEE Std 802.11-2016 (Revision of IEEE Std 802.11-2012)*, pp. 1–3534, Dec. 2016.
- [36] G. Gu and G. Peng, "The survey of gsm wireless communication system," in *Proc. 2010 International Conference on Computer and Information Application*, Dec 2010, pp. 121–124.
- [37] D. Patel and M. Won, "Experimental study on low power wide area networks (lpwan) for mobile internet of things," in *Proc. 2017 IEEE 85th Vehicular Technology Conference (VTC Spring)*, June 2017, pp. 1–5.
- [38] L. Liu, C. Oestges, J. Poutanen, K. Haneda, P. Vainikainen, F. Quitin, F. Tufvesson, and P. D. Doncker, "The cost 2100 mimo channel model," *IEEE Wireless Communications*, vol. 19, no. 6, pp. 92–99, Dec. 2012.
- [39] A. F. Molisch, K. Balakrishnan, C. chin Chong, S. Emami, A. Fort, J. Karedal, J. Kunisch, H. Schantz, U. Schuster, and K. Siwiak, "IEEE 802. 15. 4a channel model-final report," *IEEE P802*, vol. 15, Jan. 2004.
- [40] J. Medbo and P. Schramm, "Channel models for hiperlan/2 in different indoor scenarios," ETSI EP, BRAN Meeting # 3, Technical Report 3ERI085B.

- [41] V. Fernandes, H. V. Poor, and M. V. Ribeiro, “Analyses of the incomplete low-bit-rate hybrid plc-wireless single-relay channel,” *IEEE Internet of Things Journal*, vol. PP, no. 99, pp. 1–12, 2018.
- [42] V. Fernandes, W. A. Finamore, H. V. Poor, and M. V. Ribeiro, “The low-bit-rate hybrid power line/wireless single-relay channel,” *IEEE Systems Journal*, vol. PP, no. 99, pp. 1–12, 2017.
- [43] S. W. Lai and G. G. Messier, “Using the wireless and PLC channels for diversity,” *IEEE Trans. Commun.*, vol. 60, no. 12, pp. 3865–3875, Dec. 2012.
- [44] T. Holden and J. Yazdani, “Hybrid security for hybrid vehicles exploring smart grid technology, powerline and wireless communication,” in *Proc. IEEE PES Int. Conf. and Exhibition on Innov. Smart Grid Technol.*, Dec. 2011, pp. 1–5.
- [45] M. Schwartz, “Carrier-wave telephony over power lines: Early history [history of communications],” *IEEE Communications Magazine*, vol. 47, no. 1, pp. 14–18, January 2009.
- [46] T. R. Oliveira, F. J. A. Andrade, A. A. M. Picorone, H. A. Latchman, S. L. Netto, and M. V. Ribeiro, “Characterization of hybrid communication channel in indoor scenario,” vol. 31, p. 224, Sep. 2016.
- [47] V. Fernandes, M. L. Filomeno, W. A. Finamore, and M. V. Ribeiro, “An investigation on narrow band PLC-wireless parallel channel capacity,” in *Proc. XXXIV Simpósio Brasileiro de Telecomunicações*, Sep. 2016, pp. 834–838.
- [48] S. W. Lai and G. G. Messier, “The wireless/power-line diversity channel,” in *Proc. IEEE Int. Conf. on Commun.*, May. 2010, pp. 1–5.
- [49] L. d. M. B. A. Dib, V. Fernandes, and M. V. Ribeiro, “A discussion about hybrid PLC-wireless communication for smart grids,” in *Proc. XXXIV Simpósio Brasileiro de Telecomunicações*, Sep. 2016, pp. 848–852.
- [50] L. G. S. Costa, G. R. Colen, A. C. M. de Queiroz, V. L. R. da Costa, U. R. C. Vitor, F. dos Santos, and M. V. Ribeiro, “Access impedance in Brazilian in-home, broadband and low-voltage electric power grids,” *Electric Power Systems Research*, 2018, to be published.
- [51] T. R. Oliveira, A. A. Picorone, C. B. Zeller, S. L. Netto, and M. V. Ribeiro, “On the statistical characterization of hybrid plc-wireless channels,” *Electric Power Systems Research*, vol. 163, pp. 329 – 337, 2018.
- [52] T. R. Oliveira, “The characterization of hybrid PLC-wireless and PLC channels in the frequency band between 1.7 and 100 mhz for data communication,” Ph.D. dissertation, Federal University of Juiz de Fora, Mar. 2015.
- [53] S. Galli and T. Banwell, “A novel approach to the modeling of the indoor power line channel-part ii: transfer function and its properties,” *IEEE Trans. Power Del.*, vol. 20, no. 3, pp. 1869–1878, Jul. 2005.

- [54] G. R. Colen, H. Schettino, D. Fernandes, L. M. Sirimarco, F. P. V. Campos, W. A. Finamore, H. A. Latchman, and M. V. Ribeiro, "A temporal compressive resource allocation technique for complexity reduction in PLC transceivers," *Trans. Emerging Tel. Tech.*, vol. 28, no. 2, p. e2951, May 2015.
- [55] H. Meng, S. Chen, Y. L. Guan, C. L. Law, P. L. So, E. Gunawan, and T. T. Lie, "Modeling of transfer characteristics for the broadband power line communication channel," *IEEE Transactions on Power Delivery*, vol. 19, no. 3, pp. 1057–1064, Jul. 2004.
- [56] D. Anastasiadou and T. Antonakopoulos, "Multipath characterization of indoor power-line networks," *IEEE Transactions on Power Delivery*, vol. 20, no. 1, pp. 90–99, Jan. 2005.
- [57] L. T. Tang, P. L. So, E. Gunawan, Y. L. Guan, S. Chen, and T. T. Lie, "Characterization and modeling of in-building power lines for high-speed data transmission," *IEEE Transactions on Power Delivery*, vol. 18, no. 1, pp. 69–77, Jan. 2003.
- [58] M. Zimmermann and K. Dostert, "A multipath model for the powerline channel," *IEEE Transactions on Communications*, vol. 50, no. 4, pp. 553–559, Apr. 2002.
- [59] C. Konate, M. Machmoum, and J. F. Diouris, "Multi path model for power line communication channel in the frequency range of 1mhz-30mhz," in *EUROCON 2007 - The International Conference on "Computer as a Tool"*, Sept 2007, pp. 984–989.
- [60] T. K. Ho, J. J. Hull, and S. N. Srihari, "Decision combination in multiple classifier systems," *IEEE Trans. Pattern Anal. Mach. Intell.*, vol. 16, no. 1, pp. 66–75, Jan. 1994.
- [61] C. C. Y. Dorea, C. R. Goncalves, and P. A. A. Resende, "Simulation results for markov model selection: AIC, BIC and EDC," in *Proc. World Congress on Engineering and Computer Science*, vol. 2, Oct. 2014, pp. 899–901.
- [62] C. R. B. Cabral, V. H. Lachos, and C. B. Zeller, "Multivariate measurement error models using finite mixtures of skew-Student t distributions," *Journal of Multivariate Analysis*, vol. 124, pp. 179 – 198, Feb. 2014.
- [63] S. K. Mitra, *Digital Signal Processing: A Computer-Based Approach*, 3rd ed. McGraw-Hill, Jan. 2006.
- [64] R. H. Bartels, J. C. Beatty, and B. A. Barsky, *An Introduction to Splines for Use in Computer Graphics and Geometric Modelling*. Morgan Kaufmann, 1998.
- [65] S. D. Conte and C. D. Boor, *Elementary Numerical Analysis: An Algorithmic Approach*, 3rd ed. McGraw-Hill, Mar. 1980.
- [66] S. A. Dyer and J. S. Dyer, "Cubic-spline interpolation. 1," *IEEE Instrumentation Measurement Magazine*, vol. 4, no. 1, pp. 44–46, Mar. 2001.
- [67] T. R. Oliveira, C. A. G. Marques, W. A. Finamore, S. L. Netto, and M. V. Ribeiro, "A methodology for estimating frequency responses of electric power grids," *Journal of Control, Automation and Electrical Systems*, vol. 25, no. 6, pp. 720–731, 2014.

- [68] M. V. Ribeiro, G. R. Colen, F. V. P. D. Campos, Z. Quan, and H. V. Poor, “Clustered-orthogonal frequency division multiplexing for power line communication: when is it beneficial?” *IET Communications*, vol. 8, no. 13, pp. 2336–2347, Sep. 2014.
- [69] A. A. M. Picorone, T. R. Oliveira, and M. V. Ribeiro, “PLC channel estimation based on pilots signal for OFDM modulation: A review,” *IEEE Latin America Transactions*, vol. 12, no. 4, pp. 580–589, Jun. 2014.
- [70] F. M. Gardner, “Interpolation in digital modems. i. fundamentals,” *IEEE Trans, Commun.*, vol. 41, no. 3, pp. 501–507, Mar. 1993.
- [71] T. Keller and L. Hanzo, “Orthogonal frequency division multiplex synchronization techniques for wireless local area networks,” in *Proc. IEEE Int. Symp. on Personal, Indoor and Mobile Radio Communications*, vol. 3, Oct. 1996, pp. 963–967.
- [72] D. F. Cardoso, F. D. Backx, and R. Sampaio-Neto, “Improved pilot-aided channel estimation in zero padded MC-CDMA systems,” in *Proc. Int. Symp. on Wireless Pervasive Computing*, Feb. 2009, pp. 1–5.
- [73] M. Ouzzif and J. L. Masson, “Statistical analysis of the cyclic prefix impact on indoor PLC capacity,” in *Proc. IEEE Int. Symp. on Power Line Commun. Appl.*, Mar. 2009, pp. 285–289.
- [74] L. G. da S. Costa, A. C. M. de Queiroz, B. Adebisi, V. L. R. da Costa, and M. V. Ribeiro, “Coupling for power line communications: a survey,” *J. Commun. Inf. Syst.*, 2017.
- [75] F. J. C. Corripio, J. A. C. Arrabal, L. D. del Rio, and J. T. E. Munoz, “Analysis of the cyclic short-term variation of indoor power line channels,” *IEEE J. Sel. Areas Commun.*, vol. 24, no. 7, pp. 1327–1338, Jul. 2006.
- [76] A. Mathur, M. R. Bhatnagar, and B. K. Panigrahi, “PLC performance analysis over rayleigh fading channel under nakagami- m additive noise,” *IEEE Communications Letters*, vol. 18, no. 12, pp. 2101–2104, Dec. 2014.

APPENDIX A – Measurement Campaign

This Appendix summarizes the characteristics of the measurement campaign, which was detailed in [33] and [46], performed in some residences in Brazilian urban area of Juiz de Fora city. The statistical analyses of the Brazilian in-home PLC and hybrid PLC-wireless channels were supported by estimates of the CFR, acquired through this measurement campaign. The channels estimation were performed in seven different middle-class residences, some features of these places are summarized in Table 1.

The CFR measurement setup, used for acquiring the estimations of PLC CFRs, is depicted in Fig. 38. This setup consists of three main components:

- **Signal generator:** Device composed of an arbitrary signal generator board mounted in a rugged computer. A pre-designed sounding sequence is loaded into it and converted to an analog signal to be submitted to the PLC channel under analysis.
- **Data digitizer:** Acts as a receiver, measuring the transmitted sounding signal after propagating through the PLC Channel, and converts it into a digital representation for the subsequent analysis.
- **Coupler:** Circuitry used to connect both the signal generator and the data digitizer to the PLC channel under analysis. The coupler is essentially a high pass filter, blocking the main voltage signal (60 Hz in Brazil), that can damage both the signal generator and the data digitizer, presenting very low attenuations in the bandwidth of interest.

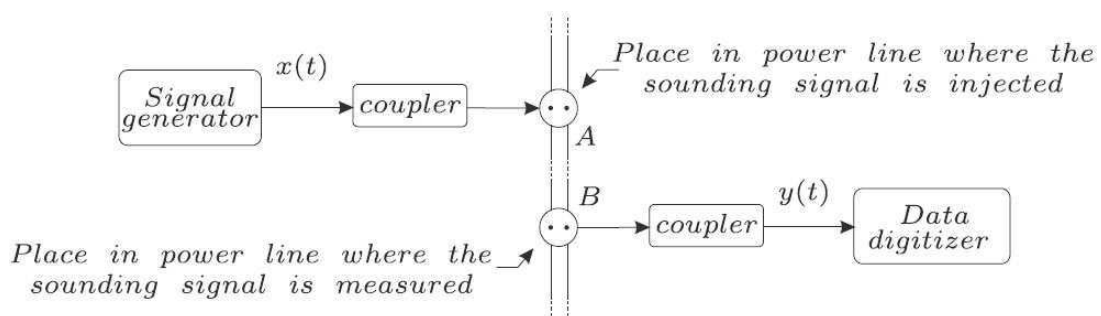


Figure 38: Block diagram of the PLC measurement setup.

From the entire campaign, 245 different combinations of pairs of outlets were measured, providing a total of 148,037 different CFR estimates, with an average of 604 consecutive CFR estimates for each PLC channel configuration.

The CFR measurement setup used for acquiring the estimations of hybrid PLC-wireless CFRs, is illustrated in Fig. 39. These measurements were carried out in the

Table 1: Characteristics of the measured residences.

Construction Type	Age (years)	Constructed area (m^2)	Considered Outlets
House # 1	30	78	12
House # 2	10	69	14
Apartment # 1	9	54	11
Apartment # 2	9	42	06
Apartment # 3	19	65	11
Apartment # 4	3	62	11
Apartment # 5	2	54	11

residences listed in Table 1, potential scattering objects and the transceivers were stationary during the measurement campaign in order to avoid Doppler effects in the wireless portion of the hybrid PLC-wireless channel. The hybrid-PLC and hybrid-wireless transceivers are rugged computers equipped with a high-speed data acquisition board and a high-speed arbitrary signal generation board that operate as receiver and transmitter, respectively. The coupler is the same circuitry used in the PLC measurement setup with the objective of blocking the main voltage signal and presenting very low attenuations in the bandwidth of interest. The adopted omnidirectional and monopole antenna operate in the frequency band ranging from 1 MHz up to 1 GHz.

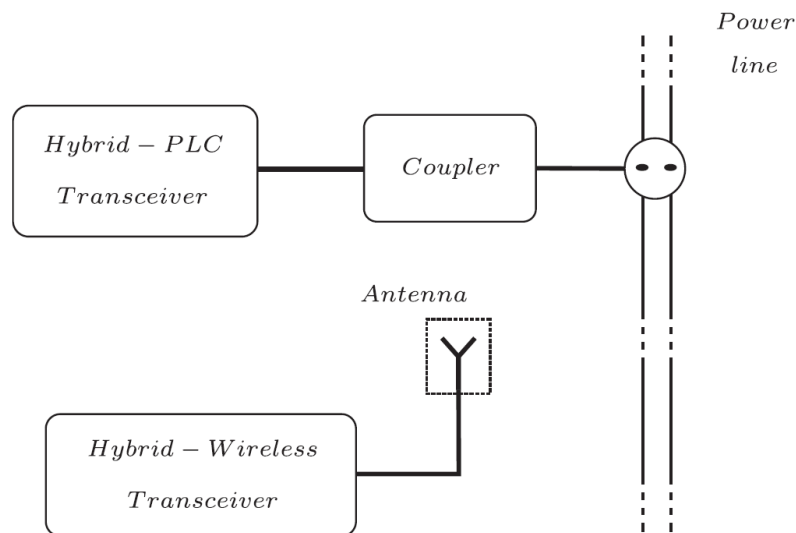


Figure 39: Block diagram of the hybrid PLC-wireless measurement setup.

By taking into account all facilities, 293 different combinations of locations for both transceivers were evaluated. The hybrid-wireless transceiver was positioned near to (*short-path channel*) and far from (*long-path channel*) the outlet in 200 and 93 combinations, respectively. Furthermore, an average of 600 estimates of CFRs were measured for each combination, resulting on a total of 175,428 different estimates of the hybrid PLC-wireless channel frequency responses, obtained during the campaign.

APPENDIX B – In-home PLC channels in the frequency band delimited by 1.7 and 100 MHz: Tables of the values of cubic splines used to model the parameter of the Beta Distribution.

Table 2: $\alpha(f)$ parameter: Coefficients of the cubic Splines for $L = 19$ nonuniform subbands.

Frequency Band (MHz)	a_u	b_u	c_u	d_u
$1.70 < f \leq 3.42$	-2.6528×10^{-5}	0.0033	-0.1197	2.5007
$3.42 < f \leq 4.44$	-2.6528×10^{-5}	5.2561×10^{-4}	0.0146	1.2292
$4.44 < f \leq 6.05$	1.7869×10^{-5}	-0.0011	0.0015	1.5211
$6.05 < f \leq 8.50$	-5.9605×10^{-6}	6.2337×10^{-4}	-0.0157	0.9666
$8.50 < f \leq 12.01$	2.0887×10^{-6}	-2.7071×10^{-4}	0.0019	0.9954
$12.01 < f \leq 17.19$	-9.2474×10^{-7}	1.8046×10^{-4}	-0.0046	0.5114
$17.19 < f \leq 22.36$	6.4104×10^{-7}	-1.1361×10^{-4}	0.0025	0.9547
$22.36 < f \leq 27.53$	-5.6131×10^{-7}	9.0243×10^{-5}	5.3515×10^{-5}	0.7099
$27.53 < f \leq 32.71$	4.7371×10^{-7}	-8.8254×10^{-5}	-2.6432×10^{-4}	1.0610
$32.71 < f \leq 43.06$	-1.7026×10^{-7}	6.2385×10^{-5}	-0.0025	0.6616
$43.06 < f \leq 48.24$	1.4089×10^{-7}	-4.5902×10^{-5}	0.0010	1.3178
$48.24 < f \leq 53.42$	1.4415×10^{-7}	-1.0984×10^{-6}	-0.0040	1.0777
$53.42 < f \leq 58.60$	-2.7951×10^{-7}	4.4742×10^{-5}	6.6073×10^{-4}	0.8167
$58.60 < f \leq 68.95$	1.4642×10^{-7}	-4.4142×10^{-5}	7.2426×10^{-4}	1.0565
$68.95 < f \leq 74.12$	-3.5410×10^{-7}	4.8981×10^{-5}	0.0018	0.6212
$74.12 < f \leq 79.30$	4.3096×10^{-7}	-6.3623×10^{-5}	1.9804×10^{-4}	0.9354
$79.30 < f \leq 84.47$	-3.8389×10^{-7}	7.3423×10^{-5}	0.0012	0.7548
$84.47 < f \leq 94.82$	9.4613×10^{-8}	-4.8652×10^{-5}	0.0039	1.2537
$94.82 < f \leq 100$	9.4613×10^{-8}	1.1522×10^{-5}	-0.0040	0.7874

Table 3: $\beta(f)$ parameter: Coefficients of the cubic Splines for $L = 19$ nonuniform subbands.

Frequency Band (MHz)	a_u	b_u	c_u	d_u
$1.70 < f \leq 3.42$	0	0.0112	-0.3463	5.1804
$3.42 < f \leq 4.44$	-9.0897×10^{-5}	0.0016	0.1020	2.8535
$4.44 < f \leq 6.05$	6.0160×10^{-5}	-0.0041	0.0503	4.8733
$6.05 < f \leq 8.50$	-1.9159×10^{-5}	0.0019	-0.0234	4.2359
$8.50 < f \leq 12.01$	7.2688×10^{-6}	-0.0010	0.0191	5.3245
$12.01 < f \leq 17.19$	-3.1854×10^{-6}	5.5773×10^{-4}	-0.0137	4.1615
$17.19 < f \leq 22.36$	3.4012×10^{-6}	-4.5522×10^{-4}	-0.0028	5.1844
$22.36 < f \leq 27.53$	-3.4336×10^{-6}	6.2635×10^{-4}	0.0153	3.8223
$27.53 < f \leq 32.71$	1.8876×10^{-6}	-4.6554×10^{-4}	0.0324	8.3953
$32.71 < f \leq 43.06$	-2.0279×10^{-7}	1.3472×10^{-4}	-0.0027	8.8443
$43.06 < f \leq 48.24$	-1.1405×10^{-6}	5.7440×10^{-6}	0.0271	12.3956
$48.24 < f \leq 53.42$	2.6168×10^{-6}	-3.5693×10^{-4}	-0.0101	13.9729
$53.42 < f \leq 58.60$	-2.6679×10^{-6}	4.7522×10^{-4}	0.0024	12.0045
$58.60 < f \leq 68.95$	1.4275×10^{-6}	-3.7318×10^{-4}	0.0132	14.4208
$68.95 < f \leq 74.12$	-4.7854×10^{-6}	5.3473×10^{-4}	0.0475	14.0510
$74.12 < f \leq 79.30$	8.4579×10^{-6}	-9.8702×10^{-4}	-4.8272×10^{-4}	19.3107
$79.30 < f \leq 84.47$	-9.4143×10^{-6}	0.0017	0.0754	18.3228
$84.47 < f \leq 94.82$	3.5082×10^{-6}	-0.0013	0.1190	34.2297
$94.82 < f \leq 100$	3.5082×10^{-6}	9.4005×10^{-4}	0.0445	34.8507

APPENDIX C – In-home hybrid PLC-WLC *short-path* channels in the frequency band delimited by 1.7 and 100 MHz: Tables of the values of cubic splines used to model the parameters of the Log-Normal Distribution.

Table 4: $\mu(f)$ parameter: Coefficients of the cubic Splines for $L = 15$ nonuniform subbands.

Frequency Band (MHz)	a_u	b_u	c_u	d_u
$1.70 < f \leq 5.08$	2.3701×10^{-6}	-6.0903×10^{-4}	0.0500	-7.9514
$5.08 < f \leq 6.54$	2.3701×10^{-6}	-1.1842×10^{-4}	-1.7145×10^{-4}	-6.6209
$6.54 < f \leq 8.50$	3.9289×10^{-6}	9.4894×10^{-5}	-8.7708×10^{-4}	-6.6686
$8.50 < f \leq 9.47$	-1.7588×10^{-5}	5.6636×10^{-4}	0.0256	-6.3004
$9.47 < f \leq 13.87$	2.4037×10^{-6}	-4.8890×10^{-4}	0.0271	-5.7031
$13.87 < f \leq 21.19$	-5.6687×10^{-7}	1.6009×10^{-4}	-0.0025	-5.4699
$21.19 < f \leq 28.03$	3.7473×10^{-7}	-9.4996×10^{-5}	0.0073	-4.1516
$28.03 < f \leq 33.40$	-3.4080×10^{-7}	6.2389×10^{-5}	0.0027	-3.9641
$33.40 < f \leq 43.46$	1.0904×10^{-7}	-5.0076×10^{-5}	0.0041	-3.3626
$43.46 < f \leq 50.49$	-8.8509×10^{-8}	1.7312×10^{-5}	-0.0027	-3.6932
$50.49 < f \leq 55.37$	1.2130×10^{-7}	-2.0924×10^{-5}	-0.0032	-3.9824
$55.37 < f \leq 65.14$	-3.1804×10^{-8}	1.5465×10^{-5}	-0.0037	-4.3889
$65.14 < f \leq 74.90$	1.7372×10^{-8}	-3.6169×10^{-6}	-0.0014	-4.7710
$74.90 < f \leq 96.87$	-1.2395×10^{-8}	6.8061×10^{-6}	-7.2408×10^{-4}	-5.0491
$96.87 < f \leq 100$	-1.2395×10^{-8}	-9.9272×10^{-6}	-0.0021	-5.1262

Table 5: $\sigma(f)$ parameter: Coefficients of the cubic Splines for the $L = 15$ nonuniform subbands.

Frequency Band (MHz)	a_u	b_u	c_u	d_u
$1.70 < f \leq 2.88$	2.1232×10^{-5}	-0.0021	0.0435	1.2187
$2.88 < f \leq 4.35$	2.1232×10^{-5}	-5.2494×10^{-4}	-0.0184	1.3724
$4.35 < f \leq 5.08$	-5.8155×10^{-5}	0.0014	0.0074	0.9206
$5.08 < f \leq 6.54$	2.0568×10^{-5}	-0.0012	0.0097	1.1473
$6.54 < f \leq 8.50$	-8.0700×10^{-6}	6.2010×10^{-4}	-0.0086	0.8867
$8.50 < f \leq 10.69$	3.7423×10^{-6}	-3.4830×10^{-4}	0.0023	1.0186
$10.69 < f \leq 17.28$	-6.3590×10^{-7}	1.5692×10^{-4}	-0.0063	0.7568
$17.28 < f \leq 22.66$	4.4496×10^{-7}	-1.0063×10^{-4}	0.0013	1.1968
$22.66 < f \leq 35.06$	-1.0044×10^{-7}	4.6212×10^{-5}	-0.0047	0.7106
$35.06 < f \leq 39.84$	1.5003×10^{-7}	-3.0325×10^{-5}	-6.8556×10^{-4}	0.8469
$39.84 < f \leq 60.25$	-1.8796×10^{-8}	1.3785×10^{-5}	-0.0023	0.6297
$60.25 < f \leq 68.55$	1.2989×10^{-7}	-9.7855×10^{-6}	-6.3475×10^{-4}	0.7014
$78.61 < f \leq 78.61$	-2.1013×10^{-7}	2.9181×10^{-5}	0.0013	0.6699
$78.61 < f \leq 94.43$	2.2893×10^{-8}	-1.4947×10^{-5}	0.0023	0.8322
$94.43 < f \leq 100$	1.0785×10^{-8}	-5.2390×10^{-7}	-9.4771×10^{-4}	0.8683

APPENDIX D – In-home hybrid PLC-WLC *long-path* channels in the frequency band delimited by 1.7 and 100 MHz: Tables of the values of cubic splines used to model the parameters of the Log-Normal Distribution.

Table 6: $\mu(f)$ parameter: Coefficients of the cubic Splines for $L = 15$ nonuniform subbands.

Frequency Band (MHz)	a_u	b_u	c_u	d_u
$1.70 < f \leq 6.44$	-1.1271×10^{-6}	1.7728×10^{-4}	0.0026	-8.4445
$6.44 < f \leq 14.84$	-1.1271×10^{-6}	-1.2068×10^{-5}	0.0119	-7.9388
$14.84 < f \leq 22.41$	1.1653×10^{-6}	-1.1350×10^{-4}	0.0081	-7.6235
$22.41 < f \leq 25.59$	-4.1434×10^{-6}	2.1163×10^{-4}	0.0172	-6.9126
$25.59 < f \leq 27.69$	4.1926×10^{-6}	-4.3475×10^{-4}	0.0056	-6.0262
$27.69 < f \leq 32.57$	-1.4955×10^{-6}	2.5704×10^{-4}	-0.0041	-6.3333
$32.57 < f \leq 33.40$	3.1809×10^{-7}	-9.2908×10^{-5}	0.0087	-5.8014
$33.40 < f \leq 40.38$	-2.6103×10^{-7}	6.4547×10^{-5}	0.0040	-5.4711
$40.38 < f \leq 44.04$	1.2268×10^{-7}	-6.8577×10^{-5}	0.0033	-4.2094
$44.04 < f \leq 48.24$	-4.0204×10^{-8}	2.4906×10^{-5}	-0.0078	-5.7833
$48.24 < f \leq 57.81$	1.8952×10^{-8}	-6.6395×10^{-7}	-0.0026	-6.6975
$57.81 < f \leq 60.74$	-2.8253×10^{-8}	1.1389×10^{-5}	-3.7214×10^{-4}	-7.1077
$60.74 < f \leq 68.94$	6.8867×10^{-8}	-6.5792×10^{-6}	6.4762×10^{-4}	-6.9439
$68.94 < f \leq 86.18$	-5.6494×10^{-8}	1.5321×10^{-5}	0.0016	-6.8672
$86.18 < f \leq 100$	-5.6494×10^{-8}	-1.7390×10^{-5}	0.0012	-6.3988

Table 7: $\sigma(f)$ parameter: Coefficients of the cubic Splines for the $L = 15$ nonuniform subbands.

Frequency Band (MHz)	a_u	b_u	c_u	d_u
$1.70 < f \leq 4.44$	1.3148×10^{-7}	-5.6568×10^{-5}	0.0030	1.4384
$4.44 < f \leq 5.91$	1.3148×10^{-7}	-1.8306×10^{-5}	-0.0043	1.3175
$5.91 < f \leq 10.45$	-2.6464×10^{-7}	4.9539×10^{-5}	0.0011	0.7124
$10.45 < f \leq 12.99$	1.0831×10^{-6}	-7.3521×10^{-5}	-0.0026	1.0896
$12.99 < f \leq 15.68$	-2.0515×10^{-6}	1.3768×10^{-4}	0.0016	0.9071
$15.68 < f \leq 19.48$	8.9917×10^{-7}	-1.2695×10^{-4}	0.0020	1.0660
$19.48 < f \leq 27.54$	-4.7172×10^{-6}	1.4280×10^{-4}	0.0036	0.8984
$27.54 < f \leq 35.84$	3.8415×10^{-7}	-9.7780×10^{-5}	0.0044	0.9779
$35.84 < f \leq 48.24$	-5.4667×10^{-7}	6.7022×10^{-5}	-2.1365×10^{-5}	0.7276
$48.24 < f \leq 58.59$	3.4176×10^{-7}	-5.5979×10^{-5}	8.0683×10^{-4}	0.8724
$58.59 < f \leq 68.94$	-1.0467×10^{-7}	3.2196×10^{-5}	-0.0012	0.7451
$68.94 < f \leq 79.30$	2.4291×10^{-7}	-2.9349×10^{-5}	-6.8042×10^{-4}	0.9511
$79.30 < f \leq 84.47$	-3.2976×10^{-8}	1.4375×10^{-5}	-0.0016	0.8571
$84.47 < f \leq 93.90$	2.9498×10^{-9}	-2.2454×10^{-6}	4.5886×10^{-4}	0.8412
$93.90 < f \leq 100$	2.9498×10^{-9}	8.7842×10^{-7}	-2.3694×10^{-5}	0.8531

APPENDIX E – List of Publications

The list of journal papers published or submitted during the graduate period is as follows:

- T. F. do A. Nogueira, G. R. Colen, V. Fernandes and M. V. Ribeiro, “Statistical Characterization and Modelings of Frequency Responses of Brazilian In-Home PLC Channels,” in *IEEE System Journal*, under review.
- V. Fernandes, T. F. do A. Nogueira, H. V. Poor and M. V. Ribeiro, “Statistical Modeling for Dedicated Energy Harvesting in Hybrid PLC-Wireless Channels,” in *IEEE Trans. on Smart Grid*, submitted.